
A METHOD TO SCAN THE PARAMETER
SPACE OF 2-D NONLINEAR BIOCHEMICAL
OSCILLATORS AND PREDICTING LIMIT
CYCLE BOUNDARIES WITH THE HELP OF
RENORMALIZATION GROUP

A THESIS SUBMITTED IN FULFILLMENT OF THE DEGREE
OF DOCTOR OF PHILOSOPHY(SCIENCE)

BY

AYAN DUTTA

INDEX No. 72/14/*PHYS.*/23

UNDER THE GUIDANCE OF

Dr. DHRUBA BANERJEE



DEPARTMENT OF PHYSICS, JADAVPUR UNIVERSITY
132, RAJA S.C. MULLICK ROAD
KOLKATA -700032

CERTIFICATE FROM THE SUPERVISOR

This is to certify that the thesis entitled "**A method to scan the parameter space of 2-D non-linear biochemical oscillators and predicting limit cycle boundaries with the help of Renormalization Group**" submitted by Sri **Ayan Dutta** who got his / her name registered on **07.04.2014**, for the award of Ph.D. (Science) degree of Jadavpur University, is absolutely based upon his own work under the supervision of **Dr. Dhruba Banerjee**, and that neither this thesis nor any part of it has been submitted for either any degree / diploma or any other academic award anywhere before.

Dhruba Banerjee
(Signature of Supervisor)

31-05-2022

Dr. DHRUBA BANERJEE
Assistant Professor
Dept. of Physics
JADAVPUR UNIVERSITY
KOLKATA - 700 032

To my family

Acknowledgements

Not every day do we get a chance to thank the people whose contributions, in some way or the other, have made our lives worthy. I take this lifetime opportunity to extend my gratitude to those who have contributed to my life in ways worth remembering.

At the very outset, I want to convey my gratitude to my thesis supervisor Dr. Dhruva Banerjee of Jadavpur University, without whose help and advice this present work would hardly have been possible. I found him a great teacher, philosopher, and guide who has always extended his arm of cooperation whenever I needed it.

I would like to thank my professors from Jadavpur University, namely, Dr. Tapas Ranjan Midya Sir, whom I owe a lot for my understanding of Classical Mechanics and Mathematical physics. Dr. Kalyan Kumar Chattopadhyay's lectures on Quantum Many-Body Theory and Electrodynamics will never be forgotten. Dr. Tapas Kumar Ballav's classes on Monte Carlo methods were a gem. Not to forget Dr. Sachindranath Das, from the Department of Instrumentation Science, one of the most sincere researchers in experimental physics I have known; I convey my gratitude to him. Prof. A.R.Chakraborty's classes on Non-linear waves were particularly interesting and will always be cherished. Dr. Dhruva Banerjee needs a special mention who nurtured my interest in the subject during my Master's days. His classes at Jadavpur University are still cherished. He has a natural flair for teaching, which I have always tried imbibing. I hope I can attend more of his lectures. I owe a lot to him, including the final opportunity to pursue Ph.D.

Opportunity demands that I thank my undergraduate college, Ramakrishna Mission Vivekananda Centenary College, Rahara, for inculcating in me discipline and some priceless values of life. I particularly thank Dr. Rajen Kundu and Dr. Madhab Bandyopadhyay of the Physics Department for their contributions to my understanding of Quantum Physics and Classical Mechanics. Dr. Sambhu Prasad Kundu and Dr. Dwijesh Majumder's lectures on Electrodynamics and Electrostatics at RKMVCC, Rahara, were engulfing. To this day, I remember Prof. Biman Mukhopadhyay of RKMVCC for clearing my concepts in Physical chemistry. He was a brilliant chemist. I am really fortunate to have received his guidance. I thank the late Prof. S. Majumder for helping me with my mathematics during my graduation. Lastly, I convey my gratitude to Shyamal da (Dr. Shyamal Bhar), who has been our senior at JU, for his guidance and indispensable suggestions.

I would like to mention some unforgettable teachers from my childhood days, Mrs. Lipika Chattopadhyay, Mrs. Lipika Ghosh, Mrs. Rita Sarkar, Mr. Pradip Pal, and Mr. Abhijit Biswas, Mrs. Sanchita Banerjee, Mrs. Sumana Basu and Mrs. Pamela Paul from St. Xavier's Institution, Panihati. Their support and care made my school days really special. Apart from them, my mathematics teacher Mr. Atanu Kumar Pandit (Atanu Sir), is someone to whom I shall remain grateful always for reasons galore, and my physics teacher Mr. Subir Sengupta (Subir Sir), occupies a special place in my heart since he is the one who had inspired me to take up physics.

Every human being is in an insurmountable debt to his/her parents, and mine is no exception. I thank them for giving me this life and all the perquisites this life has to offer. It is for them that I could get a proper education which they have always pushed and advocated for. They have always believed in me and have provided

for every demand of mine. I think I haven't adequately thanked them. My little brother Toton is the one whose arrival in this world made my childhood special. He was my partner in every mischief. From playing cricket to flying kites on the roof and the time spent at our ancestral home in Sukchar, are my best memories to date. The late nights we spent studying together, along with those jokes and thoughtful discussions, cannot ever be forgotten. I thank him for always being my supporter.

I thank God for presenting me with a childhood full of worthy friends like Ujjwal, Rinku, Pakuni, Morol, Bhai, Sourav da, and Babushona. I am forever young because of you all. Junior brothers like Rick, Tukai, Soumyo, Toto, Dampi, Sumanta and seniors like Golu da and Bumba da occupy a special place in my heart. Growing up around you people has been a joyride. I found great friends in Sukalyan, Pratik and Samir at RKMVCC . Seniors Sauvik da and Soham da made those late afternoon classes interesting during the grads. Luckily we are still in touch. Tanmoy and Rajdip's jokes were gems and provided great entertainment between the grueling sessions at college. At Jadavpur University, I met some really interesting friends; Ankur, Surajit da, Amitabh da, Tanumoy, Senaul, Sutanya, and Wahida became my closest friends buddies and are to this date. I shall continue to cherish every moment of those three years we spent together at JU. Ankur is a great friend and has always extended his arm of help whenever needed. Sharing laboratory space with Chitrak and Jyotipriya has been quite interesting and motivating. Our late evening discussions took my days' tiredness away. Somnath is the junior who has helped me a lot and needs a special mention. I thank him for whatever he has done for me. Lastly, I express my deep gratitude to our senior at the JU research lab, Dr. Debapriya Das (Debapriya di), for her constant support and encouragement. She has always stood by her juniors

through thick and thin during research and has always extended her help whenever needed.

Next, I wish to thank the people without whose help I could not have completed my Master's. Smt. Chhabi Bhattacharyya, Sri Sanjiv Ranjan, and Sri Ashit Baran Roy's cooperation made it possible for me to attend classes at JU. I shall always remain grateful to them. I found a great enthusiast in Sri Joy Sona Ghosh, alumni of JU Mathematics Department and my colleague. Our discussions on mathematics, particle physics, relativity, and cosmology while returning home from work every day in the Kolkata metro are truly enjoyed.

I extend my utmost gratitude to my friend, life partner, and my much better half Sutanya for her immense love, constant care, and encouragement is the reason behind my being able to finish this mammoth task. Times have not been easy sometimes, but she has always stayed by me and believed in my abilities. She is the most intelligent woman I have ever come across with a kind heart. She has a wonderful ability to take away my worries and has always filled me with confidence. She is a brilliant dancer, a big foodie, and a brilliant cook. I still think that it's our common love for *rosogollas* that has brought us together. I can never ask for more from her. I wish her luck in her future endeavors and thank her for gifting me this great partnership. I must thank Mr. Tapas Sarkar and Mrs. Sarbani Sarkar, my in-laws, for being our pillar of constant support.

Last but not least, I thank all the staff of Jadavpur University, whose constant hard work gets this great institution going.

Ayan Dutta

ABSTRACT

Index No. 72/14/Phys./23

TITLE : A method to scan the parameter space of 2-D nonlinear biochemical oscillators and predicting limit cycle boundaries with the help of Renormalization Group.

This thesis is motivated to find a suitable mathematical tool or a method that will facilitate scanning of the entire parameter space of a non-Lienard type non-linear biochemical oscillator. The parameter space of two-dimensional non-Lienard type non-linear oscillators having at most two system parameters guiding the dynamics of the system is divided into two regions by a curve called the stability curve. Values of the system parameters guiding the overall dynamics of the system from one side of this stability curve cause the system to exhibit isolated closed orbits or limit cycles, while parameter values from the other side of the stability curve cause the system to have stable fixed points. On the curve, the system is supposed to undergo a Hopf bifurcation. The developed mathematical tool can help to scan the parameter space and change the parameter values in a suitable desired manner. Sel'kov model of Glycolysis has been taken up to introduce the procedure since the parameter space of this process is suitable for portraying the effectiveness of the method.

We have started out with very general discussions of the system dynamics of two-dimensional non-linear oscillators and how their dynamical characteristics change with the change in parameter values. The various types of fixed points possible in a dynamical system and conditions for the formation of limit cycles have been discussed in the first chapter. The second chapter emphasizes the importance of the Perturbative Renormalization Group. The application of the Perturbative renormalization group leading to the formation of flow equations has been discussed in detail. The advantage of RG in comparison to ordinary perturbation theory has been discussed, along with its usefulness as a probe in proving the applicability of the presently developed method is studied.

The third chapter of this volume throws light on the application of perturbation theory in the case of two-dimensional non-Linear type non-linear oscillators. Perturbative renormalization group has been applied in the case of the Sel'kov model of Glycolysis, leading to amplitude flow equations which give the distance of the center to the point where the limit cycle cuts the X-axis. These results have been predicted for different parameter values inside the limit cycle region of the parameter space. The parameter values have been varied using an external handle in the form of an external parameter ' δ ' suitably introduced into the system equations so as to be able to scan the parameter space. The method, however, suffers from some restrictive constraints which limit its applicability to the parameter space, as we shall see in detail.

The fourth chapter of the present report proposes the mathematical procedure which eliminates the restrictions on the external parameter ' δ ', thus bettering our method earlier presented in chapter 3. This procedure is better fitted in the scanning of the parameter space of the two-dimensional non-Lienard type biochemical oscillators to a large extent, as we shall see in detail, and the same has been proven by comparison of results predicted by the Perturbative Renormalization Group and numerical plots. Lastly, the bibliography for the work has been listed.

Ayan Dutta
(Signature of Candidate)
31-05-2022

Dhruba Banerjee
(Signature of Supervisor) 31-05-2022
Dr. DHRUBA BANERJEE
Assistant Professor
Dept. of Physics
JADAVPUR UNIVERSITY
KOLKATA - 700 032

List of Publications

- A Dutta, D Das, D Banerjee, JK Bhattacharjee, *Estimating the boundaries of a limit cycle in a 2D dynamical system using renormalization group*, Communications in Nonlinear Science and Numerical Simulation, Volume 57, April 2018, Pages 47-57.
- A Dutta, J Roy, D Banerjee, *Predicting Limit Cycle Boundaries Deep Inside Parameter Space of a 2D Biochemical Nonlinear Oscillator Using Renormalization Group*, International Journal of Bifurcation and Chaos, Vol. 31, No. 11, 2150162 (2021).

Contents

Acknowledgements	i
Abstract	vi
List of Publications	viii
1 Introduction	1
1.1 Motivation and Aim	1
1.2 Literature Review	2
1.2.1 Dynamical Systems : Fixed points & Clas- sification	2
1.2.2 Nonlinear oscillators : Dependence on parameters	14
2 Perturbative Renormalization Group (RG)	20
2.1 Advantage of RG	20
2.2 A theoretical probe	27
3 Scanning the parameter space: A primitive trial	30
3.1 Introduction	30
3.2 The Procedure	31
3.3 Results	46
3.4 Appendix	52
4 Scanning the parameter space: A subtle approach	55

4.1	Introduction	55
4.2	The Method	56
4.3	Results	68
4.4	Appendix A	73
4.5	Appendix B	76
4.6	Appendix C	83
5	Prospects and Conclusion	92
	Bibliography	95

List of Figures

1.1	Phase portraits for different values of ‘a’(Strogatz,2018) 5	
1.2	Combination of eigenvectors(Strogatz,2018)	10
1.3	Classification of fixed points(Strogatz,2018)	10
1.4	Types of Limit Cycles(Strogatz,2018)	15
1.5	Trapping region \mathbb{R} (Strogatz,2018)	16
1.6	Real eigenvalues(a) and complex conjugates(b) im- plying stability of a fixed point(Strogatz,2018) . . .	17
1.7	Change of eigenvalue position with parameter vari- ation	18
2.1	Exact solution vs Solution offered by Perturbation theory(Strogatz,2018)	23
3.1	Parameter space of Glycolytic oscillator	34
3.2	Limit cycle for $\delta = 0.002$ and intercept on X-axis is $A=0.088$	41
3.3	Limit cycle for $\delta = 0.0015$ and intercept on X-axis at $A = 0.075$	48
3.4	Limit cycle for $\delta = 0.002$ and intercept on X-axis at $A = 0.088$	48
3.5	Limit cycle for $\delta = 0.0025$ and intercept on X-axis at $A = 0.097$	49
3.6	Limit cycle for $\delta = 0.0025$ and intercept on X-axis at $A = 0.097$	50

3.7	Limit cycle for $\delta = 0.05$ and intercept on X-axis at $A = 0.665$	50
4.1	Stability diagram for varying delta(δ)	59
4.2	Limit cycle for $\delta = 0.001$ and boundary calculated at $A_{numerical} = 0.03$	70
4.3	Limit cycle for $\delta = 0.01$ and boundary calculated at $A_{numerical} = 0.10$	71
4.4	Limit cycle for $\delta = 0.10$ and boundary calculated at $A_{numerical} = 0.36$	71
4.5	Limit cycle for $\delta = 0.12$ and boundary calculated at $A_{numerical} = 0.42$	72

Chapter 1

Introduction

1.1 Motivation and Aim

Study of dynamical systems [1–6] provide a framework for understanding the functioning of biological processes such as glycolysis, cell cycles, genetic regulatory networks, etc. Investigations of these fundamental life-sustaining processes using kinetic models have helped understand these complex bio-systems and have given rise to systems biology as a new field in biological research.

Dynamic (or kinetic) models have long been in practice to understand the function of biological systems [7–9]. One main thing about these dynamical models is their dependence on various parameters. The foremost challenge to be faced while modeling a biological system is, therefore, the problem of parameter estimation. Parameter estimation aims to find the unknown parameters of the model which give the best fit to an experimental data set. Any change in the concentration of metabolites, proteins, or genetic components within a biological network dictates changes in the values of the parameters, which in turn causes the biochemical systems to exhibit dynamical behavior.

The kinetic or mathematical models [10, 11] of such biochemical processes portray how the set of parameters dictates the overall dynamics of the system. Depending on a particular system

of interest, that system may have one or more than one parameter controlling its overall behaviour [12]. For the two parameters involved, the parameter space is a 2-dimensional space further subdivided into zones depending on the dynamical behavior of the system. Any change in the value of the parameters while roaming from one region of the parameter space to another causes the system dynamics to change drastically on the phase plane. Each of these phase portraits represents a physiologically important state of the original biochemical process. The effects of parameter variation is thus of immense interest to biologists studying various phenomena going on inside living cells in the form of various biological processes [8, 13].

Thus motivated by the importance of parameters and parameter space in the case of non-linear biochemical oscillators, the current thesis aims to find a mathematical procedure by which the parameter space of a 2-dimensional non-linear biochemical oscillator may be scanned effectively. We intend to establish the method by predicting limit cycle boundaries accurately for parameter values lying anywhere within the limit cycle zone of the parameter space of such oscillators.

1.2 Literature Review

1.2.1 Dynamical Systems : Fixed points & Classification

Dynamical systems are systems that evolve with time. While studying a dynamical system, we intend to find how that trajectory of the system evolves in time on the phase plane. Given this basic fact, generations of scientists and engineers have applied various mathematical and computational methods [14–19] to solve dynamical systems which happen to be both linear and non-linear.

While the linear systems [20] could be dealt with much ease, solving non-linear systems proved to be quite a formidable task when approached with ordinary mathematical methods. In the discussions to follow, we shall confine ourselves to 2-dimensional linear and non-linear systems and their dynamical behaviors on the phase plane.

Linear systems are the simplest in the category of dynamical systems in 2-dimensions and play an important role in the classification of fixed points of non-linear systems. A two-dimensional linear system is a system of the following form :

$$\begin{aligned}\dot{x} &= ax + by \\ \dot{y} &= cx + dy\end{aligned}$$

where a, b, c, d are parameters of the system. We can write the system in a more compact way vectorially by writing

$$\dot{\mathbf{X}} = \mathbf{A}\mathbf{X} \tag{1.1}$$

where $A = \begin{bmatrix} a & b \\ c & d \end{bmatrix}$ and $\mathbf{X} = \begin{bmatrix} x \\ y \end{bmatrix}$. The system is said to be linear in the sense that if there are two solutions of the system given by \mathbf{X}_1 and \mathbf{X}_2 , then any linear combination of the two solutions given by $c_1\mathbf{X}_1 + c_2\mathbf{X}_2$ is also a solution of the system. Now for any choice of the matrix A , if $X = 0$, we obtain $\dot{X} = 0$, implying the fact that $X = 0$ is always a fixed point of the system. By a fixed point, we mean points of equilibrium of the system on the phase plane so that a sufficiently small disturbance away from it damp out in time, in which case the fixed point is a stable fixed point and if small disturbances sufficiently close to it grow in time, the fixed point will be referred to as unstable. In practice fixed point of a system is obtained by putting to zero the right-hand side of equation (1.1)

and solving for ‘x’ and ‘y’.

The solutions of equation (1.1) are given as $x = x(t)$ and $y = y(t)$ and are found to be trajectories on the phase plane. The above system is said to be autonomous since the time variable ‘t’ does not appear in the RHS of equation (1.1). The solutions $x(t)$ and $y(t)$ trace out a curve on the phase plane and given the appropriate initial conditions in the form of $x = x_0$, $y = y_0$ at $t = t_0$ where x_0 and y_0 are the initial values at time t_0 ; there can be one and only one solution satisfying this condition when (x_0, y_0) is an ‘ordinary point’ i.e., a point where conditions of regularity are satisfied on the phase plane. This, however, does not mean that there can be at most one phase path through the point (x_0, y_0) on the phase diagram since the same point can serve as the initial condition for other starting times as well.

To get a better understanding of what we mean let us solve the system equations (1.1) given that the matrix $A = \begin{bmatrix} a & 0 \\ 0 & -1 \end{bmatrix}$ and draw the phase portrait as ‘a’ varies from $-\infty$ to $+\infty$ by simple qualitative discussions as follows : The given system is thus

$$\begin{bmatrix} \dot{x} \\ \dot{y} \end{bmatrix} = \begin{bmatrix} a & 0 \\ 0 & -1 \end{bmatrix} \begin{bmatrix} x \\ y \end{bmatrix} \quad (1.2)$$

whilst matrix multiplication gives

$$\dot{x} = ax$$

$$\dot{y} = -y$$

The solution of the above two equations are simply given by :

$$x(t) = x_0 e^{at} \quad (1.3)$$

$$y(t) = y_0 e^{-t} \quad (1.4)$$

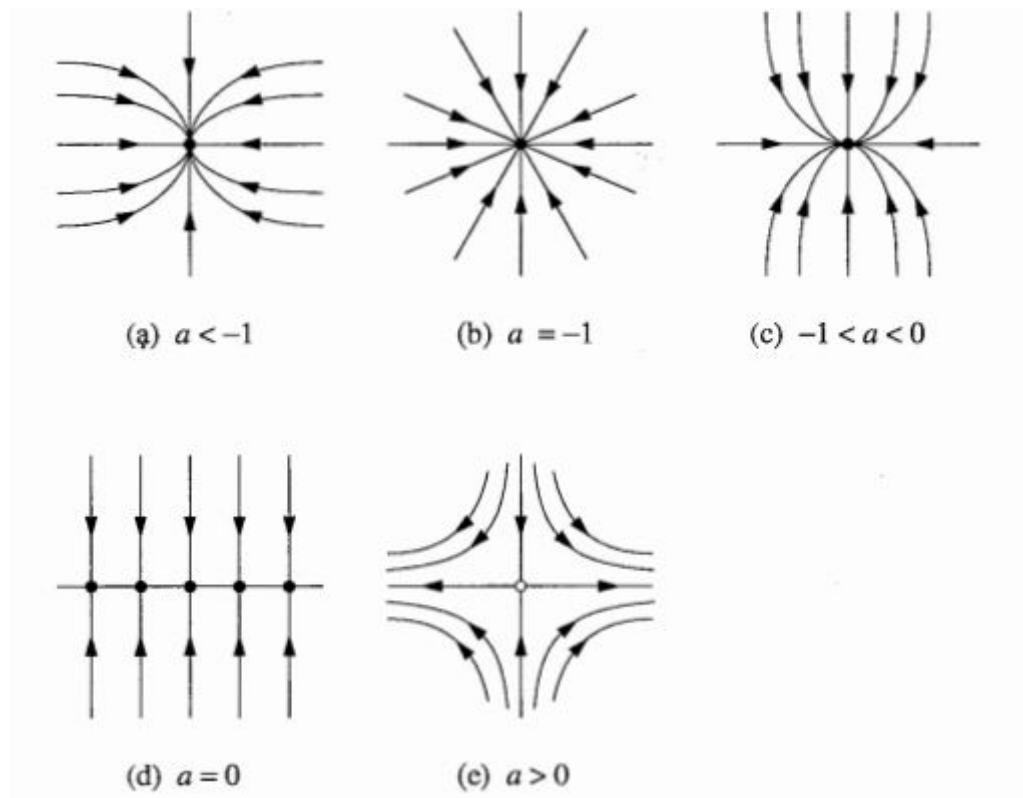


Figure 1.1: Phase portraits for different values of 'a' (Strogatz, 2018)

To understand the solutions (1.3) and (1.4) and classify the various type of possible fixed points of the current dynamical system, we take a close look at their phase portraits in the above figures and try to portray the results qualitatively.

In each of the above cases, $y(t)$ decays exponentially. When $a < 0$, $x(t)$ also decays exponentially and therefore all trajectories must approach origin as $t \rightarrow \infty$. The direction of approach is what will depend on the size of 'a' compared to -1 .

In Figure 1.1(a), $a < -1$, implying $x(t)$ is decaying more rapidly than $y(t)$. Thus as 'a' is very negative, the decay along the x-axis is instantaneous, and the trajectories along the x-axis will fall onto the y-axis (i.e., will fall off in the x-direction quickly and

come very close to the y-axis) and then approach the origin as per the rate of decay along the y-axis thus making them look tangential to the y-axis. Looking backward for $t \rightarrow -\infty$, the trajectories will become parallel to the faster-decaying direction (x-direction). In such a case the fixed points of the system given by $(x^*, y^*) = (0, 0)$ is called a stable node.

In Figure 1.1(b), $a = -1$ and thus from equation (1.3) and (1.4), we see that the decay rates in both the directions are equal. The equations also show that $y(t) / x(t) = \text{constant}$. Therefore all trajectories are straight lines through origin. In this case the point (x^*, y^*) is called a symmetrical node or star.

If the value of ‘ a ’ lies between -1 and 0, we should again have a node, but in this case, the x-direction will be more slowly decaying, and the trajectories must approach the origin along the x-direction. This is portrayed in Figure 1.1(c).

If $a = 0$ the decay will only occur along the y-direction with $x(t) = x_0$. This means that there is an entire line of fixed points along the x-axis and all the trajectories approach these fixed points along vertical lines, as shown in Figure 1.1(d).

Finally in Figure 1.1(d), $a > 0$, then the fixed point $(x^*, y^*) = (0, 0)$ becomes unstable as the growth in the x-direction is exponential. So most of the trajectories will go away from the fixed point and go out to infinity. An exception will occur if a trajectory start on the y-axis ; it then walks a tightrope to the origin. In forward time, the trajectories will be asymptotic to the x-axis and to the y-axis in backward time. In this case the fixed point $(x^*, y^*) = (0, 0)$ is said to be a saddle point. The y-axis is called the stable manifold of the saddle point $(x^*, y^*) = (0, 0)$ defined as the set of initial conditions x_0 such that $x(t) \rightarrow x^*$ as $t \rightarrow \infty$. In the same manner the

unstable manifold of the saddle point $(x^*, y^*) = (0, 0)$ is the set of initial conditions such that $x(t) \rightarrow x^*$ as $t \rightarrow -\infty$. Here the x-axis is the unstable manifold. It is notable how a typical trajectory approaches the unstable manifold as $t \rightarrow \infty$, and approaches the stable manifold as $t \rightarrow -\infty$.

Having described the trajectories arising out of the different situations in a dynamical system, there are some standard definitions in the literature about the stability of fixed points of a dynamical system. Briefly put we can say that the fixed point $(x^*, y^*) = (0, 0)$ is an attracting fixed point in the Figures 1.1(a-c) if all trajectories starting near $(x^*, y^*) = (0, 0)$ approach it as $t \rightarrow \infty$. That is, $x(t) \rightarrow x^*$ as $t \rightarrow \infty$. So, if x^* attracts all trajectories in the phase plane, it may be called globally attracting. A fixed point is said to be Liapunov stable if all trajectories starting sufficiently close to the fixed point remain close to it for all time. In Figure 1.1(a-d), the origin is Liapunov stable. Figure 1.1(d) shows that a fixed point can be Liapunov stable but not attracting in which case the particular fixed point will be called neutrally stable. Nearby trajectories are neither attracted to nor repelled from a neutrally stable point. Now, if a fixed point is *both* Liapunov stable and attracting, we call it stable or asymptotically stable. Finally, the fixed point $(x^*, y^*) = (0, 0)$ is unstable as in Figure 1.1(e) because it is neither attracting nor Liapunov stable.

Thus, having roughly understood the possible phase space dynamics and types of trajectories and fixed points in a linear dynamical system, we now turn our attention to the general case of an arbitrary 2×2 matrix aiming to classify all the possible phase portraits. Our example above has provided a clue that the x and y axes have played a crucial geometric role in determining the direction of the trajectories as $t \rightarrow \pm\infty$. Interestingly they also contained

some special **straight line trajectories**: a trajectory starting on one of the coordinate axes stayed on that axis forever and exhibited exponential growth and decay along it.

To formulate a general study, we shall seek trajectories of the form

$$\mathbf{X}(t) = e^{\lambda t} \mathbf{V} \quad (1.5)$$

where $\mathbf{V} \neq 0$ is a fixed vector to be determined and λ gives the growth or decay rate as appropriate of a particular problem. We can imagine that if a solution like Equation 1.5 exists it will correspond to an exponential motion along a line spanned by the vector \mathbf{V} .

To find the conditions required to be satisfied by the vector \mathbf{V} and the growth/decay rate λ , we shall directly substitute $\mathbf{X}(t) = e^{\lambda t} \mathbf{V}$ into $\dot{\mathbf{X}} = \mathbf{A}\mathbf{X}$ and obtain $\lambda e^{\lambda t} \mathbf{V} = e^{\lambda t} \mathbf{A}\mathbf{V}$. If the factor $e^{\lambda t}$ is cancelled from both sides we get the following equation:

$$\mathbf{A}\mathbf{V} = \lambda \mathbf{V} \quad (1.6)$$

Equation (1.6) above depicts that our desired type of straight line solutions exist only if \mathbf{V} is an **eigenvector** of \mathbf{A} with corresponding **eigen value** λ . We shall call this solution given by equation (1.5) an **eigen solution**. Thus it becomes of general interest at this point to find the **eigen values** of the matrix \mathbf{A} which are given by the **characteristic equation**: $\det(\mathbf{A} - \lambda \mathbf{I}) = 0$, where \mathbf{I} is the identity matrix.

For a 2x2 matrix, $\mathbf{A} = \begin{bmatrix} a & b \\ c & d \end{bmatrix}$ the characteristic equation becomes,

$$\begin{vmatrix} a - \lambda & b \\ c & d - \lambda \end{vmatrix} = 0.$$

Expanding the determinant gives us :

$$\lambda^2 - \tau\lambda + \Delta = 0 \quad (1.7)$$

where,

$$\tau = \text{trace}(\mathbf{A}) = a + d,$$

$$\Delta = \text{det}(\mathbf{A}) = ad - bc.$$

Solving equation (1.7) we get the following :

$$\lambda_1 = \frac{\tau + \sqrt{\tau^2 - 4\Delta}}{2}, \quad \lambda_2 = \frac{\tau - \sqrt{\tau^2 - 4\Delta}}{2} \quad (1.8)$$

The solution equations (1.8) indicate that the eigenvalues depend only on the trace and determinant of the matrix \mathbf{A} .

The first thing here to be considered is the case when the eigenvalues are distinct i.e., $\lambda_1 \neq \lambda_2$ in which case the corresponding eigenvectors \mathbf{V}_1 and \mathbf{V}_2 are linearly independent, and hence span the entire plane. Then according to linear algebra any initial condition \mathbf{X}_0 can be written as a linear combination of eigenvectors like $\mathbf{X}_0 = c_1\mathbf{V}_1 + c_2\mathbf{V}_2$ (Figure 1.2 below).

Thus the general solution for $\mathbf{X}(t)$ which satisfies the initial conditions and is a linear combination of both the solutions to equation(1.1) is simply :

$$\mathbf{X}(t) = c_1 e^{\lambda_1 t} \mathbf{V}_1 + c_2 e^{\lambda_2 t} \mathbf{V}_2 \quad (1.9)$$

All the above discussions lead us to a simple classification of the fixed points of a dynamical system along with their type and stability on a simple diagram given in the next page:

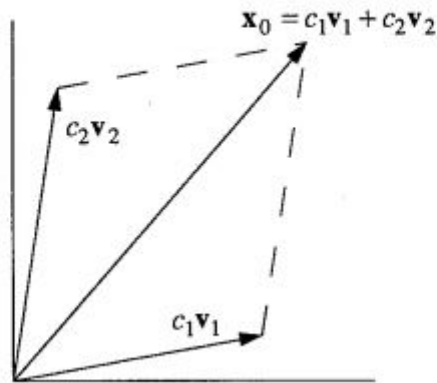


Figure 1.2: Combination of eigenvectors(Strogatz,2018)

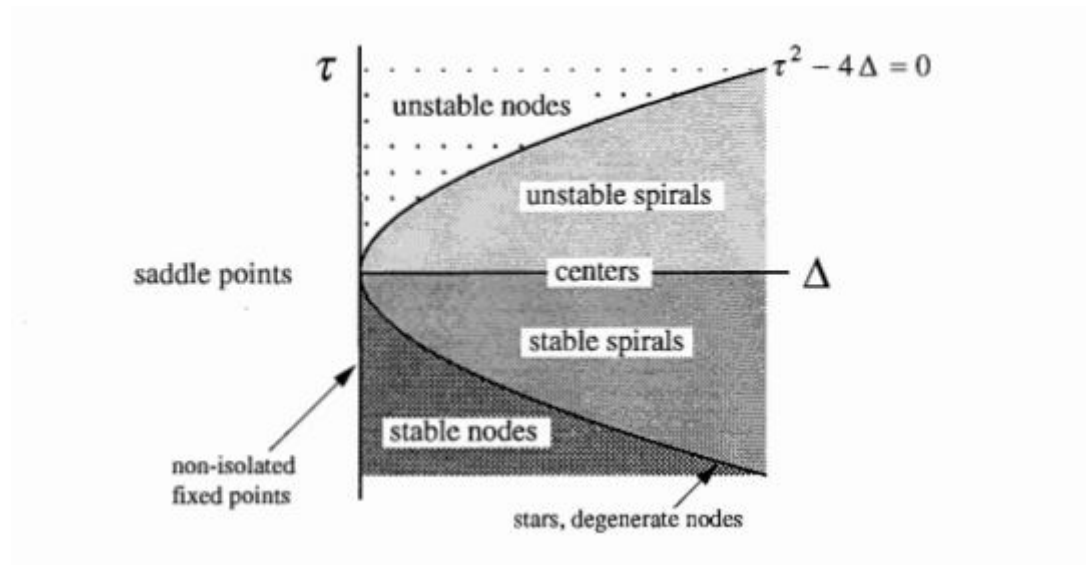


Figure 1.3: Classification of fixed points(Strogatz,2018)

In the figure 1.3 above the axes are the trace τ and the determinant Δ of the matrix \mathbf{A} . The informations in the figure 1.3 are implied by the following formulae :

$$\lambda_{1,2} = \left(\frac{\tau \pm \sqrt{\tau^2 - 4\Delta}}{2} \right) \text{ (the eigenvalues of matrix } \mathbf{A} \text{)}$$

$$\Delta = \lambda_1 \lambda_2 \text{ (the determinant of the matrix } \mathbf{A} \text{)}$$

$$\tau = \lambda_1 + \lambda_2 \text{ (the trace of the matrix } \mathbf{A} \text{)}$$

The following points lead us to the Figure 1.3:

If $\Delta < 0$, the eigenvalues are real and have opposite signs; hence the fixed point is a saddle point.

If $\Delta > 0$, the eigenvalues are either real with the same sign (nodes), or complex conjugate spirals and centers. Nodes satisfy the condition $\tau^2 - 4\Delta > 0$ and spirals satisfy $\tau^2 - 4\Delta < 0$. The parabola in the Figure 1.3 given by the equation $\tau^2 - 4\Delta = 0$ is the borderline between nodes and spirals; star nodes and degenerate nodes live on this parabola. The stability of the nodes and spirals are determined by the trace τ . When $\tau < 0$, both eigenvalues have negative real parts, so the fixed point is stable. Unstable nodes and spirals have $\tau > 0$. Neutrally stable centres live on the borderline $\tau = 0$, where the eigenvalues are purely imaginary.

If $\Delta = 0$, at least one of the eigenvalues is zero. The origin is then not an isolated fixed point. There is either a whole line of fixed points as in Figure 1.1(d), or a plane of fixed points if $\mathbf{A} = \mathbf{0}$.

Figure 1.3 indicate that saddle point nodes and spirals are the major types of fixed points. Centres, stars, degenerate nodes and non-isolated fixed points are *borderline cases* that occur along the curves in the (Δ, τ) plane. Among the borderline cases, centers are, however, the most important.

We shall now move on to non-linear systems and apply the above ideas to study the phenomena arising in such systems and study the overall phase dynamics of non-linear systems.

Two dimensional nonlinear systems

The general form of a nonlinear system in two dimensions

is given by :

$$\begin{aligned}\dot{x} &= f(x,y) \\ \dot{y} &= g(x,y)\end{aligned}$$

where $f(x,y)$ and $g(x,y)$ are given functions. This system can be written in a vector form as

$$\dot{\mathbf{x}} = \mathbf{f}(\mathbf{x})$$

where $\mathbf{x} = (x,y)$ is a point in the phase plane and $\dot{\mathbf{x}}$ is the velocity vector at that point. The vector field traces out a solution $\mathbf{x}(t)$ by flowing along the vector field in time. The entire plane is filled with trajectories as each point can be selected to play the role of initial conditions. Thus the phase plane will look like an ordinary x-y plane on which the solutions to the vector field will be in the form of curves $(x(t), y(t))$ where $x(t)$ and $y(t)$ are the solutions. The constant solutions called as fixed points in the literature are obtained by putting $f(x,y) = 0$, $g(x,y) = 0$ and solving for x and y . These constant solutions or fixed points will be represented as (x^*, y^*) . If the time variable 't' does not enter into the right hand side i.e., inside the functions $f(x,y)$ and $g(x,y)$, the system will be called **autonomous**. On the phase diagram, any typical point (x,y) is a **state** of the system. The differential equation for the phase paths is given by

$$\frac{\dot{x}}{\dot{y}} = \frac{dy}{dx} = \frac{f(x,y)}{g(x,y)}.$$

It may be interesting to note here that there is one and only one phase path through any state (x,y) of the system no matter at what time 't' the point is encountered. Thus infinitely many solutions of the system equations, differing only by time displacements,

will produce the same phase path. Two dimensional non-linear systems like the above are treated qualitatively by linearizing it at an **equilibrium point** or **fixed point** and studying the overall dynamics of the system close to the fixed point. If the nature of the fixed points can be settled in this way, the broad picture of the phase diagram then becomes clear.

Consider the system

$$\dot{x} = f(x, y) \quad (1.10)$$

$$\dot{y} = g(x, y) \quad (1.11)$$

Suppose that (x^*, y^*) is a fixed point, i.e., $f(x^*, y^*) = g(x^*, y^*) = 0$. We can therefore write by a Taylor expansion,

$$f(x, y) = ax + by + M(x, y), \quad g(x, y) = cx + dy + N(x, y)$$

where

$$a = \left(\frac{\partial f}{\partial x} \right)_{(x^*, y^*)}, \quad b = \left(\frac{\partial f}{\partial y} \right)_{(x^*, y^*)}, \quad c = \left(\frac{\partial g}{\partial x} \right)_{(x^*, y^*)}, \quad d = \left(\frac{\partial g}{\partial y} \right)_{(x^*, y^*)}.$$

and $M(x, y)$ and $N(x, y)$ are of lower order of magnitude than the linear terms as (x, y) approaches the point (x^*, y^*) . The **linear approximation** to the system in the neighbourhood of the fixed point is then written as

$$\dot{x} = ax + by \quad (1.12)$$

$$\dot{y} = cx + dy \quad (1.13)$$

and the matrix say, $\mathbf{A} = \begin{bmatrix} a & b \\ c & d \end{bmatrix}$ with its four elements 'a', 'b', 'c' and 'd' given above is called the **Jacobian** of the system. We expect the solutions of equations (1.12) and (1.13) to be geometrically similar to those of the original system near the fixed point, which

is, however, fulfilled in most cases; there are, however exceptions beyond the scope of the present article. The rest of the analysis for classifying the fixed points in a two-dimensional non-linear system is done as per the prescription given for two-dimensional linear systems.

1.2.2 Nonlinear oscillators : Dependence on parameters

Dynamical systems (linear and non-linear) in two dimensions are represented by coupled differential equations. In two dimensions such differential equations take the general form :

$$\begin{aligned}\dot{x} &= f(x, y) \\ \dot{y} &= g(x, y)\end{aligned}$$

where $f(x, y)$ and $g(x, y)$ are given functions of two variables x and y . The system dynamics of the above equations, in general, is a plot of the simultaneous solutions $(x(t), y(t))$ of the equations under some given initial condition on the $x - y$ plane. Such a plot is called a phase diagram.

It may so happen in certain cases that the phase diagram for a particular system contains a single, unstable equilibrium point surrounded by an isolated closed trajectory. The word *isolated* means that the neighboring trajectories are not closed, they either spiral toward or veer away from that closed trajectory, then the closed trajectory is called a **limit cycle** [21].

If all the neighbouring trajectories approach the closed curve the limit cycle is *stable* or *attracting*. Otherwise the limit cycle is either *unstable* or in some exceptional cases *half stable*.

The presence of stable limit cycles in a phase portrait indicates that the system under consideration can exhibit self-sustained

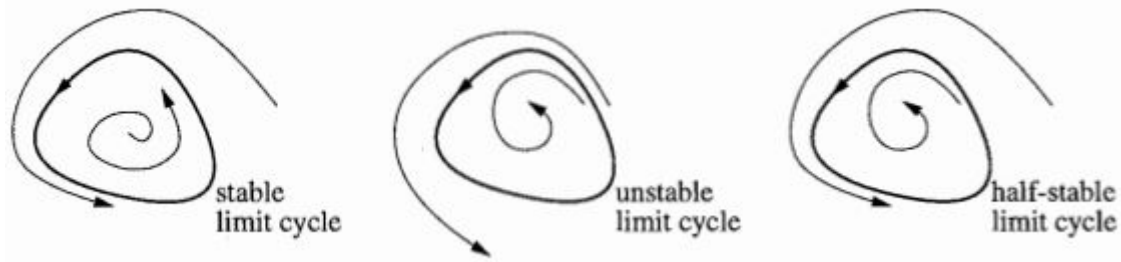


Figure 1.4: Types of Limit Cycles(Strogatz,2018)

oscillations, i.e., they oscillate even in the absence of an external periodic forcing [22,23]. Such systems are often referred to as non-linear oscillators, and the phenomena of non-linear oscillations [24] derive their name from such kind of system oscillations [25–27]. It is interesting to notice that the isolated closed orbits or *limit cycles* originate from purely non-linear phenomena as in linear systems, closed orbits can never be isolated. Limit cycles thus originate from the structure of the system and its dependence on parameters.

There are valid procedures in the literature [28] that can rule out the possibility of the occurrence of periodic orbits in systems, the discussion of which is beyond the scope of the present work. At the same time, there are methods that establish the existence of closed orbits in particular systems. The main theoretical statement towards establishing the existence of isolated closed orbits or limit cycles is the **Poincare-Bendixson Theorem** [2, 18], which states that if :

1. \mathbb{R} is a closed, bounded subset of the plane ;
2. $\dot{\mathbf{x}} = \mathbf{f}(\mathbf{x})$ is a continuously differentiable vector field on an open set containing \mathbb{R} ;
3. \mathbb{R} does not contain any fixed points; and
4. There exists a trajectory C that starts in \mathbb{R} and remains in \mathbb{R} for all future time.

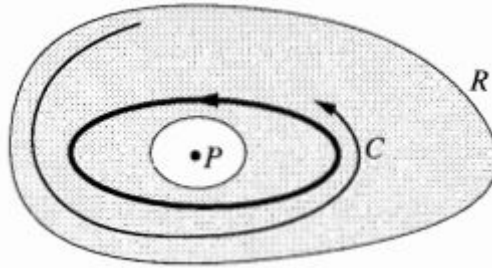


Figure 1.5: Trapping region \mathbb{R} (Strogatz,2018)

Then either C is a closed orbit, or it spirals toward a closed orbit as $t \rightarrow \infty$. So \mathbb{R} contains a closed orbit (Figure 1.5). The proof of the theorem is beyond the scope of this article, but according to the literature, it is sufficient to establish the phenomenon of non-linear oscillations in certain systems.

Apart from all that is said above, the non-linear oscillations of a dynamical system depend largely on the variation of parameters of the non-linear system. Any change in the value of the system parameters brings about a change in the phase portrait. In one-dimensional non-linear problems, such a change can be associated with the creation, destruction, or destabilization of fixed points of the system, whereas in two dimensions, the same is accompanied by the creation, destruction, or destabilization of closed orbits as well. It is where the importance of change in the parameter values of a 2-dimensional non-linear system comes in, and thus we start describing ways in which oscillations can be turned on or off. The process which makes such changes in the phase portrait happen is known in the literature as **bifurcation** [29–31].

Thus if the phase portrait of a certain dynamical system changes its topological structure as a parameter is varied, we say that a **bifurcation** has occurred. There are many types of commonly possible bifurcations in one, and two dimensional systems, namely the saddle-node, transcritical, and pitchfork bifurcations but

another type of bifurcation called the *Hopf bifurcation* [31, 32] is the one which has no counterpart in one-dimensional systems. It is a way in which a fixed point loses its stability without colliding with any other fixed points. Also, Hopf bifurcations can generate limit cycles and other periodic solutions. How? let's have a close look.

Supposing we have a two-dimensional system with a stable fixed point and a parameter, say μ , we have to find the possibilities of the fixed point losing its stability on varying the value of the parameter μ . The eigenvalues of the Jacobian matrix of the system (Page 13) serve as the key. If the fixed point is stable, the eigenvalues λ_1 and λ_2 of the Jacobian must both be real and negative, i.e., we must have $\text{Re } \lambda < 0$. Another way we can have a stable fixed point is that both the λ 's must be complex conjugates while keeping the condition $\text{Re } \lambda < 0$ as shown in the figure below.

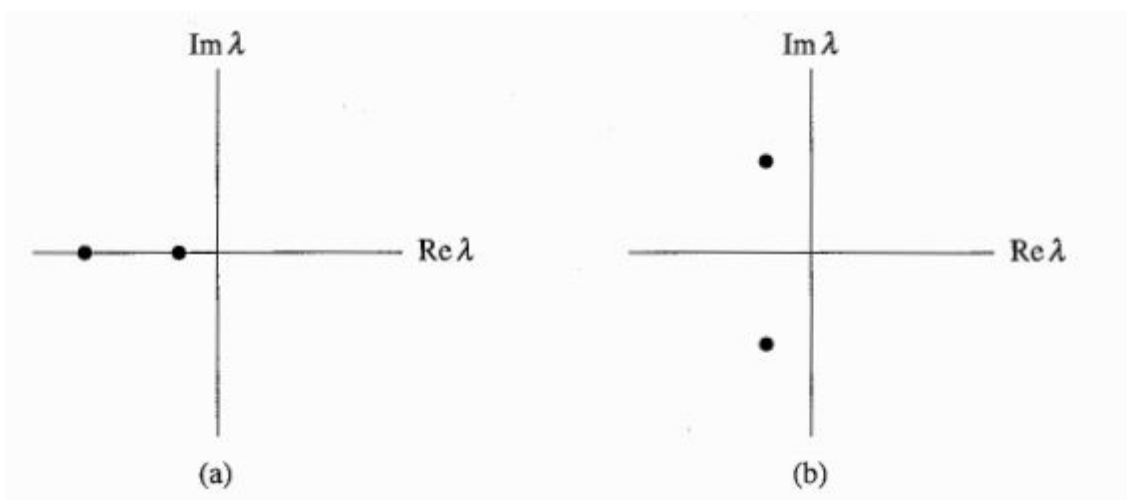


Figure 1.6: Real eigenvalues(a) and complex conjugates(b) implying stability of a fixed point(Strogatz,2018)

To destabilize the fixed point, we need one or both of the eigenvalues to cross into the right half-plane as the parameter μ varies. This amounts to saying that either both the eigenvalues λ_1 and λ_2 are real and positive, or they are again complex conjugates with their real parts greater than zero, i.e., $\text{Re } \lambda > 0$.

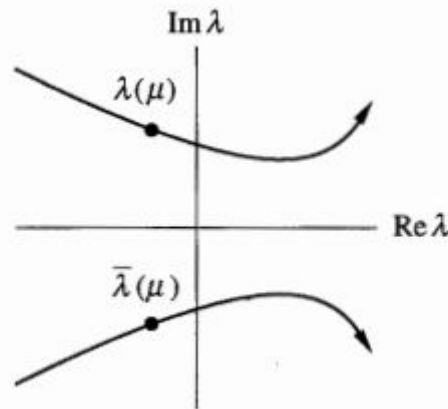


Figure 1.7: Change of eigenvalue position with parameter variation (Strogatz,2018)

According to literature, the crossing over of the eigenvalues is a direct consequence of Hopf Bifurcation, and the eigenvalues follow a curved path during the crossover and cross the imaginary axis with a nonzero slope, as shown in Figure 1.7.

The method above is the standard underlying method by which a Hopf bifurcation occurs on the variation of parameters in a non-linear system. Now a non-linear system can have more than one parameter, which is generally the case in most non-Lienard systems expressed in the general form of equations (1.10) and (1.11). In such cases the eigenvalues of the Jacobian matrix \mathbf{A} of the system will generally depend on both the parameters naturally, and this dependence can be expressed by the equation (1.7). Now the condition to get periodic solutions in those systems is quite straightforward. Mathematically we explore the condition when the trace (τ) and the determinant (Δ) of the Jacobian matrix are both greater than zero so that the fixed point of the system is unstable, and we can assume that a Hopf bifurcation has resulted in the loss of stability of the system fixed point making it an unstable spiral with the formation of a stable closed orbit around it. The latter, however, can occur when only the condition $\tau^2 - 4\Delta < 0$ is satisfied, which is also the condition for the formation of an unstable spiral. The

idea is that a stable fixed point has lost its stability, and as such, trajectories starting on it spiral away very slowly, failing to return to the same point where it started after every rotation about the fixed point. The trajectory thus slowly approaches a closed orbit or the limit cycle.

For $\tau^2 - 4\Delta > 0$ the fixed point is an unstable fixed point and trajectories starting from it go out to infinity monotonically and exponentially and as such there is no question of formation of a limit cycle. So the condition when the Hopf bifurcation is happening is the condition $\tau^2 - 4\Delta = 0$, which draws a border separating the cases $\tau^2 - 4\Delta > 0$ and $\tau^2 - 4\Delta < 0$. A method to classify periodic orbits is laid down in the works of Amartya Sarkar, Sagar Chakraborty and Jayanta Kr. Bhattacharjee [33]. However, $\tau^2 - 4\Delta = 0$ gives an equation connecting the various parameters of the system and which results in a curve separating different regions of the parameter space of the system in two dimensions as we will see shortly. This curve is the curve on which the system fixed point is assumed to show characteristics of a *center*, indicating that on this curve we get the condition satisfied by the parameters when the Hopf bifurcation is taking place. This is the part that we intend to exploit to establish a method to scan the parameter space of non-linear biochemical oscillators. The chapters 3 and 4 will be dedicated to showing this in detail about how this can be done and how we can effectively prove it theoretically.

Chapter 2

Perturbative Renormalization Group (RG)

The present chapter is intended to give the reader a taste of Renormalization group(RG) as put forward in the works of Delamotte & Chen, Goldenfeld and Oono [34, 35] and how it comes in handy when we are studying oscillating nonlinear dynamical systems from a perturbative point of view. We shall see in detail what perturbative renormalization means and its advantage over normal perturbation theory has been discussed. We shall also see how RG can be used as a probe to establish our method put forward in this text.

2.1 Advantage of RG

Oscillating nonlinear systems [36–38] can be grouped under two broad types namely, **Lienard** systems and **non-Lienard** systems. Lienard systems constitute a family of autonomous second order nonlinear differential equations that exhibit limit cycles or centres under certain conditions. These systems can model various chemical, physical and biological nonlinear phenomena and, in general can be written as a second order homogeneous nonlinear differential equation of the form :

$$\ddot{x} + \mu f(x)\dot{x} + g(x) = 0 \quad (2.1)$$

The well known van der Pol oscillator, the Duffing oscillator & the Quartic oscillators are a few examples. Equation (2.1) can be put into our known form by writing :

$$\dot{x} = y \quad (2.2)$$

$$\dot{y} = -g(x) - f(x)y \quad (2.3)$$

Lienard's theorem [2,39] suggests that the system above will have unique, stable limit cycle around the origin if the following conditions are satisfied :

1. $f(x)$ & $g(x)$ are continuously differentiable for all x .
2. $g(-x) = -g(x)$ for all x , i.e., $g(x)$ is an odd function.
3. $g(x) > 0$ for $x > 0$.
4. $f(-x) = f(x)$ for all x i.e., $f(x)$ is an even function.
5. The odd function $F(x) = \int_0^x f(u)du$ has exactly one positive zero at $x = a$, is negative for $0 < x < a$, is positive and non decreasing for $x > a$, and $F(x) \rightarrow \infty$ as $x \rightarrow \infty$.

The conditions on $g(x)$ mean that the restoring force tends to reduce any displacement, whereas the assumptions on $f(x)$ imply that the damping is negative at small $|x|$, and positive at large $|x|$. This means small oscillations are pumped up, and large ones are damped down, and the system, therefore, settles to a self-sustained oscillation of some intermediate amplitude.

The parameter μ in equation(2.1) can dictate the dynamics of the system considerably. For if $\mu \gg 1$, it's the strongly non-linear limit, where the limit cycle consists of a slow buildup followed by a sudden discharge and so on. The oscillations, in this case, are called **relaxation oscillations**. Another alternative is the

condition when $0 \leq \mu \ll 1$, which is the limit of **weakly non-linear oscillations** [2].

The first thing that we are interested in about non-linear oscillations is to be able to predict their shape, period and amplitude of limit cycles. The analysis employs ordinary perturbation theory [40, 41] where it is assumed that the oscillator at the lowest order behaves as a simple harmonic oscillator which we know fully; the higher orders are just slightly perturbed versions of the SHO. This technique, however, has a flaw in that it fails after a certain predetermined time which paves the way to the introduction of a powerful technique known as Renormalization group [42, 43] into the analysis. Let us see what this means.

The *quartic* oscillator is given by the equation :

$$\ddot{x} = -\omega^2 x - \lambda x^3 \quad (2.4)$$

where λ is assumed to be small. Introducing perturbation theory involves expanding the variable 'x' as

$$x(t) = x_0 + \lambda x_1(t) + \lambda^2 x_2(t) + \dots$$

Putting this in equation(2.4) and equating the coefficients of powers of λ from both sides we get the following equations at the zeroth order and at the first order :

$$\lambda_0 : \ddot{x}_0 + \omega^2 x_0 = 0 \quad (2.5)$$

$$\lambda_1 : \ddot{x}_1 + \omega^2 x_1 = -x_0^3 \quad (2.6)$$

The zeroth order solution is given by

$$x_0(t) = A_0 \cos(\omega t + \theta_0)$$

Plugging this into equation(2.6) gives

$$\ddot{x}_1 + \omega^2 x_1 = -A_0^3 \cos^3(\omega t + \theta_0)$$

using the solution of the first order equation along with that of the zeroth order the final solution $x(t)$ is in general given by :

$$x(t) = A_0 \cos(\omega t + \theta_0) - \frac{3A_0^3}{8\omega} \lambda (t - t_0) \sin(\omega t + \theta_0) + \lambda \left[-\frac{3A_0^3}{16\omega^2} \cos(\omega t + \theta_0) - \frac{A_0^3}{32\omega^2} \cos 3(\omega t + \theta_0) \right] + \dots \quad (2.7)$$

Here ‘ A_0 ’ and ‘ θ_0 ’ are constants generally determined by initial conditions at an arbitrary $t = t_0$; in our case, $t_0 = 0$ however; we notice that the second term is *divergent*. If (2.7) has to be a solution of equation(2.4), it has to be a *convergent* series. However at, a fixed ‘ t ’ equation(2.7) provides a good approximation as long as λ is small enough - more specifically, we need $\lambda(t - t_0) \ll 1$ so that the higher correction terms are negligible. However, normally we are interested in a fixed λ , and not fixed ‘ t ’. In this case we see the perturbation approximation up to first order to work for times $t \ll O(1/\lambda)$ i.e., we must have $t \ll \frac{1}{\lambda}$, for times given by $\lambda(t - t_0) > 1$ the perturbation theory breaks down and the solution diverges.

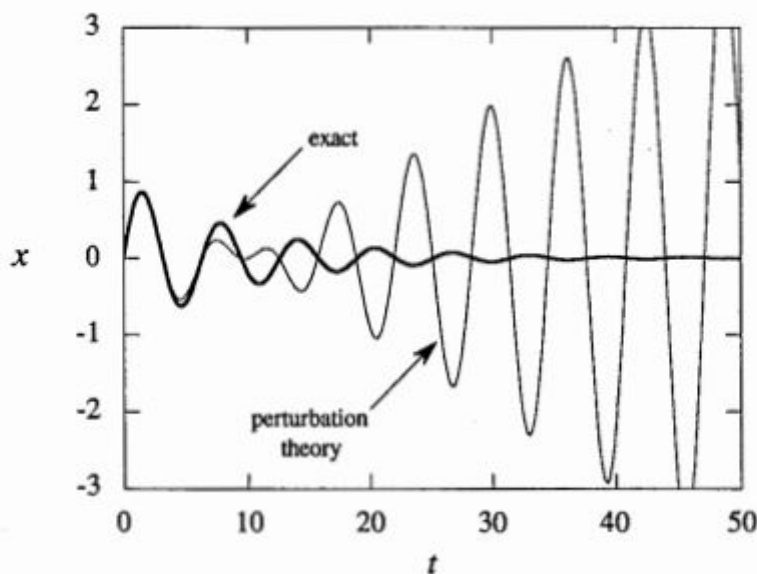


Figure 2.1: Exact solution vs Solution offered by Perturbation theory(Strogatz,2018)

Figure 2.1 is a portrait of the situation with $\lambda = 0.1$, which shows the perturbation theory to fail after $t = 10$ s. The exact line is the plot of the exact solution of the equation and used here for comparison purpose and the details of which are omitted.

The failure of ordinary perturbation theory can be attributed to the assumption that the frequency of the dynamics is a constant. However, this is not so in non-linear problems as the non-linearity makes the frequency of the oscillator a function of the amplitude.

Renormalization Group (RG) put forth recently by Chen, Goldenfeld, and Oono [34, 35, 44] is a powerful tool that can regularise a divergent perturbation series by introducing an arbitrary time τ and splitting the time scale ' $t - t_0$ ' by writing ' $(t - \tau) + (\tau - t_0)$ ' and absorb the terms containing ' $\tau - t_0$ ' into the renormalized counterparts ' A ' and ' θ ' of amplitude (A_0) and phase (θ_0). This is possible as A_0 and (θ_0) are no longer constants of motion in the presence of non-linear terms. The method is executed by introducing a multiplicative renormalization constant $Z_1 = 1 + \sum_1^\infty a_n \lambda^n$ and another additive renormalization constant $Z_2 = \sum_1^\infty b_n \lambda^n$ such that $A_0(t_0) = Z_1(t_0, \tau)A(\tau)$ and $\theta_0(t_0) = \theta(\tau) + Z_2(t_0, \tau)$. The coefficients ' a_n ' and ' b_n ' ($n \geq 0$) are chosen meticulously order by order in λ to eliminate the terms containing ' $\tau - t_0$ '. as introduced in standard RG [35]. At the end one naturally arrives at the RG-flow equations involving ' A ' and ' θ ' given by : $\frac{dA}{d\tau} = f(A, \theta)$ and $\frac{d\theta}{d\tau} = g(A, \theta)$. Solving the RG-flow equations, one gets the renormalized ' A ' and ' θ ' in terms of which the divergences in the perturbation series get contained. Thus the Renormalization group method starts out with a naive perturbative expansion with no initial assumptions, which results in the generation of 'secular' terms due to non-linearities present in the problem. To get rid of the 'sec-

ular' terms, an arbitrary time τ is introduced into the problem and the perturbation series is rewritten in terms of the renormalization constants. This effectively rids us of the trouble-causing 'secular' terms. Finally, we replace ' τ ' with ' t ' to obtain the global solution to the problem. Corrections to amplitude and frequency will arise quite naturally as we follow the above procedure order by order in specific cases.

In our case we assume $t_0 = 0$ in equation(2.7) and the same is rewritten as :

$$x(t) = A_0 \cos(\omega t + \theta_0) - \frac{3A_0^3}{8\omega} \lambda . t . \sin(\omega t + \theta_0) + \lambda \left[-\frac{3A_0^3}{16\omega^2} \cos(\omega t + \theta_0) - \frac{A_0^3}{32\omega^2} \cos 3(\omega t + \theta_0) \right] + \dots \quad (2.8)$$

Now we have to write the divergent term as :

$-\frac{3A_0^3}{8\omega} \lambda . (t - \tau + \tau) . \sin(\omega t + \theta_0)$ and introduce renormalization constants $Z_1(\tau)$ and $Z_2(\tau)$ as:

$$A_0(0) = Z_1(\tau)A(\tau) = A(\tau)(1 + a_1\lambda + \dots) \quad (2.9)$$

$$\theta_0(0) = Z_2(\tau) + \theta(\tau) = \theta(\tau) + b_1\lambda + \dots \quad (2.10)$$

Plugging equations(2.9) and (2.10) in equation(2.8) the τ divergence in $\tau \sin(\omega t + \theta_0)$ is nullified by choosing the values of the coefficients a_1 and b_1 suitably. One can easily find that at the first order of perturbation the values are given by $a_1 = 0$ and $b_1 = \tau \frac{3A_0^2(\tau)}{8\omega}$ and then equation(2.8) taken upto first order in perturbation becomes :

$$\begin{aligned}
x = A(\tau) \cos(\omega t + \theta(\tau)) + \lambda \left[-\frac{3A^3(\tau)}{16\omega^2} \cos(\omega t + \theta(\tau)) \right. \\
- \frac{A^3(\tau)}{32\omega^2} \cos 3(\omega t + \theta(\tau)) \\
\left. - (t - \tau) \frac{3A^3(\tau)}{8\omega} \sin(\omega t + \theta(\tau)) \right] \quad (2.11)
\end{aligned}$$

Now since τ is an arbitrary time scale and the dynamics has to be independent of τ hence we must have $\frac{dx}{d\tau} = 0$. Then on differentiating one finds the RG-flow equations take the following form :

$$\frac{dA}{d\tau} = 0 \quad (2.12)$$

$$\frac{d\theta}{d\tau} = \frac{3A^2\lambda}{8\omega} \quad (2.13)$$

Equation(2.12) implies that in the first order, amplitude(A) is a constant and equation(2.13) implies that $\theta = \tau \frac{3A^2\lambda}{8\omega}$. Now, the global solution is obtained by putting $\tau = t$ (because τ is arbitrary) and the final solution at the first order of perturbation takes the following form :

$$\begin{aligned}
x = A(\tau) \cos \left(\omega + \frac{3A^2\lambda}{8\omega} \right) t \\
- \lambda \left[\frac{3A^3}{16\omega^2} \cos(\omega t + \theta) + \frac{A^3}{32\omega^2} \cos 3(\omega t + \theta) \right]. \quad (2.14)
\end{aligned}$$

Equation(2.14) is the renormalized form and the global solution of x upto the first order and the important point to notice here is that RG has helped us get rid of the secular divergence present in the problem thereby proving its advantage over ordinary perturbation theory.

2.2 A theoretical probe

The fact that RG is advantageous in contrast to ordinary perturbation theory in removing divergences in series solutions to non-linear oscillators has been discussed in detail in the previous section. The present section will briefly throw light on how the renormalization group can be used as a probe in non-linear dynamics.

It is well known from available literature [45–47] that the renormalization group process naturally leads to flow equations in amplitude and frequency when applied to dynamical problems. The flow equations are of utmost importance as they help to draw some general conclusions about the global nature of the solutions to various differential equations. In the most general case, flow equations at various orders of perturbation are a result of renormalizing the amplitude and phase of an oscillation so that the divergences arising due to the presence of secular terms are nullified. The flow equations have the following universal form :

$$\frac{dA}{d\tau} = f(A, \theta) \quad (2.15)$$

$$\frac{d\theta}{d\tau} = g(A, \theta) \quad (2.16)$$

where $f(A, \theta)$ and $g(A, \theta)$ are arbitrary functions of amplitude (A) and phase (θ) arising at different order of perturbation, i.e., at the different orders of perturbation the functional forms of these functions will be different. For autonomous systems one can check that the functions f & g depends on the amplitude(A) only.

A topic of great interest in non-linear oscillations is to differentiate whether the non-linear oscillatory system has a non-linear *center* i.e., trajectories around the fixed point are a family of closed

orbits or the system exhibits a *limit cycle*, i.e., there is only a single isolated closed orbit surrounding the fixed point in question. According to literature [28] *Renormalization Group* does the work quite reliably and helps predict *centres* and *limit cycles* accurately than any other method. The recipe offered by the renormalization group is simple.

For *centre*, the amplitude flow equation obtained by putting-

$$\frac{dA}{d\tau} = f(A) = 0$$

is satisfied always for $A = 0$ implying that the fixed point is a focus or *centre*. *Centres* are surrounded by a family of circles with radii fixed by initial conditions of the problem and remain so at any time and at any order of perturbation. On the other hand, for the existence of a *limit cycle* the amplitude flow equation obtained by putting -

$$\frac{dA}{d\tau} = f(A) = 0$$

with the function $f(A)$ is such that the flow is finite and the value of this finiteness can be calculated from the value of A obtained from solving the equation, and this is satisfied for some value $A = A_j$ indicating that an isolated periodic orbit of amplitude A_j surrounds the fixed point. In practice, the equation $f(A) = 0$ gives a polynomial in A with at least one root real and greater than zero, as we shall see later.

The flow equations are used in our work as part of a probing technique where we use our developed method to go deep inside the limit cycle zone of the parameter space of a non-linear biochemical oscillator and calculate the limit cycle boundary using perturbative renormalization group scheme obtaining the flow equation for the values of the parameters at that particular point of the pa-

parameter space. Next, we numerically plot the same limit cycle and obtain its boundary for the same value of parameters and tally the results obtained in both cases. *Renormalization group* is thus used as a probe and plays a passive role in establishing our work.

Chapter 3

Scanning the parameter space: A primitive trial

3.1 Introduction

In the present chapter, our preliminary attempt to develop a method to scan the parameter space of a 2-dimensional non-linear oscillator has been discussed in detail. The process of successfully applying perturbation theory in the case of 2-dimensional non-linear oscillators will also be discussed in detail. Lastly, it will be discussed how *renormalization group* can be applied to the problem to quantify the method put forward.

Poincare-Bendixson theorem is the key theoretical result in non-linear dynamics that proposes the conditions for the existence of *isolated* closed orbits in particular non-linear systems. The theory of the formation of limit cycles is an elaborately studied topic in non-linear dynamics. It illustrates the importance of parameter spaces in such non-linear systems. A study on how the parameter space can be scanned or examined to facilitate the study of system dynamics when we go deeper inside the limit cycle region is rare in the literature. Also, for non-Lienard systems of differential equations, the application of the perturbative renormalization group can be quite a challenge and is not quite straightforward, as in the case of Lienard systems.

3.2 The Procedure

To address the issues discussed in the introduction, we have chosen the Sel'kov model of Glycolysis, which serves as a beautiful and interesting example. The mathematical model of the Glycolytic biochemical process, first introduced by Sel'kov [48] in terms of the concentrations of two reagents of the reaction pathway, one is adenosine diphosphate, and another is fructose-6-phosphate is given by :

$$\dot{x} = -x + ay + x^2y \quad (3.1)$$

$$\dot{y} = b - ay - x^2y \quad (3.2)$$

where 'x' and 'y' represent the concentrations of adenosine diphosphate and fructose-6-phosphate, respectively and $a > 0$ and $b > 0$ are two adjustable parameters. The linear stability analysis of the above system starts by finding the fixed points of the system, which are obtained by putting $\dot{x} = 0$ and $\dot{y} = 0$ simultaneously and solving for x and y . It is easily found that the fixed points of the Sel'kov model of glycolysis are $x^* = b$ and $y^* = \frac{b}{a + b^2}$. The Jacobian of the system equations(3.1) and (3.2) is

$$J = \begin{bmatrix} \frac{\partial f}{\partial x} & \frac{\partial f}{\partial y} \\ \frac{\partial g}{\partial x} & \frac{\partial g}{\partial y} \end{bmatrix}_{(x^*, y^*)} = \begin{bmatrix} (-1 + \frac{2b^2}{a + b^2}) & (a + b^2) \\ (\frac{-2b^2}{a + b^2}) & -(a + b^2) \end{bmatrix} \quad (3.3)$$

which will be playing an important role in our theory but let us first see how perturbation theory can be employed in case of non-Lienard systems.

We know from experience that in case of Lienard systems (Duffing oscillator or van der Pol oscillator) the general system can

be written in the following form

$$\begin{aligned}\dot{x} &= y \\ \dot{y} &= -\omega^2 x - \varepsilon f(x, y)\end{aligned}\quad (3.4)$$

where ω is the natural frequency and $f(x, y)$ is a nonlinear polynomial function in ‘x’ and ‘y’. It may be emphasized here that the effect of the non-linearity $f(x, y)$ is a perturbative modification to the base oscillation, which is a simple harmonic oscillation with the natural frequency ω . Thus perturbation theory, up to some order, leads us to flow equations in amplitude and phase whose fixed points tell us where the system will settle as per the recipe of *renormalization group*. It is well known theoretically that if for a general non-linear oscillatory system equation(3.4) (with amplitude A and phase θ), the dependent variable ‘x’ is perturbatively expanded as

$$x = x_0 + \varepsilon x_1 + \varepsilon^2 x_2 + \dots \quad (3.5)$$

then at the n^{th} order of perturbation, the resonant(or secular) terms appear as

$$\ddot{x}_n + \omega^2 x_n = f(A, \theta) \sin(\omega t + \theta) + g(A, \theta) \cos(\omega t + \theta) \quad (3.6)$$

+ non secular terms.

then the amplitude and phase flow equations at the n^{th} order in perturbation are obtained from renormalization group quite easily as:

$$\frac{dA}{dt} = -\varepsilon^n \cdot \frac{1}{2\omega} \cdot f(A, \theta) + \text{lower order corrections} \quad (3.7)$$

$$\frac{d\theta}{dt} = -\varepsilon^n \cdot \frac{1}{2A\omega} \cdot g(A, \theta) + \text{lower order corrections} \quad (3.8)$$

To implement the perturbative renormalization group to the problem of the Sel’kov model of glycolysis, the first thing to note is that there is no perturbation parameter in the problem to start with. Since we intend to apply the perturbative renormalization group

to our problem, we have to recast the Sel'kov model described by equations(3.1) & (3.2) in a suitable way. The first step to this is shifting the origin of the coordinates from $(0,0)$ to the fixed point (x^*, y^*) where $x^* = b$ and $y^* = \frac{b}{a+b^2}$. We achieve this with the help of a linear transformation by writing

$$x = X + x^* \quad (3.9)$$

$$y = Y + y^* \quad (3.10)$$

where the original system equations (3.1) and (3.2) take the following form :

$$\dot{X} = \left(\frac{b^2 - a}{b^2 + a} \right) X + (a + b^2)Y + \left(\frac{b}{a + b^2} \right) X^2 + 2bXY + X^2Y \quad (3.11)$$

$$\dot{Y} = \left(\frac{-2b^2}{a + b^2} \right) X - (a + b^2)Y - \left(\frac{b}{a + b^2} \right) X^2 - 2bXY - X^2Y \quad (3.12)$$

Linear stability analysis performed on the transformed system given by equations(3.11) and (3.12) portray that the trace of the stability matrix will vanish if the following equality is satisfied :

$$(b^2 - a) = (b^2 + a)^2 \quad (3.13)$$

Equation(3.13) when solved for 'a' gives the following equation of a curve on the parameter space of the Glycolytic system :

$$a = \frac{1}{2} \left[\sqrt{1 + 8b^2} - (1 + 2b^2) \right] \quad (3.14)$$

This curve demarcates two different zones on the parameter space of the original system, as in Figure 3.1. On one side of it, the origin is a *stable fixed point*, and on the other, the origin is an *unstable*

fixed point. On the curve, the origin is expected to behave like a *centre*. We shall concentrate on the region where the origin is unstable since this is the region where the origin turns unstable, resulting in repelling trajectories away from it and towards some fixed orbit or a so-called *limit cycle*. Hence the region where the origin becomes unstable will henceforth be referred to as the ‘*limit cycle*’ region.

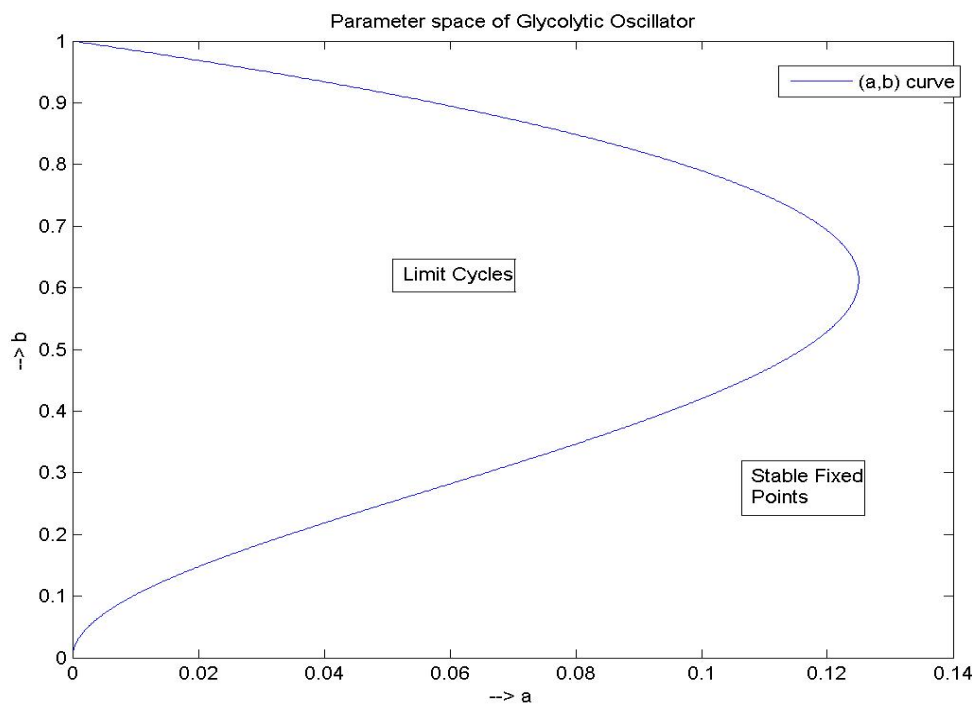


Figure 3.1: Parameter space of Glycolytic oscillator

The existence of the limit cycle will, however, continue to be predicted by the Poincare-Bendixson theorem, but the location and size of the cycle cannot be quantified by this theorem. This is where perturbation theory is required to arrive at the amplitude flow equation whose fixed point can supposedly help us locate the limit cycle. But before we see how perturbation theory can be implemented for the Glycolytic oscillator, we need to specify the values of the parameters controlling the dynamics of the oscillator. For studying characteristics of limit cycles and other important prop-

erties, we may need to select parameter values from all over the 'limit cycle' region of the parameter space. So we must figure out a way to enter the limit cycle zone of the parameter space, which is achieved in the following way:

Since the right end extremum of the parameter space curve occurs at the points $a = \frac{1}{8}$ and $b = \sqrt{\frac{3}{8}}$, we introduce an adjustable parameter ' δ ' and choose a point inside the 'limit cycle' region of the parameter space as $a = \frac{1}{8} - \delta$ and $b = \sqrt{\frac{3}{8}}$. Then substituting the parameters ' a ' and ' b ' in the original equation this way, we can scan the parameter space by simply choosing the value of the parameter ' δ '. For $\delta > 0$, we are inside the limit cycle region, and for $\delta < 0$, we are in the stable fixed point region. The magnitude of the parameter ' δ ' and its sign together define our position on the parameter space. Its magnitude however is a measure of how far we go on either side of the bifurcation curve given by equation (3.14). The value of the parameter ' b ' is kept constant as per choice, which hints at moving along a straight line ' $b = constant$ ' in the parameter space. The method, however, has some limitations, as we shall see, but for the time being, let us now turn our attention towards implementing the perturbative renormalization group in the case of Non-Lienard systems.

Inserting ' $a = \frac{1}{8} - \delta$ ' and ' $b = \sqrt{\frac{3}{8}}$ ' in the system equations (3.11) and (3.12) we obtain the following pair of equations by treating ' δ ' as small and hence retaining terms only linear in ' δ ' :

$$\dot{X} = \frac{1}{2}X + \frac{1}{2}Y + 3\delta X - \delta y + \left(\sqrt{\frac{3}{2}} + \sqrt{6\delta}\right)X^2 + \sqrt{\frac{3}{2}}XY + X^2Y \quad (3.15)$$

$$\dot{Y} = -\frac{3}{2}X - \frac{1}{2}Y - 3\delta X + \delta Y - \left(\sqrt{\frac{3}{2}} + \sqrt{6}\delta\right)X^2 - \sqrt{\frac{3}{2}}XY - X^2Y \quad (3.16)$$

These equations are arrived at by choosing ‘ δ ’ as a small adjustable parameter but one should not assume that ‘ δ ’ is the perturbation parameter of the problem. We therefore expand the dependent variables ‘ X ’ and ‘ Y ’ in the system equations in terms of a perturbation parameter ‘ λ ’ as

$$X = X_0 + \lambda X_1 + \lambda^2 X_2 + \dots \quad (3.17)$$

$$Y = Y_0 + \lambda Y_1 + \lambda^2 Y_2 + \dots \quad (3.18)$$

But there is no ‘ λ ’ in the RHS of equations (3.15) and (3.16). Here we slightly distort the problem and deliberately insert the perturbation parameter ‘ λ ’ in the two equations such that they are written as

$$\dot{X} = \frac{1}{2}X + \frac{1}{2}Y + \lambda \left[3\delta X - \delta Y + \left(\sqrt{\frac{3}{2}} + \sqrt{6}\delta\right)X^2 + \sqrt{\frac{3}{2}}XY + X^2Y \right] \quad (3.19)$$

$$\dot{Y} = -\frac{3}{2}X - \frac{1}{2}Y - \lambda \left[3\delta X - \delta Y + \left(\sqrt{\frac{3}{2}} + \sqrt{6}\delta\right)X^2 + \sqrt{\frac{3}{2}}XY + X^2Y \right] \quad (3.20)$$

The equations (3.19) and (3.20) are more conducive for the application of perturbative analysis. This is so because, at the zeroth order, the trace of the stability matrix evaluated at the origin is zero. Hence in this order, both ‘ X ’ and ‘ Y ’ oscillate simple harmonically with different phases. The effect of the perturbation is then to correct this zeroth-order result and drive the system to settle onto some isolated closed orbit or *limit cycle*. The artificial insertion of

the perturbation parameter does not cost us much in terms of accuracy, as at the end, one will be putting ‘ $\lambda = 1$ ’.

Now we have two first-order coupled differential equations from which we have to construct second-order differential equations in either ‘X’ or ‘Y’. Let us first differentiate equation(3.19) once with respect to time which gives

$$\begin{aligned} \ddot{X} = \frac{1}{2}\dot{X} + \frac{1}{2}\dot{Y} + \lambda \left[3\delta\dot{X} - \delta\dot{Y} + \left(\sqrt{\frac{3}{2}} + \sqrt{6}\delta \right) 2X\dot{X} \right. \\ \left. + \sqrt{\frac{3}{2}}\dot{X}Y + \sqrt{\frac{3}{2}}X\dot{Y} + 2X\dot{X}Y + X^2\dot{Y} \right] \end{aligned} \quad (3.21)$$

At the zeroth order equation (3.21) will look like :

$$\ddot{X}_0 = \frac{1}{2}\dot{X}_0 + \frac{1}{2}\dot{Y}_0$$

Putting detailed expressions of \dot{X}_0 and \dot{Y}_0 from equations(3.19) and (3.20) in the above equation one can get the following zeroth order uncoupled equation for X_0 as

$$\ddot{X}_0 + \frac{1}{2}X_0 = 0 \implies X_0 = A \cos \left(\frac{t}{\sqrt{2}} + \theta \right) = A \cos \alpha \quad (3.22)$$

The solution for Y_0 is obtained by feeding the solution for X_0 back in the equation (3.19) to get :

$$Y_0 = 2\dot{X}_0 - X_0 \implies Y_0 = \sqrt{3}A \cos(\alpha + \phi) \quad (3.23)$$

The phase difference ϕ is given together by the expressions $\sin \phi = \sqrt{\frac{2}{3}}$ and $\cos \phi = -\sqrt{\frac{1}{3}}$. Thus having the solutions upto the zeroth order sorted out and given by equations (3.22) and (3.23) let us now move on to the first order. At the first order of perturbation in X the

equation (3.21) looks like :

$$\begin{aligned} \ddot{X}_1 + \frac{1}{2}X_1 = 3\delta\dot{X}_0 - \delta\dot{Y}_0 + \sqrt{6}(1 + 2\delta)X_0\dot{X}_0 + \sqrt{\frac{3}{2}}\dot{X}_0Y_0 \\ + \sqrt{\frac{3}{2}}X_0\dot{Y}_0 + 2X_0\dot{X}_0Y_0 + X_0^2\dot{Y}_0 \quad (3.24) \end{aligned}$$

The R.H.S of the above equation when expanded using the solutions for X_0 and Y_0 will give secular sin and cos terms of the form $\sin\left(\frac{t}{\sqrt{2}} + \theta\right)$ and $\cos\left(\frac{t}{\sqrt{2}} + \theta\right)$ along with non-secular terms. The secular terms are responsible for producing divergent solutions and must be scanned quite diligently so that at this stage *renormalization group* can be invoked to absorb the divergences according to prescriptions laid down in the second chapter of this volume. Quite naturally, one should get flow equations in amplitude and frequency, which go on to correct the amplitude and frequency in the next order of perturbation, whereas at the same time, one may be able to predict the limit cycle boundary on the X-axis by finding the fixed point of the amplitude flow equation. To obtain the flow equations in amplitude and frequency by invoking *renormalization group* could be quite challenging for a lengthy equation of type (3.24). Since the main aim is just to obtain the flow equations, this could be directly written by merely inspecting the RHS of the equation (3.24). At this point, we divert from our discussion to recollect the solutions of two simple differential equations, which will be of immense help.

The RHS of the said equation when expanded will give terms of the following four types : $C_1 \sin(\omega t + \theta)$, $C_2 \cos(\omega t + \theta)$, $C_3 \sin l(\omega t + \theta)$ and $C_4 \cos k(\omega t + \theta)$. Where C_1, C_2, C_3 & C_4 are just the constant coefficients. Let us see how the solution to a nonhomogeneous differential equation involving the terms look

like. The solution to the following differential equation

$$\ddot{y} + \omega^2 y = P \cos K(\omega t + \theta) + Q \sin L(\omega t + \theta) \quad (3.25)$$

1. When $K = L = 1$ is given by

$$y(t) = \frac{P}{4\omega^2} \cos(\omega t + \theta) + \frac{Q}{4\omega^2} \sin(\omega t + \theta) + \frac{t}{2\omega} \left[P \sin(\omega t + \theta) - Q \cos(\omega t + \theta) \right] \quad (3.26)$$

2. When $K \neq L \neq 1$ is given by

$$y(t) = \frac{P}{\omega^2(1 - K^2)} \cos K(\omega t + \theta) + \frac{Q}{\omega^2(1 - L^2)} \sin L(\omega t + \theta) \quad (3.27)$$

Thus it is evident from the solutions of equation (3.25) above that terms containing secular sine and cosine give rise to divergences of the form $D_1.t.\cos(\omega t + \theta)$ and $D_2.t.\sin(\omega t + \theta)$, where D_1 & D_2 are the coefficients of the *divergent terms*. The divergences have to be contained by invoking the method of *renormalization group* discussed and can be a lengthy process. The flow equations however can be written down by just having a close look at the divergent terms. The process is simple [49]. If the divergent term is of the form $D_1.t.\cos(\omega t + \theta)$, then this term contributes to the amplitude flow equation as $\frac{dA}{d\tau} = D_1$. On the other hand if the divergent term is of the form $D_2.t.\sin(\omega t + \theta)$ then this term will contribute to the phase flow equation as $\frac{d\theta}{d\tau} = -\frac{D_2}{A}$.

Returning to the context of writing down a solution to equation (3.24), one can write it down straight away by comparing the RHS of equation(3.24) with the already laid down solutions of the equation(3.25) given at SL No. 1 & 2 above. Then it becomes quite easy to find the coefficients D_1 and D_2 of the divergent terms by mere inspection. After figuring out D_1 and D_2 , writing down the

amplitude and phase flow equations are quite straightforward as per the recipe given in the previous paragraph.

Elaborating the RHS of equation (3.24), we find that the third ($X_0\dot{X}_0$), fourth (\dot{X}_0Y_0) and fifth ($X_0\dot{Y}_0$) terms do not produce any secular sine divergence. They either give constant or terms containing $\sin 2\alpha$ or $\cos 2\alpha$ terms, none of which contribute to the amplitude equation we intend to find. However, the first two and last two terms on the RHS of Eq. (3.24) do give secular $\sin \alpha$. Putting together all the coefficients of secular $\sin \alpha$ on the right-hand side of Eq. (3.24), we name it A_1 . As per prescriptions, the amplitude flow equation is given by :

$$\frac{dA}{dt} = \lambda \frac{A}{\sqrt{2}} \left[\frac{4}{\sqrt{2}} \delta - \frac{3}{4\sqrt{2}} A^2 \right] \quad (3.28)$$

Hence the value of the amplitude at the limit cycle is given by

$$\frac{dA}{dt} = 0 \quad (3.29)$$

$$A = \sqrt{\frac{16}{3} \delta} \quad (3.30)$$

the other root being at $A = 0$ (i.e., the origin). The value of the amplitude thus obtained in Eq.(3.30) is the distance from the origin to the point of intersection of the limit cycle with the X-axis, which we have predicted perturbatively. The same can be done along Y-axis also if we had applied perturbative renormalization group to the Y- equation, i.e., Eq. (3.20) or by an orthogonal transformation which would be discussed briefly in the Appendix.

Thus we have developed a crude method to scan the parameter space of a non-Lienard non-linear biochemical oscillator, and we have successfully applied the perturbative renormalization group to this class of non-Lienard oscillatory systems. Now by

varying the value of the parameter ‘ δ ,’ we shall try to penetrate deep into the limit cycle zone of the parameter space of the non-Lienard oscillator, which in our case is the Sel’kov model of Glycolysis and predict the limit cycle boundary or amplitude of limit cycle on the X-axis for every value of parameters a , b & δ using the result obtained from the application of *renormalization group* and given by Eq. (3.30). If *renormalization group* is able to predict the amplitude quite accurately, we shall assume that the method to scan the parameter space is working good. In this context renormalization group is used just as a probe to prove the accuracy of the method.

If we assume the value of ‘ δ ’ as $\delta = 0.002$, then Eq. (3.30) predicts that the limit cycle cuts the X-axis at the point $A = 0.103$ up to three places of decimals. If the same curve is plotted using any mathematical software with the value of the parameters ‘ $a = \frac{1}{8} - \delta$ ’ and ‘ $b = \sqrt{\frac{3}{8}}$ ’ it is found to be $A = 0.088$, as in the diagram below.

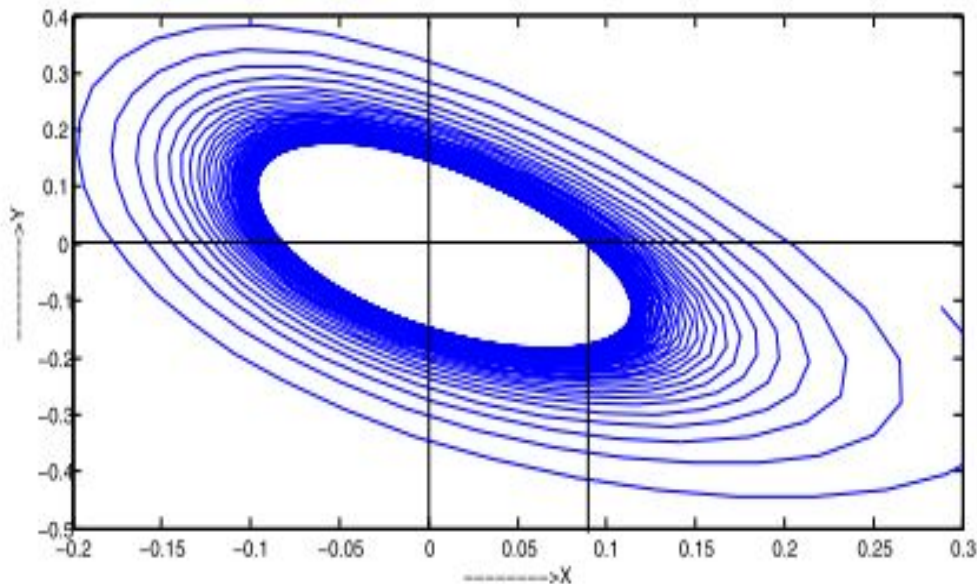


Figure 3.2: Limit cycle for $\delta = 0.002$ and intercept on X-axis is $A=0.088$

Up to the first order in perturbation, this is close enough but is not accurate enough. The first order results slightly overshoot the

actual value obtained in the numerical plot at the first order in perturbation. To predict the results more accurately, we shall move on to the second-order in perturbation.

Before we move on to the second order the first order solution in X_1 has to be elaborately calculated. Eq. (3.24) can easily be elaborated and rearranged in the form

$$\begin{aligned} \ddot{X}_1 + \frac{1}{2}X_1 = & A_{1x} \sin \alpha + B_{1x} \cos \alpha + A_{2x} \sin 2\alpha \\ & + B_{2x} \cos 2\alpha + A_{3x} \sin 3\alpha + B_{3x} \cos 3\alpha \quad (3.31) \end{aligned}$$

where the coefficients are given as:

$$\begin{aligned} A_{1x} &= -2\sqrt{2}\delta A + \frac{3A^3}{4\sqrt{2}} \\ B_{1x} &= \delta A - \frac{A^3}{4} \\ A_{2x} &= -\sqrt{3}\delta A^2 \\ B_{2x} &= -\sqrt{\frac{3}{2}}A^2 \\ A_{3x} &= \frac{3A^3}{4\sqrt{2}} \\ B_{3x} &= -\frac{3A^3}{4} \end{aligned}$$

Eq.(3.31) looks just like equation (3.25) whose solution on integration and applying renormalization group is obtained in the following form

$$\begin{aligned} X_1 = & \frac{A_{1x}}{2} \sin \alpha + \frac{B_{1x}}{2} \cos \alpha - \frac{2A_{2x}}{3} \sin 2\alpha - \frac{2B_{2x}}{3} \cos 2\alpha \\ & - \frac{A_{3x}}{4} \sin 3\alpha - \frac{B_{3x}}{4} \cos 3\alpha \quad (3.32) \end{aligned}$$

For second order calculations the explicit solutions of X_0 X_1 , Y_0 and Y_1 are required. Now X_0 X_1 & Y_0 are already defined by Eqs.

(3.22), (3.23) and (3.32). The first order equation for the variable Y is obtained similarly by differentiating Eq. (3.20) once with respect to time and is given by

$$\begin{aligned} \ddot{Y}_1 + \frac{1}{2}Y_1 = & -3\delta X_0 + \delta Y_0 - 3\delta\dot{X}_0 + \delta\dot{Y}_0 + \sqrt{\frac{3}{2}}\left(X_0^2 + X_0Y_0 + \right. \\ & \left. \dot{X}_0Y_0 + X_0\dot{Y}_0\right) - \sqrt{6}(1+2\delta)X_0\dot{X}_0 - X_0^2Y_0 \\ & - X_0^2\dot{Y}_0 - 2X_0\dot{X}_0Y_0 \quad (3.33) \end{aligned}$$

The RHS of Eq. (3.33) above when expanded and rearranged takes the following form

$$\begin{aligned} \ddot{Y}_1 + \frac{1}{2}Y_1 = & A_{1y} \cos \alpha + B_{1y} \sin \alpha + A_{2y} \cos 2\alpha \\ & + B_{2y} \sin 2\alpha + A_{3y} \cos 3\alpha + B_{3y} \sin 3\alpha + C_y \quad (3.34) \end{aligned}$$

with the coefficients defined as

$$\begin{aligned} A_{1y} &= -4A\delta + A^3 \\ B_{1y} &= \sqrt{2}\delta A - \frac{A^3}{4\sqrt{2}} \\ A_{2y} &= \sqrt{\frac{3}{2}}\left(\frac{1}{2} - \delta\right)A^2 \\ B_{2y} &= \frac{\sqrt{3}}{2}(1+2\delta)A^2 \\ A_{3y} &= A^3 \\ B_{3y} &= -\frac{A^3}{4\sqrt{2}} \\ C_y &= -\sqrt{\frac{3}{2}}\delta A^2 \end{aligned}$$

Equation(3.34) when integrated yields the solution Y_1 given by

$$\begin{aligned} Y_1 = & \frac{A_{1y}}{2} \cos \alpha + \frac{B_{1y}}{2} \sin \alpha - \frac{2A_{2y}}{3} \cos 2\alpha - \frac{B_{2y}}{3} \sin 2\alpha \\ & - \frac{A_{3y}}{4} \cos 3\alpha - \frac{B_{3y}}{4} \sin 3\alpha + 2C_y \quad (3.35) \end{aligned}$$

Second Order Calculation:

The second order equation in X obtained by differentiating Eq.(3.19) once with respect to X or by collecting the terms with coefficient λ^2 in Eq. (3.21) is given by

$$\begin{aligned} \ddot{X}_2 + \frac{1}{2}X_2 = & 3\delta\dot{X}_1 - \delta\dot{Y}_1 + \sqrt{6}(1 + 2\delta)(X_0\dot{X}_1 + \dot{X}_0X_1) \\ & + \sqrt{\frac{3}{2}}(\dot{X}_0Y_1 + \dot{X}_1Y_0 + X_0\dot{Y}_1 + X_1\dot{Y}_0) + 2\dot{X}_0X_1Y_0 \\ & + 2X_0\dot{X}_1Y_0 + 2X_0\dot{X}_0Y_1 + 2X_0X_1\dot{Y}_0 + X_0^2Y_1 \quad (3.36) \end{aligned}$$

To obtain the amplitude flow equation according to the prescription laid down by *renormalization group* the coefficient of secular $\sin \alpha$ term in the right-hand side of the above equation needs to be figured out. The calculation at this order of perturbation is more challenging than the previous however is not impossible if done carefully. We shall not dig into the calculational details at this stage and straight away enumerate the result; the total coefficient of the secular $\sin \alpha$ arising from the terms in the RHS of Eq.(3.36) is given as

$$\begin{aligned} A_2 = & \frac{A_{1x}}{2} \left(1 - \sqrt{\frac{3}{2}} \right) A^2 + A_{1y} \left(\frac{\delta}{2\sqrt{2}} - \frac{3}{8\sqrt{2}} A^2 \right) \\ & + B_{1x} \left(-\frac{3\delta}{2\sqrt{2}} + \frac{3}{4\sqrt{2}} A^2 \right) + B_{2x} \left(\frac{1}{2\sqrt{3}} - \frac{\sqrt{2}}{3} + \frac{2\delta}{\sqrt{3}} \right) A \\ & + \left(\frac{A_{2y}}{2\sqrt{3}} - \sqrt{2}C_y \right) A - \left(\frac{A_{3y}}{16\sqrt{2}} + \frac{B_{3x}}{8\sqrt{2}} \right) A^2 \quad (3.37) \end{aligned}$$

the above form of A_2 when simplified using the explicit expressions

of the constants takes the following form :

$$A_2 = -\frac{7\delta^2}{2\sqrt{2}}A + \left[\left(\frac{21}{8\sqrt{2}} + 2\sqrt{3} - 2\sqrt{2} \right) \delta + \frac{1}{\sqrt{3}} - \frac{1}{4\sqrt{2}} \right] A^3 - \left(\frac{3\sqrt{3}}{16} + \frac{5}{32\sqrt{2}} \right) A^5 \quad (3.38)$$

Combining this with the first order result in Eq. (3.28) and using the prescription of writing the flow equations we finally arrive at the amplitude flow equation to the second order in perturbation with $\omega = \frac{1}{\sqrt{2}}$ as

$$\begin{aligned} \frac{dA}{dt} &= \left(-\frac{\sqrt{2}}{2} \right) [\lambda A_1 + \lambda^2 A_2] \\ &= A \left(2\lambda \delta + \frac{7}{4} \lambda^2 \delta^2 \right) + A^5 \lambda^2 \left(\frac{3\sqrt{3}}{16\sqrt{2}} + \frac{5}{64} \right) \\ &\quad - A^3 \left[\frac{3}{8} \lambda + \lambda^2 \left(\frac{1}{\sqrt{6}} - \frac{1}{8} + \left(\frac{21}{16} + \sqrt{6} - 2 \right) \delta \right) \right] \end{aligned} \quad (3.39)$$

Now, recalling that the parameter ‘ δ ’ was assumed to be small while arriving at the equations (3.15) and (3.16), only terms linear in delta are retained and terms with higher powers in λ are ignored in the above equation. The final amplitude flow equation in second order is thus

$$\frac{dA}{dt} \simeq A [0.229\lambda A^4 - \{0.375 + \lambda(1.762\delta + 0.283)\}A^2 + 2\delta] \quad (3.40)$$

Thus, at last, we have arrived at the second-order amplitude flow equation applying the perturbative renormalization group to the Sel’kov model of the Glycolytic oscillator. The result at Eq. (3.40) would be tested for different values of parameters ‘a’ and ‘b’ of the system obtained by varying the value of parameter ‘ δ ’, which is a measure of how much deep we go inside the limit cycle region of the parameter space, and the result would be compared with the mathematical

plot of the system equations using the same value of parameters ‘a’ and ‘b’.

3.3 Results

The preceding section has introduced a simple method to scan the parameter space of a two dimensional non-linear non-Lienard biochemical oscillator and the technique to apply perturbation theory in the case of two-dimensional non-linear non-Lienard oscillators. The perturbative renormalization group has been applied to such oscillators satisfactorily, which resulted in amplitude and phase flow equations in the case of such oscillators at different orders of perturbation [50].

Results up to the second order in perturbation show clearly that in the case of the Sel’kov model of Glycolysis, only amplitude gets corrected in the first and second-order of perturbation. Higher orders have been kept beyond the scope of this volume to keep matters simple. The amplitude flow equation in the second order is given by Eq. (3.40). The fixed points of the equation, obtained by putting $\frac{dA}{dt} = 0$ i.e.,

$$A \left[0.229\lambda A^4 - \{0.375 + \lambda(1.762\delta + 0.283)\}A^2 + 2\delta \right] = 0 \quad (3.41)$$

gives the location of the limit cycle described as the distance from the origin to the point where the X-axis intersects the limit cycle. From Eq. (3.41), it is clear that the origin ($A = 0$) remains an unstable fixed point of the system to the second order. There is also a term quadratic in A^2 in Eq.(3.41), whose smaller root brings us the required correction in the value of A over the value obtained in the first order from Eq. (3.30).

While evaluating the roots of the quadratic, ‘ λ ’ must be put equal to 1 to bring back the original pair of equations given by Eq. (3.19) and (3.20). It may be recalled that λ was introduced to cast the system equations in a suitable manner so as to make them conducive to the application of perturbation theory.

The parameter ‘ δ ’, on the other hand, was introduced as a part of our method to facilitate scanning of the parameter space. In our calculations, as we reiterate here, only terms linear in ‘ δ ’ were retained in the transformed system equations (3.15) and (3.16) from the very beginning. Now having calculated the second-order amplitude flow equation, our task will be to verify how closely the results offered by the perturbative renormalization group in the form of positions of the boundaries of the limit cycles for different values of the system parameters ‘ a ’ and ‘ b ’ (obtained by varying the parameter ‘ δ ’), can predict the actual limit cycle boundaries of the system when plotted numerically for the same values of the system parameters. If the two results are close, we shall go on to say that our method to scan the parameter space is working good. The values of the parameter ‘ δ ’, however, have to be chosen judiciously.

The focus will be on the value of the limit cycle boundary given by the value of ‘ A ’. When $\delta = 0.0015$, the numerical plotting gives us $A = 0.075$. The first order result predicted by Eq.(3.30) at $A = 0.089$, and the second-order correction given by Eq.(3.41) brings it down to $A = 0.068$, which is reasonably close to the actual value predicted by numerical methods. Figure 3.3 shows the actual position of the limit cycle boundary at $A = 0.075$.

With $\delta = 0.002$ the numerical pot gives $A = 0.088$. The first order predicts it at $A = 0.103$ while the second order corrects it and pulls it down to $A = 0.079$ which is again closer to the actual numerical value (Figure 3.4).

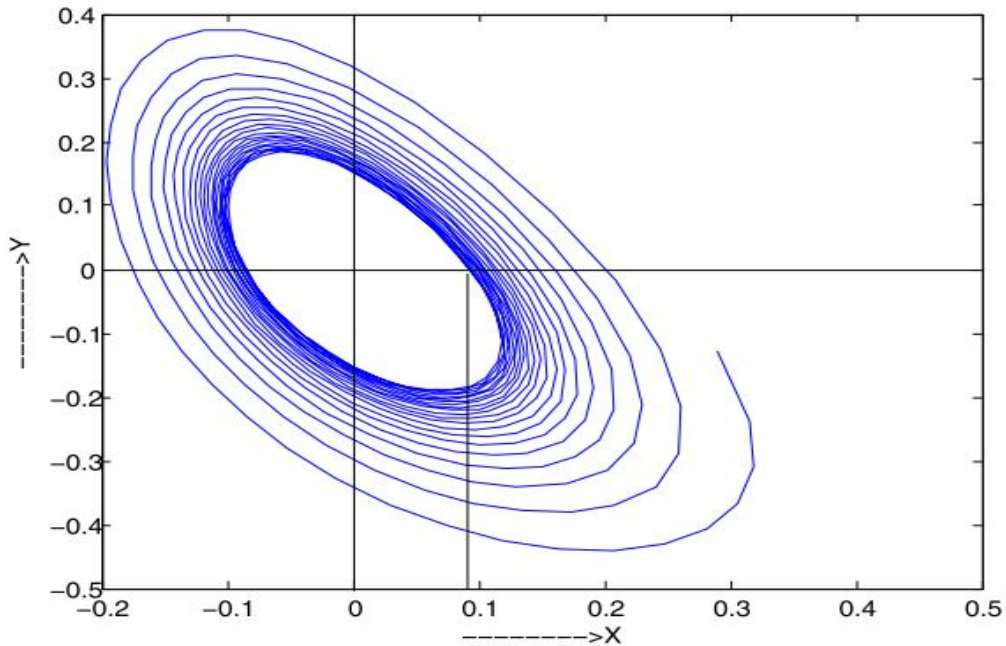


Figure 3.3: Limit cycle for $\delta = 0.0015$ and intercept on X-axis at $A = 0.075$

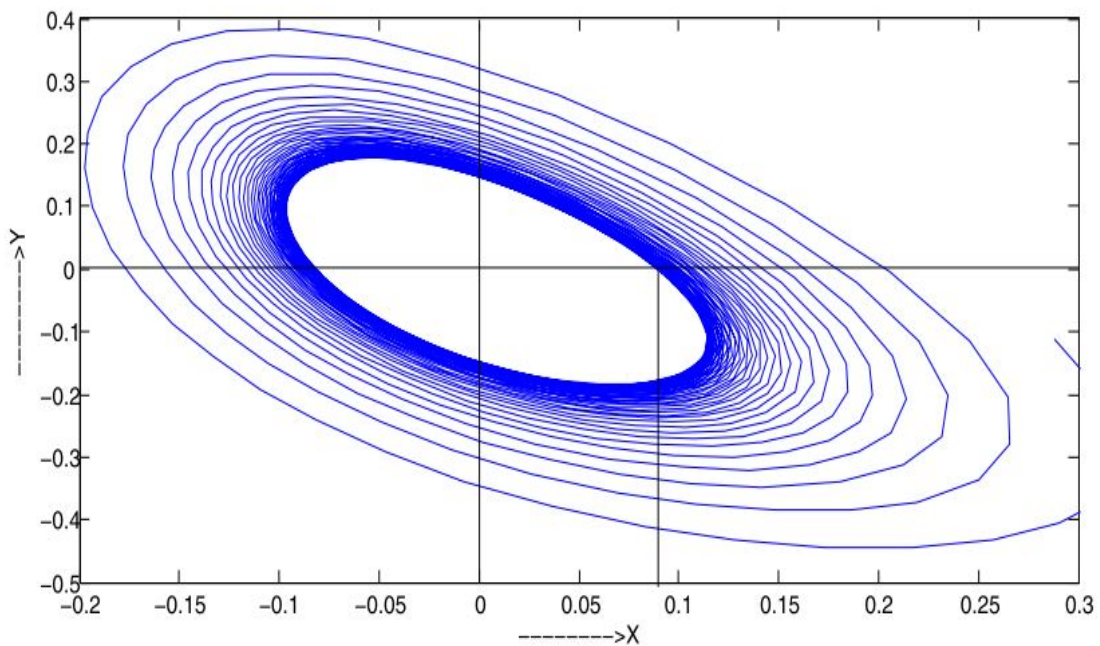


Figure 3.4: Limit cycle for $\delta = 0.002$ and intercept on X-axis at $A = 0.088$

For $\delta = 0.0025$ the numerical the position of the limit cycle as predicted by the numerical plot is at $A = 0.097$ and the first order and second order results predicted by perturbative renormalization group are $A = 0.115$ and $A = 0.086$ respectively. Figure 3.5 below is the numerical plot for the values of the system parameters for $\delta = 0.0025$.

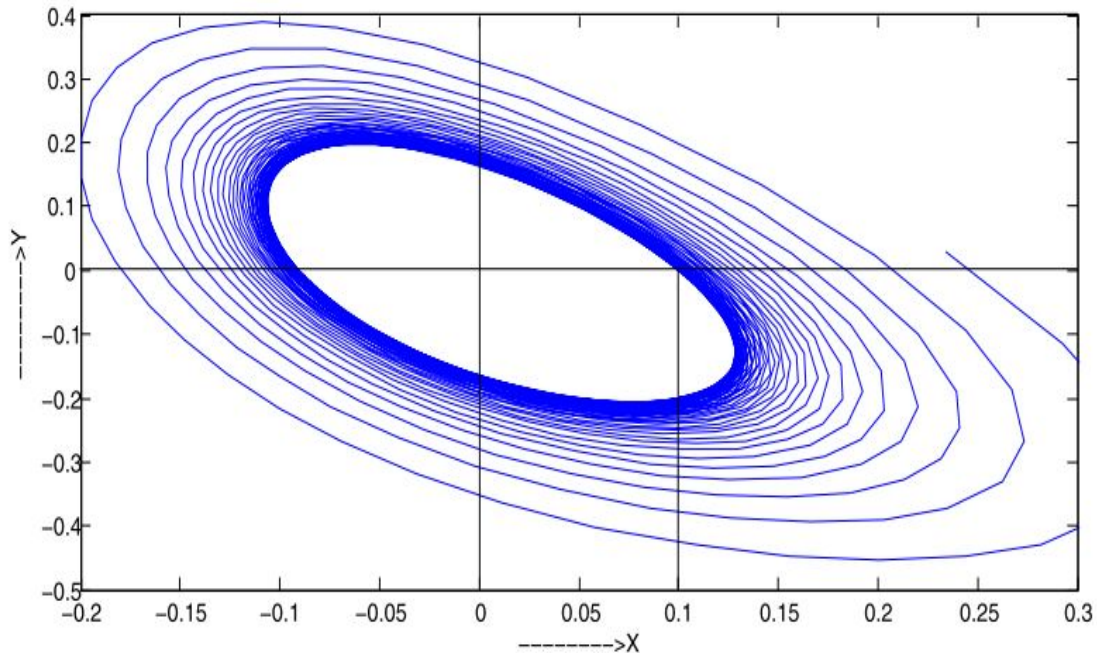


Figure 3.5: Limit cycle for $\delta = 0.0025$ and intercept on X-axis at $A = 0.097$

It is easily noticeable that for values of the parameter δ kept small enough up to 2% of the width of the limit cycle zone given by $a = \frac{1}{8}$ (Figure 3.1), the results predicted by perturbative calculations are close enough to the actual numerical results.

If we want to dig deeper inside the limit cycle zone of the parameter space by selecting a slightly higher value of the parameter δ , for example, say if we choose $\delta = 0.01$, the boundary of the limit cycle predicted by the numerical plot (Figure 3.6) and those predicted by first order and second order of perturbation are given by $A = 0.21$, $A = 0.23$ and $A = 0.17$ respectively are still reliably accurate.

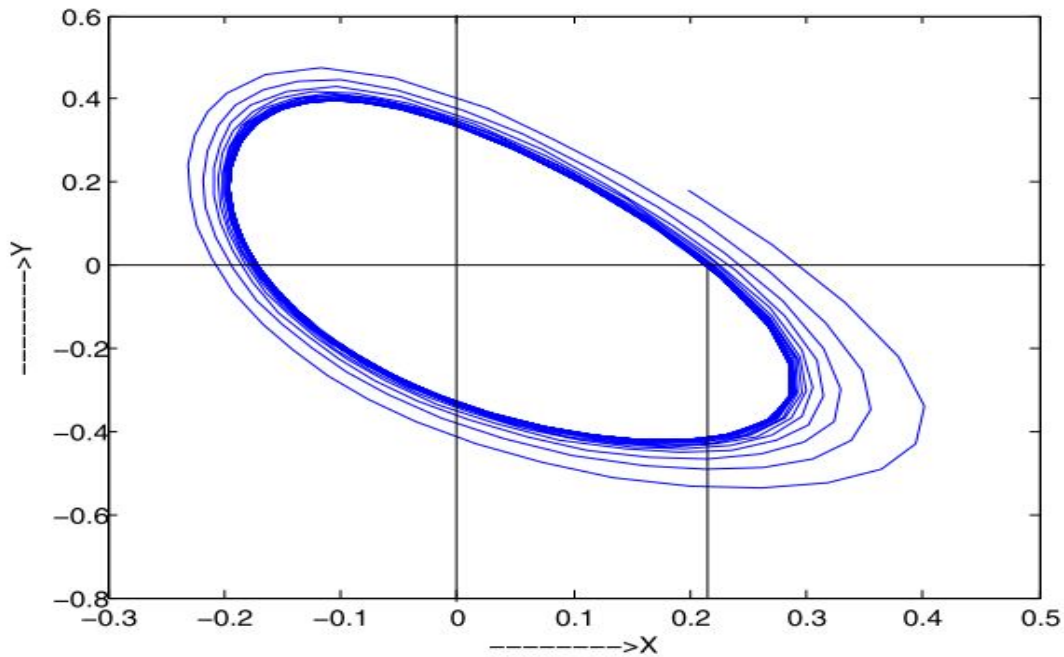


Figure 3.6: Limit cycle for $\delta = 0.0025$ and intercept on X-axis at $A = 0.097$

For still higher values of ' δ ' say for $\delta = 0.05$ the boundary of limit cycle predicted by numerical plot (Figure 3.7) and the first and second order of perturbative renormalization group are respectively given by $A = 0.665$, $A = 0.516$ and $A = 0.380$.

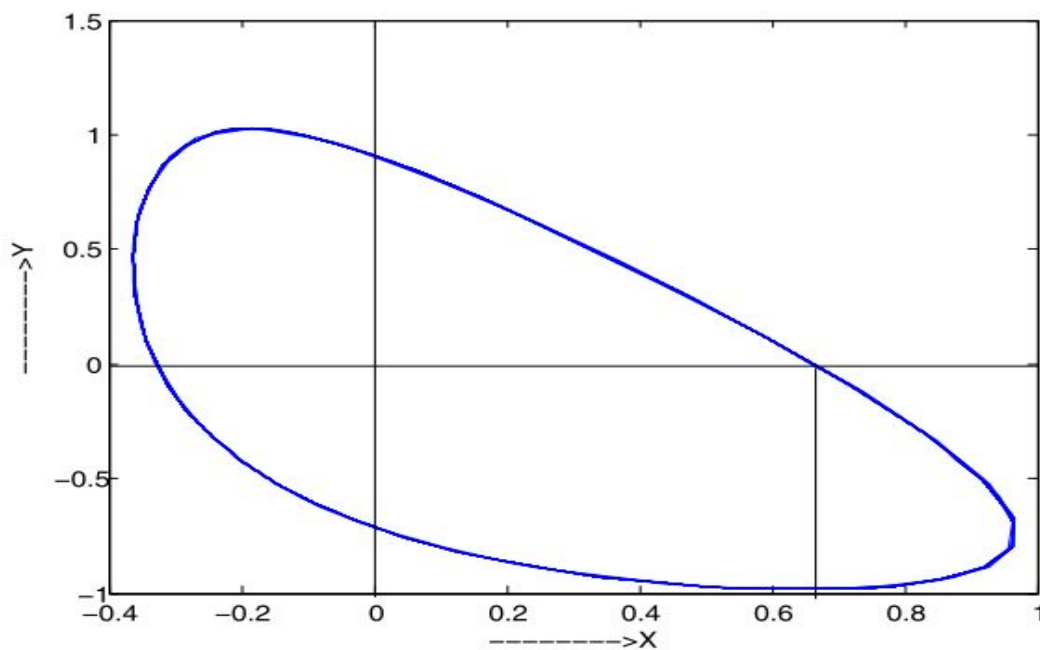


Figure 3.7: Limit cycle for $\delta = 0.05$ and intercept on X-axis at $A = 0.665$

This is because, in this case, the linearization in δ is done in the Eqs. (3.15) and (3.16) fail, and terms with higher powers of δ need to be included in the study.

To summarize the chapter, we have made an attempt to scan the parameter space of a non-Lienard non-linear biochemical oscillator, viz., the Sel'kov model of Glycolysis. This has been done by introducing an additional parameter ' δ ' in the system equations in such a way that it helps us go deeper inside the limit cycle zone of the parameter space. Our endeavour was to select system parameter values 'a' and 'b' inside the limit cycle zone by varying the externally introduced parameter ' δ ' and predict limit cycle boundaries for those selected parameter values by use of perturbative renormalization group and compare them with the numerical results. We have succeeded to some extent in scanning the parameter space and predicting limit cycle boundaries for values of selected system parameters inside the limit cycle region. However our method here required us to keep ' δ ' small, thus restricting our ability to scan the total parameter space or the total limit cycle region. This had to be done to keep the algebra simple as we know that ugliness and order of perturbations go hand in hand and if we had included higher powers of the parameter ' δ ' initially, the process of introducing perturbation theory in this case of a non-Lienard type oscillator would have turned quite a formidable task.

3.4 Appendix

In this short Appendix, we will explain the procedure to find the distance from the fixed point (i.e., the origin) to the point where the limit cycle cuts the Y-axis, as said on Page-39. Since we intend to introduce the procedure to the reader, we shall remain confined to the first order in perturbation only as calculations for the higher orders will be no different than what is done in the first order.

The idea is to rotate the coordinate axes by an angle $\beta = \frac{\pi}{2}$ so that the Eqs. (3.11) and (3.12) can be recast with ‘X’ replaced by ‘ $-Y$ ’ and ‘Y’ replaced by ‘ $+X$ ’ as

$$\dot{X} = -(a + b^2)X + \frac{2b^2}{a + b^2}Y - \frac{b}{a + b^2}Y^2 + 2bXY - XY^2 \quad (3.42)$$

$$\dot{Y} = -(a + b^2)X + \frac{b^2 - a}{a + b^2}Y - \frac{b}{a + b^2}Y^2 + 2bXY - XY^2 \quad (3.43)$$

Now putting the values $b = \sqrt{\frac{3}{8}}$ and $a = \frac{1}{8} - \delta$ and retaining terms upto an order linear in ‘ δ ’, the above two equations with the perturbation parameter ‘ λ ’ inserted take the following form ,

$$\dot{X} = -\frac{1}{2}X + \frac{3}{2}Y + \lambda \left[\delta X + 3\delta Y - \sqrt{\frac{3}{2}}(1 + 2\delta)Y^2 + \sqrt{\frac{3}{2}}XY - XY^2 \right] \quad (3.44)$$

$$\dot{Y} = -\frac{1}{2}X + \frac{1}{2}Y + \lambda \left[\delta X + 3\delta Y - \sqrt{\frac{3}{2}}(1 + 2\delta)Y^2 + \sqrt{\frac{3}{2}}XY - XY^2 \right] \quad (3.45)$$

Now looking at the various orders in perturbation we see that the zeroth order equation in variable ‘X’ is given by

$$\ddot{X}_0 + X_0 = 0 \quad (3.46)$$

The solution to the above equation can be taken as

$$X_0 = A \cos \alpha$$

with $\alpha = \frac{1}{\sqrt{2}}.t + \theta$ with $\omega = \frac{1}{\sqrt{2}}$.

Similarly the zeroth order equation for the variable 'Y' can be written down using equations (3.44) as

$$Y_0 = \frac{2}{3}\dot{X}_0 + \frac{1}{3}X_0 \quad (3.47)$$

which may be put in the explicit form by using the zeroth order result for the X variable as

$$Y_0 = \frac{A}{3} \cos \alpha - \frac{A\sqrt{2}}{3} \sin \alpha \quad (3.48)$$

Thus having obtained the zeroth order solutions for the two variables X and Y we now move forward with the first order. As before the first order equations can be written down by double differentiating the Eq.(3.44) and using Eq.(3.45) as

$$\begin{aligned} \ddot{X}_1 + \frac{1}{2}X_1 &= \delta X_0 + 3\delta Y_0 - \sqrt{\frac{3}{2}}(1 + 2\delta)Y_0^2 + \sqrt{\frac{3}{2}}X_0Y_0 - X_0Y_0^2 \\ &+ \delta\dot{X}_0 + 3\delta\dot{Y}_0 - \sqrt{6}(1 + 2\delta)Y_0\dot{Y}_0 + \sqrt{\frac{3}{2}}\dot{X}_0Y_0 \\ &+ \sqrt{\frac{3}{2}}X_0\dot{Y}_0 - \dot{X}_0Y_0^2 - 2X_0Y_0\dot{Y}_0 \quad (3.49) \end{aligned}$$

As before the right hand side of the above equation is expanded using the expressions of X_0 and Y_0 after which we expect to get a equation of the form

$$\ddot{X}_1 + \frac{1}{2}X_1 = P \cos \alpha + Q \sin \alpha + \text{non - secular terms} \quad (3.50)$$

Now it is well known that the coefficient of the $\sin \alpha$ term will alone contribute to the amplitude flow equation given by

$$\frac{dA}{dt} = -\frac{Q}{2\omega}$$

We do not go into more details in the calculation and directly write down the result here given by

$$\frac{dA}{dt} = -\frac{\sqrt{2}A}{2} \left[-\sqrt{2}\delta A - \sqrt{\frac{1}{2}}\delta A - \frac{1}{\sqrt{2}}\delta A + \frac{1}{9\sqrt{2}}A^3 + \frac{7}{36\sqrt{2}}A^3 - \frac{1}{18\sqrt{2}}A^3 \right]$$

which implies

$$\frac{dA}{dt} = \frac{A}{\sqrt{2}} \left(2\sqrt{2}\delta - \frac{1}{4\sqrt{2}}A^2 \right) \quad (3.51)$$

The boundary of the limit cycle or the distance between the origin from the point where the limit cycle intersects the Y-axis is obtained by putting

$$\frac{dA}{dt} = 0$$

which in turn gives

$$A = \sqrt{16\delta}$$

.

Turning back to our numerical plots, we see that this is again a good prediction, although slightly overestimated. Second-order corrections(not shown here for the Y direction) are expected to bring the results closer to the actual numerical value; however, we must calculate it for reasonably small values of δ . Therefore, by rotating the coordinate axes through an arbitrary angle β and effecting orthogonal transformation on Eqs (3.11) and (3.12), one can get good estimates of the size and shape of the limit cycle over the entire range of $0 \leq \beta \leq 2\pi$. This way, results in the Y-direction can also be easily calculated.

Chapter 4

Scanning the parameter space: A subtle approach

4.1 Introduction

In this chapter, a more general method to scan the parameter space of a non-linear non-Lienard biochemical oscillator is presented. Unlike the method discussed in the previous chapter, this requires no restrictions to be imposed on the value of the parameter ‘ δ ’, thus enabling one to scan the entire parameter space of the biochemical oscillator with ease. This facilitates the prediction of limit cycle boundaries for parameter values at points deep inside the limit cycle region of the parameter space. The process of application of perturbation theory for non-Lienard type non-linear oscillators, as introduced in the previous chapter, will be followed, and the use of perturbative renormalization group as a probe to verify the results will be retained.

The method starts with shifting the origin of the original system equations of Sel’kov model of Glycolysis given by Eqs. (3.1) and (3.2) with the common prescription of writing $X = x - x^*$ and $Y = y - y^*$ where $(x^*, y^*) = (b, \frac{b}{a + b^2})$ is the fixed point of the system in the phase space. The Jacobian of the system is computed

at the fixed point (x^*, y^*) as usual in Eq. (3.3) given by

$$J = \begin{bmatrix} \left(-1 + \frac{2b^2}{a+b^2}\right) & (a+b^2) \\ \left(\frac{-2b^2}{a+b^2}\right) & -(a+b^2) \end{bmatrix} \quad (4.1)$$

For the system to have a stable limit cycle, the fixed point (x^*, y^*) is required to lose its stability post a supercritical Hopf Bifurcation so that a trapping region is created around the fixed point and any trajectory starting inside this trapping region jumps to the nearby isolated closed orbit also called a limit cycle. The prescription for this to happen is already discussed as the conditions laid down by the Poincare Bendixson theorem in the previous chapter. However, the direct link between a fixed point losing its stability post a Hopf Bifurcation and the Jacobian of the corresponding nonlinear system is that the trace (τ) and the determinant (Δ) of the Jacobian should be greater than zero subject to the condition $\tau^2 - 4\Delta < 0$ as per discussions in chapter 1.

In this chapter, we shall make greater use of the Jacobian of the nonlinear system in introducing the external parameter ‘ δ ’ into the system equations so that there are no restrictions on the value of the parameter ‘ δ ’. We shall see how this works in detail and how the parameter δ needs to be introduced into the system equations so as to get the desired results.

4.2 The Method

The Sel’kov model of Glycolysis given by the Eqs.(3.1) and (3.2) are a set of non-Lienard type non-linear equations with its Jacobian given by Eq. (4.1) above evaluated at the fixed point of the system $(x^*, y^*) = (b, \frac{b}{a+b^2})$. As already known, the criteria for the

formation of limit cycle imposes upon the Jacobian the conditions

1. $Trace(\tau) > 0$
2. $Determinant(\Delta) > 0$
3. $\tau^2 - 4\Delta < 0$

The trace(τ) and the determinant(Δ) of the Jacobian for the Sel'kov model of Glycolysis are written in the explicit form as

$$\tau = \frac{2b^2}{a+b^2} - (1+a+b^2) \quad (4.2)$$

$$\Delta = a+b^2 \quad (4.3)$$

It is thus clear that the determinant (Δ) of the system is by default greater than zero since the system parameters 'a' and 'b' are greater than zero. However speculation may remain about the fate of the trace (τ) since it is a difference of two positive terms. The condition for the system to have a stable limit cycle (or an unstable fixed point) is thus

$$(1+a+b^2) < \frac{2b^2}{a+b^2} \quad (4.4)$$

The curve separating the two regions of the parameter space of the system i.e., the limit cycle region and the region where the fixed point is stable is clearly obtained by plotting the following equation:

$$\frac{2b^2}{a+b^2} = (1+a+b^2) \quad (4.5)$$

The curve defining the above equation can be found at Figure 3.1. Equation(4.5) when solved for the parameter 'a' takes the functional form

$$a = \frac{1}{2} \left[\sqrt{1+8b^2} - (1+2b^2) \right]$$

given by Eq. (3.14). It is imperative to note that on this curve the system shows centre like oscillations . If we have to scan the entire parameter space we need to introduce an external parameter ' δ ' in

Eq.(4.5) in such a way that any variation in the value of δ may take us inside or outside the limit cycle zone as and when we want so. We achieve this by writing

$$\frac{2b^2}{a+b^2} = (1+a+b^2) + \delta \quad (4.6)$$

By doing so, it is assured that for $\delta = 0$ we place ourselves on the curve separating the two regions of the parameter space. For $\delta > 0$ satisfying equality in Eq. (4.6) means that $(1+a+b^2) < \frac{2b^2}{a+b^2}$ and we are inside the limit cycle zone while for $\delta < 0$ we have $(1+a+b^2) > \frac{2b^2}{a+b^2}$ and we are outside the limit cycle zone and in the region of stable fixed points. This little improvisation dramatically changes the scenario as we shall see. In the light of our improvisation given by Eq.(4.6) the original transformed system equations obtained by shifting the origin from $(0,0)$ to $(x^*, y^*) = (b, \frac{b}{a+b^2})$ and given by Eqs. (3.11) and (3.12) takes a new form given by

$$\begin{aligned} \dot{X} = (a+b^2+\delta)X + (a+b^2)Y + \left(\frac{b}{a+b^2}\right)X^2 \\ + 2bXY + X^2Y \quad (4.7) \end{aligned}$$

$$\begin{aligned} \dot{Y} = \left(\frac{-2b^2}{a+b^2}\right)X - (a+b^2)Y - \left(\frac{b}{a+b^2}\right)X^2 \\ - 2bXY - X^2Y \quad (4.8) \end{aligned}$$

A new stability equation, parametric in ' δ ' is obtained from Eq.(4.6) which when solved for the original system parameter 'a' of the Glycolytic oscillator has the following form

$$a = \frac{1}{2} \left[\sqrt{(2b^2 + \delta + 1)^2 - 4(b^4 + \delta b^2 - b^2)} - (2b^2 + \delta + 1) \right] \quad (4.9)$$

The stability diagram for the Sel'kov model of Glycolysis will be mandated from now onwards by equations (4.6) and (4.9) for different values of parameter ' δ ' as shown in Figure (4.1) below.

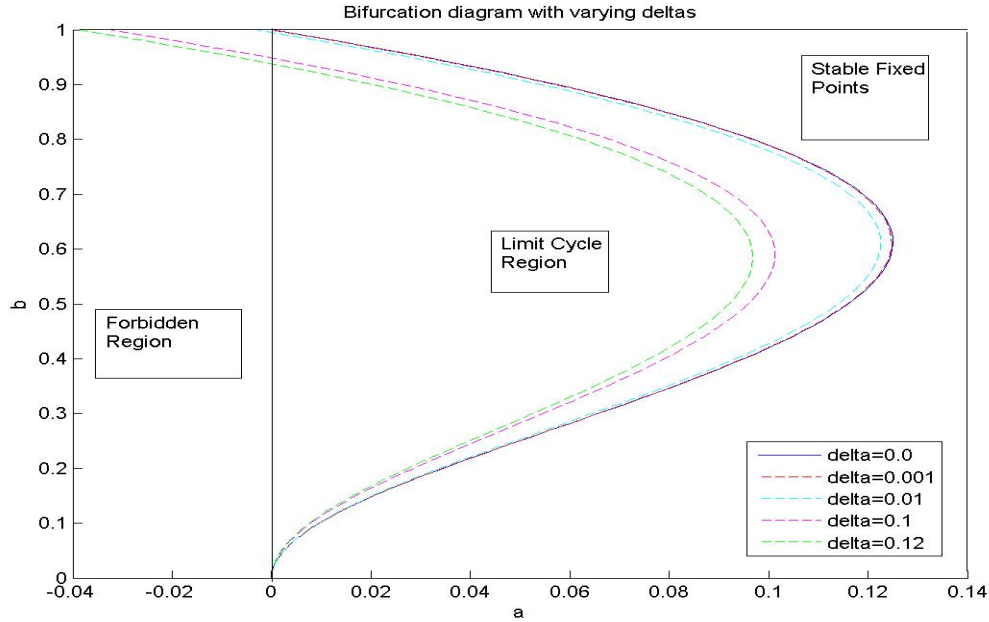


Figure 4.1: Stability diagram for varying delta(δ)

The next thing that is to be done is to check the newly introduced method by applying perturbative renormalization group up to 2^{nd} order in perturbation to the transformed system equations (4.7) and (4.8), finding limit cycle boundaries then comparing the results obtained with actual numerically predicted results as we had done previously in chapter 3.

For making the Eqs. (4.7) and (4.8) conducive to the application of perturbation theory so that the zeroth-order the system variables given by X_0 and Y_0 may show purely simple harmonic oscillations we rewrite the equations as

$$\dot{X} = (a + b^2)X + (a + b^2)Y + \lambda \left[\delta X + \left(\frac{b}{a + b^2} \right) X^2 + 2bXY + X^2Y \right] \quad (4.10)$$

$$\dot{Y} = \left(\frac{-2b^2}{a+b^2} \right) X - (a+b^2)Y - \lambda \left[\left(\frac{b}{a+b^2} \right) X^2 + 2bXY + X^2Y \right] \quad (4.11)$$

λ here is the externally introduced perturbation parameter of the problem.

As before, we shall form two second-order inhomogeneous non-linear differential equations in variables X and Y of the system by differentiating the equations (4.10) and (4.11) once with respect to time (refer **Appendix A**). These equations at this stage will look like

$$\ddot{X} + \omega^2 X = \lambda \left[k\delta X + \delta\dot{X} + \frac{2b}{k} X\dot{X} + 2b(\dot{X}Y + X\dot{Y}) + 2X\dot{X}Y + X^2\dot{Y} \right] \quad (4.12)$$

where the frequency of oscillation is $\omega = \sqrt{2b^2 - k^2}$ and $k = a + b^2$ is a constant.

$$\ddot{Y} + \omega^2 Y = \lambda \left[-\frac{\omega^2}{k} \Gamma - \frac{2b^2\delta}{k} X - \frac{2b}{k} X\dot{X} - 2b(X\dot{Y} + \dot{X}Y) - 2X\dot{X}Y - X^2\dot{Y} \right] \quad (4.13)$$

$$\text{where } \Gamma = \frac{b}{k} X^2 + 2bXY + X^2Y$$

At this point, we are ready to apply the perturbative renormalization group starting with any one of the equations above but as usual, let us stick to the X equation only and find the limit cycle boundary on the X -axis as done previously. We start out by

expanding the variables X and Y as

$$X = X_0 + \lambda X_1 + \lambda^2 X_2 + \dots \quad (4.14)$$

$$Y = Y_0 + \lambda Y_1 + \lambda^2 Y_2 + \dots \quad (4.15)$$

which leads to the following zeroth order equation for X :

$$\ddot{X}_0 + \omega^2 X_0 = 0 \quad (4.16)$$

with the solution for X_0 as

$$X_0 = A \cos \alpha \quad (4.17)$$

where $\alpha = (\omega t + \theta)$ is the phase of the oscillation and A is as usual the amplitude. The zeroth order equation for Y however must be carefully obtained from Eq.(4.11) given by

$$\dot{X}_0 = k(X_0 + Y_0) \quad (4.18)$$

i.e.,

$$Y_0 = \frac{1}{k}[\dot{X}_0 - kX_0] \quad (4.19)$$

Using Eq.(4.17) in Eq.(4.19) , the zeroth order solution for Y_0 is given by

$$Y_0 = -\frac{A\omega}{k} \sin \alpha - A \cos \alpha \quad (4.20)$$

It is easy to calculate that the phase difference between X_0 and Y_0 is given by $\phi = \tan^{-1} \left(-\frac{a+b^2}{\omega} \right)$.

First order calculations

The first order equations in the variables X and Y as obtained from the equations (4.12) and (4.13) can be written as

$$\begin{aligned} \ddot{X}_1 + \omega^2 X_1 = k\delta X_0 + \delta \dot{X}_0 + \frac{2b}{k} X_0 \dot{X}_0 + 2b \dot{X}_0 Y_0 + 2b X_0 \dot{Y}_0 \\ + 2X_0 \dot{X}_0 Y_0 + X_0^2 \dot{Y}_0 \end{aligned} \quad (4.21)$$

$$\begin{aligned} \ddot{Y}_1 + \omega^2 Y_1 = & -\frac{\omega^2 b}{k^2} X_0^2 - \frac{2b\omega^2}{k} X_0 Y_0 - \frac{\omega^2}{k} X_0^2 Y_0 - \frac{2b^2}{k} \delta X_0 \\ & - \frac{2b}{k} X_0 \dot{X}_0 - 2b (X_0 \dot{Y}_0 + \dot{X}_0 Y_0) \\ & - 2X_0 \dot{X}_0 Y_0 - X_0^2 \dot{Y}_0 \quad (4.22) \end{aligned}$$

Expanding the right hand side of Eq.(4.21) with the help of Eqs. (4.18) and (4.20) it can be expressed in the following simple form (please refer **Appendix B**)

$$\begin{aligned} \ddot{X}_1 + \omega^2 X_1 = & A_1 \sin \alpha + B_1 \cos \alpha + C_1 \sin 2\alpha + D_1 \cos 2\alpha \\ & + E_1 \sin 3\alpha + F_1 \cos 3\alpha \quad (4.23) \end{aligned}$$

where the values of the coefficients are given by

$$\begin{aligned} A_1 &= \frac{3A^3\omega}{4} - \delta\omega A \\ B_1 &= k\delta A + \frac{A^3\omega^2}{4k} \\ C_1 &= 2bA^2\omega - \frac{bA^2\omega}{k} \\ D_1 &= -\frac{2bA^2\omega^2}{k} \\ E_1 &= \frac{3A^3\omega}{4} \\ F_1 &= -\frac{3A^3\omega^2}{4k} \end{aligned}$$

The solution of Eq.(4.23) can be straight away written down as per the prescriptions laid down in the Eqs. (3.25), (3.26) and (3.27) in the last chapter and after absorbing the divergences introduced by the secular terms at the RHS of Eq.(4.23) following the procedure

of renormalization as

$$X_1(t) = \frac{A_1}{4\omega^2} \sin \alpha + \frac{B_1}{4\omega^2} \cos \alpha - \frac{C_1}{3\omega^2} \sin 2\alpha - \frac{D_1}{3\omega^2} \cos 2\alpha \\ - \frac{E_1}{8\omega^2} \sin 3\alpha - \frac{F_1}{8\omega^2} \cos 3\alpha \quad (4.24)$$

It is easy to note that the $\sin \alpha$ and $\cos \alpha$ terms in the RHS of Eq.(4.23) are the so-called secular terms responsible for the introduction of divergent terms in the solution. These divergent terms, on the other hand, contribute to the amplitude and phase flow equations as per prescriptions of the Renormalization group process discussed in detail in the preceding chapter. Following the procedures laid down in the literature, it may be figured out that the first-order flow equations for X_1 are given by :

$$\left. \frac{dA}{dt} \right|_1 = -\frac{A_1}{2\omega} = -\frac{1}{2\omega} \left(\frac{3A^3\omega}{4} - \delta\omega A \right) \quad (4.25)$$

which is the amplitude flow equation upto 1st order of perturbation. The phase flow equation upto 1st order of perturbation is

$$\frac{d\theta}{dt} = -\frac{B_1}{2A\omega} \quad (4.26)$$

Similarity, the solution of the Y equation upto the first order of perturbation can easily be calculated to be

$$Y_1(t) = \frac{A_2}{4\omega^2} \sin \alpha + \frac{B_2}{4\omega^2} \cos \alpha - \frac{C_2}{3\omega^2} \sin 2\alpha - \frac{D_2}{3\omega^2} \cos 2\alpha \\ - \frac{E_2}{8\omega^2} \sin 3\alpha + \frac{F_2}{\omega^2} \quad (4.27)$$

where the constant coefficients are given by:

$$\begin{aligned}
 A_2 &= \frac{\omega^3 A^3}{4k^2} + \frac{A^3 \omega}{4} \\
 B_2 &= \frac{2A^3 \omega^2}{k} - \frac{2b^2 A \delta}{k} \\
 C_2 &= \frac{\omega^3 A^2 b}{k^2} + \frac{bA^2 \omega}{k} - 2bA^2 \omega \\
 D_2 &= \frac{3\omega^2 bA^2}{k} - \frac{\omega^2 bA^2}{2k^2} \\
 E_2 &= \frac{\omega^3 A^3}{4k^2} + \frac{A^3 \omega}{4} \\
 F_2 &= \frac{\omega^2 bA^2}{k} \left(1 - \frac{1}{2k} \right)
 \end{aligned}$$

The amplitude and phase flow equations for the 1st order in Y can easily be written off as per the formula $\frac{dA}{dt} = -\frac{A_2}{2\omega}$ and $\frac{d\theta}{dt} = -\frac{B_2}{2A\omega}$. We however limit ourselves to finding boundaries of limit cycles of the system on the X-axis only.

Second order calculations

The solutions for X_0, Y_0, X_1 & Y_1 given by Eqs.(4.17), (4.20), (4.24) and (4.27) makes way for the second-order calculations in perturbation theory. We shall stick to finding the amplitude flow equation at the second-order of perturbation for the variable X_2 only. This is quite easy, as writing down the flow equation in either amplitude or phase requires one to construct the differential equation in X_2 and gather the coefficients of the $\sin \alpha$ and $\cos \alpha$ terms at the RHS of the equation and then form the flow equations as per recipe laid down in chapter 3. One need not solve the equation to get the expression for ' $X_2(t)$ '.

The equation for X_2 can be obtained from the perturbative

expansion of the Eq.(4.12) with the help of Eqs. (4.14) and (4.15) and equating the terms of the order λ^2 from both sides and is given by (refer **Appendix C**)

$$\begin{aligned} \ddot{X}_2 + \omega^2 X_2 = & k\delta X_1 + \delta \dot{X}_1 + \frac{2b}{k} (X_0 \dot{X}_1 + X_1 \dot{X}_0) + 2b (\dot{X}_0 Y_1 + Y_0 \dot{X}_1) \\ & + 2b (X_0 \dot{Y}_1 + X_1 \dot{Y}_0) + 2X_1 \dot{X}_0 Y_0 + 2X_0 \dot{X}_1 Y_0 \\ & + 2X_0 \dot{X}_0 Y_1 + 2X_1 X_0 \dot{Y}_0 + X_0^2 \dot{Y}_1 \quad (4.28) \end{aligned}$$

To obtain the amplitude and phase flow equations at this order of perturbation, one needs to expand the RHS in light of the Eqs.(4.17), (4.20), (4.24) and (4.27). By doing so it is a matter of time when one finds the above equation to assume the general form given below :

$$\ddot{X}_2 + \omega^2 X_2 = P \cos \alpha + Q \sin \alpha + \text{nonsecular terms} \quad (4.29)$$

The above equation is similar to Eq.(3.25) and (3.26). The divergent part of the solution of Eq.(4.29) arising due to the secular terms is of the type

$$\frac{t}{2\omega} [P \sin \alpha - Q \cos \alpha]$$

Therefore the amplitude and phase flow equations will simply be given by -

$$\frac{dA}{dt} = -\frac{Q}{2\omega} \quad (4.30)$$

$$\frac{d\theta}{dt} = -\frac{P}{2A\omega} \quad (4.31)$$

as per the recipe given in the previous chapter. Thus to obtain the amplitude flow equation one needs to collect the coefficients of all $\sin \alpha$ terms in the RHS of Eq. (4.28). A meticulous expansive calculation of the RHS of Eq.(4.28) shows that the coefficient of

the $\sin \alpha$ term is given by

$$Q = \frac{k\delta A_1}{4\omega^2} - \frac{\delta B_1}{4\omega} + \frac{bAD_1}{3\omega k} + \frac{bAD_2}{3\omega} - \frac{bAD_1}{3\omega} - \frac{2bAF_2}{\omega} - \frac{bAC_1}{3k} + \frac{A^2 A_1}{8k} - \frac{A^2 E_1}{16k} + \frac{3A^2 B_1}{8\omega} - \frac{A^2 F_1}{16\omega} - \frac{3A^2 B_2}{16\omega} \quad (4.32)$$

The key to finding this is to look for the terms in the RHS of Eq.(4.28) with the following combinations of sin and cos functions ($\sin \alpha \cos 2\alpha$), ($\cos \alpha \sin 2\alpha$), ($\cos 3\alpha \sin 2\alpha$) and ($\cos 2\alpha \sin 3\alpha$). It is easy to understand that only these combinations can give rise to secular sin terms, the coefficients of which when taken together looks like Eq.(4.32). Equation (4.32) needs to be further expanded using the explicit expressions of the constant coefficients $A_1, B_1, C_1, D_1, E_1, F_1, A_2, B_2, C_2, D_2, E_2, F_2$ (see page 60 & 61) and after a careful and rigorous simplification gives

$$Q = - \left(\frac{6\omega}{32k} \right) A^5 + \left(\frac{3b^2\delta}{8k\omega} + \frac{9k\delta}{16\omega} - \frac{3\omega\delta}{16k} + \frac{b^2\omega}{2k^2} - \frac{b^2\omega}{k} \right) A^3 - \left(\frac{k\delta^2}{2\omega} \right) A \quad (4.33)$$

Thus the amplitude flow equation at the second order of perturbation given by Eq.(4.30) looks like

$$\left. \frac{dA}{dt} \right|_2 = -\frac{Q}{2\omega} \quad (4.34)$$

where ' Q ' is the coefficient of $\sin \alpha$ given by Eq.(4.33). The final second order flow equation can then be written down as

$$\left. \frac{dA}{dt} \right|_{2ndOrder} = \lambda \left. \frac{dA}{dt} \right|_1 + \lambda^2 \left. \frac{dA}{dt} \right|_2 \quad (4.35)$$

which is explicitly written as

$$\begin{aligned} \left. \frac{dA}{dt} \right|_{2^{nd} Order} &= \lambda \left[\frac{\delta}{2} A - \frac{3}{8} A^3 \right] + \lambda^2 \left[\left(\frac{3}{32k} \right) A^5 \right. \\ &+ \left(-\frac{3b^2\delta}{16k\omega^2} - \frac{9k\delta}{32\omega^2} + \frac{3\delta}{32k} - \frac{b^2}{4k^2} + \frac{b^2}{2k} \right) A^3 \\ &\left. + \left(\frac{k\delta^2}{4\omega^2} \right) A \right] \quad (4.36) \end{aligned}$$

Equations(4.25) and (4.36) depict the amplitude flow equations in the first and second orders of perturbation on the X-axis, the fixed point of which gives the distance of the origin from the point where the limit cycle cuts the X-axis. As done in the earlier chapter, we shall compare the boundaries of the limit cycles on the X-axis as predicted by the perturbative renormalization group with those numerically plotted with values of parameters ‘a’ and ‘b’ of the system deep inside the limit cycle zone of the parameter space. The values of the parameters ‘a’ and ‘b’ are varied by varying the value of the external parameter ‘ δ ’. If we find that the perturbatively calculated results are in close agreement with the numerical results, we shall infer that our posed method is working good.

4.3 Results

As usual, the boundaries of the limit cycles for the biochemical glycolytic oscillator on the X-axis at various orders of perturbation are obtained from the fixed points of the Eq.(4.25) and Eq.(4.36) obtained by putting the RHS of these equations to zero.

The limit cycle boundary on the X-axis upto first order in perturbation is obtained by putting

$$\begin{aligned} \left. \frac{dA}{dt} \right|_1 &= 0 \\ \text{or, } -\frac{1}{2\omega} \left(\frac{3A^3\omega}{4} - \delta\omega A \right) &= 0 \\ \text{or, } A \left(\frac{3A^2}{4} - \delta \right) &= 0 \end{aligned}$$

$$\therefore A = 0 \quad \& \quad A = \sqrt{\frac{4\delta}{3}} \quad (4.37)$$

$A = 0$ represents the origin i.e., the fixed point. The second value of the amplitude 'A' represents our coveted result.

The second order result for the boundary of the limit cycle on the X-axis in this case is obtained by putting the RHS of Eq. (4.35) to zero, i.e.,

$$\left. \frac{dA}{dt} \right|_{2ndOrder} = 0$$

which implies

$$\begin{aligned} \left(\frac{3}{32k} \right) A^4 + \left(-\frac{3b^2\delta}{16k\omega^2} - \frac{9k\delta}{32\omega^2} + \frac{3\delta}{32k} - \frac{b^2}{4k^2} + \frac{b^2}{2k} - \frac{3}{8} \right) A^2 \\ + \left(\frac{k\delta^2}{4\omega^2} + \frac{\delta}{2} \right) = 0 \quad (4.38) \end{aligned}$$

The above equation being quadratic in A^2 has a solution given by :

$$A^2 = \frac{-M \pm \sqrt{M^2 - 4LN}}{2L}$$

where L , M and N are respectively given by :

$$L = \frac{3}{32k}$$

$$M = -\frac{3b^2\delta}{16k\omega^2} - \frac{9k\delta}{32\omega^2} + \frac{3\delta}{32k} - \frac{b^2}{4k^2} + \frac{b^2}{2k} - \frac{3}{8}$$

$$N = \frac{k\delta^2}{4\omega^2} + \frac{\delta}{2}$$

Finally ‘A’ is given by :

$$A = \sqrt{\frac{-M \pm \sqrt{M^2 - 4LN}}{2L}} \quad (4.39)$$

Equation(4.39) gives the position of the limit cycle predicted by the 2nd order of perturbative renormalization group.

Let us now concentrate on whether the variation of the parameter ‘ δ ’ according to the method presented can predict the boundary of the limit cycles more accurately. For this, we shall keep the value of the system parameter ‘ b ’ constant and equal to $\sqrt{\frac{3}{8}}$, i.e., the value of ‘ b ’ at the extremum of the stability curve of the oscillator. The value of the system parameter ‘ a ’ here has been calculated from Eq.(4.9), appropriate for a particular stability curve depending on the value of the parameter ‘ δ ’ on that curve. We shall compare the position of the limit cycle boundary on the X-axis as predicted by perturbative renormalization group at the first and second orders of perturbation with the numerical results corresponding to same values of the parameters ‘ δ ’, ‘ a ’, and ‘ b ’.

For $\delta = 0.001$ and $b = \sqrt{\frac{3}{8}}$ the value of system parameter ‘ a ’ as given by Eq.(4.9) as ‘ $a = 0.124$ ’. The limit cycle boundary at the first order and second order of perturbation is given by $A_{firstorder} = 0.0365$ and $A_{secondorder} = 0.0366$. The limit cycle boundary obtained numerically for the same value of the parameters is $A_{numerical} = 0.03$ which is very close to the calculated value and is given in Figure 4.2.

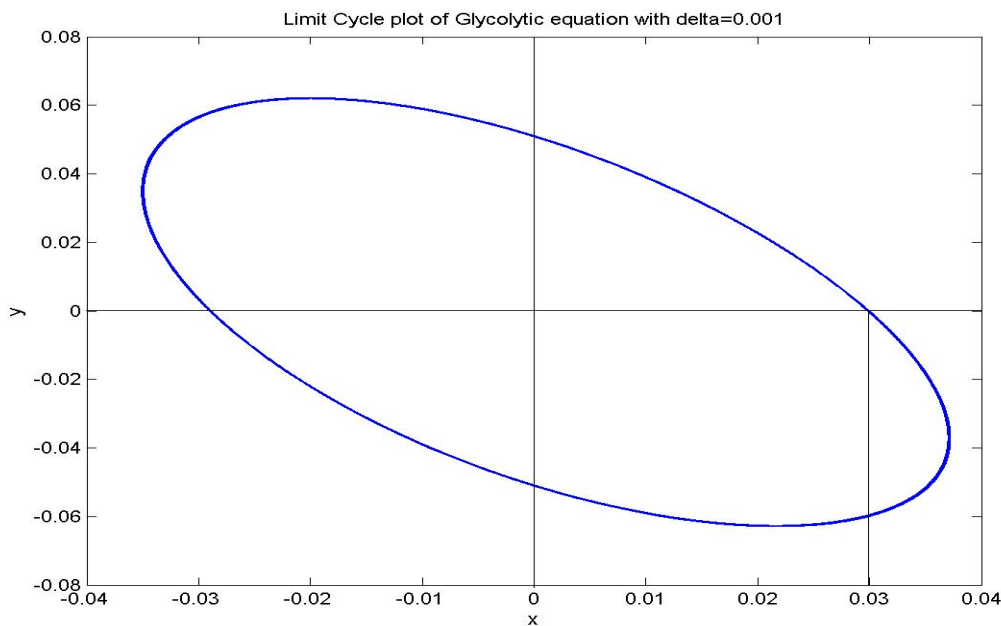


Figure 4.2: Limit cycle for $\delta = 0.001$ and boundary calculated at $A_{numerical} = 0.03$

Next, we choose the value of the parameter $\delta = 0.01$ and for the same value of the system parameter ‘ b ’ and the calculated value of the parameter ‘ a ’ from Eq.(4.9) is 0.122. For this case, the boundary of the limit cycle on the X-axis given by the distance of the origin from the point where the limit cycle cuts the X-axis is predicted at $A_{firstorder} = 0.1155$ and $A_{secondorder} = 0.1153$ at the first and second order of perturbation. The numerical value of the boundary of the limit cycle for the same parameter values plotted in Figure 4.3 is at $A_{numerical} = 0.10$. Thus the values obtained by perturbative calculation and that obtained from the numerical plot are very close.

For higher values of δ , say for $\delta = 0.10$ the boundary of the limit cycle predicted by perturbative renormalization group at the first and second order and that given by numerical plot are at $A_{firstorder} = 0.3651$, $A_{secondorder} = 0.03599$ and $A_{numerical} = 0.36$ all of which agree to a great extent as in Figure 4.4.

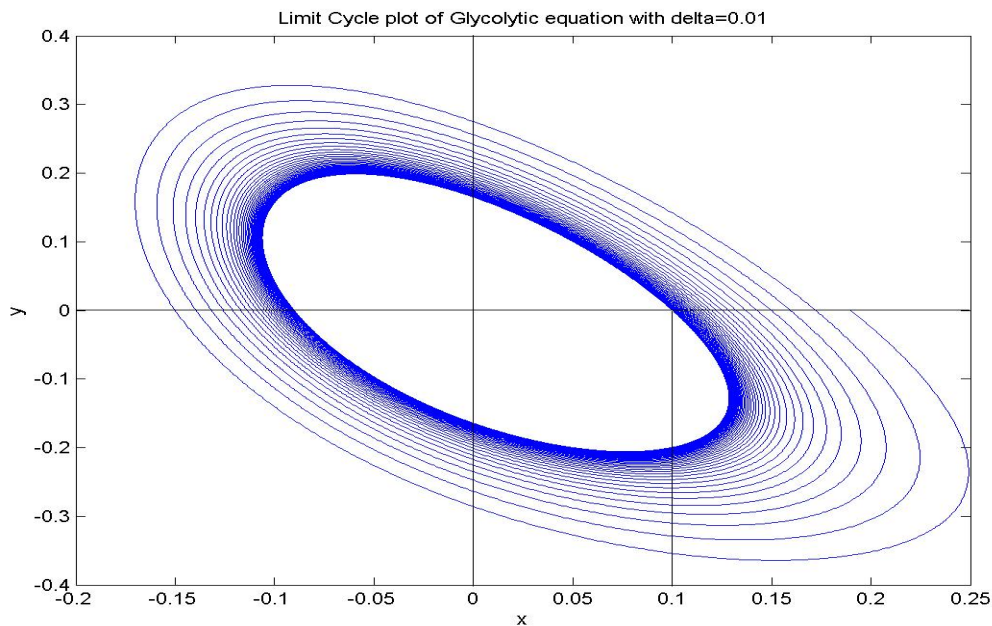


Figure 4.3: Limit cycle for $\delta = 0.01$ and boundary calculated at $A_{numerical} = 0.10$

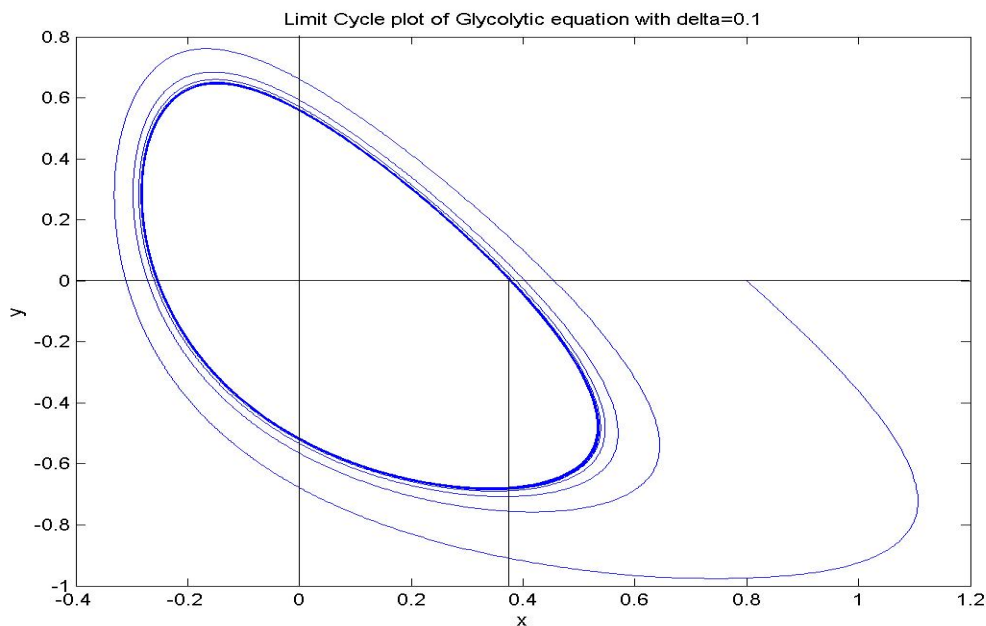


Figure 4.4: Limit cycle for $\delta = 0.10$ and boundary calculated at $A_{numerical} = 0.36$

Lastly for still higher values of the parameter ‘ δ ’, i.e., for $\delta = 0.12$ the boundary of the limit cycle as predicted by first and second order of perturbative renormalization group is at $A_{firstorder} = 0.4000$, $A_{secondorder} = 0.3933$ respectively and that predicted by numerical plot is at $A_{numerical} = 0.42$ implying that the results also agree for a quite higher value of the parameter ‘ δ ’, shown at Figure 4.5 below.

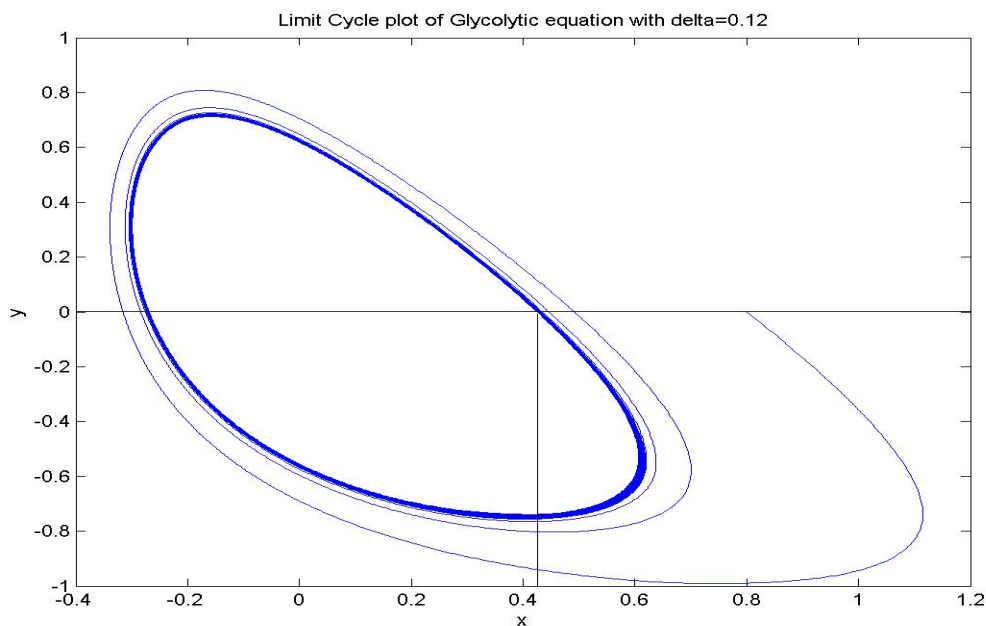


Figure 4.5: Limit cycle for $\delta = 0.12$ and boundary calculated at $A_{numerical} = 0.42$

Thus the results obtained are quite satisfactory since the theoretically calculated boundaries of limit cycles for various values of the parameters ‘ δ ’, ‘ a ’ and ‘ b ’ using perturbative renormalization and our method to scan the parameter space are in good agreement with the results obtained from numerical plots. This proves that the method described to scan the parameter space in this chapter is way better than the method we had presented in the previous chapter in a way that it can predict accurate results, and the limit cycle boundaries can be calculated at any depth inside the limit cycle region as presented in the work of Dutta et al. [51].

4.4 Appendix A

Formulating Eqs.(4.12) & (4.13)

Given the Eqs.(4.10) and (4.11) i.e.,

$$\dot{X} = (a + b^2)X + (a + b^2)Y + \lambda \left[\delta X + \left(\frac{b}{a + b^2} \right) X^2 + 2bXY + X^2Y \right]$$

and

$$\dot{Y} = \left(\frac{-2b^2}{a + b^2} \right) X - (a + b^2)Y - \lambda \left[\left(\frac{b}{a + b^2} \right) X^2 + 2bXY + X^2Y \right]$$

the next step towards formulating the equation for \ddot{X} is given by

$$\ddot{X} = (a + b^2)\dot{X} + (a + b^2)\dot{Y} + \lambda \left[\delta \dot{X} + \frac{2b}{a + b^2} X \dot{X} + 2b(X\dot{Y} + \dot{X}Y) + 2X\dot{X}Y + X^2\dot{Y} \right] \quad (4.40)$$

or,

$$\ddot{X} = (a + b^2)\dot{X} + (a + b^2)\dot{Y} + \lambda \left[\delta \dot{X} + \frac{2b}{a + b^2} X \dot{X} + 2b(X\dot{Y} + \dot{X}Y) + 2X\dot{X}Y + X^2\dot{Y} \right]$$

or,

$$\begin{aligned} \ddot{X} = & (a + b^2) \left[(a + b^2)X + (a + b^2)Y + \lambda (\delta X + \Gamma) \right] \\ & + (a + b^2) \left[-\frac{2b^2}{a + b^2}X - (a + b^2)Y - \lambda (\Gamma) \right] \\ & + \lambda \left[\delta \dot{X} + \frac{2b^2}{(a + b^2)} X \dot{X} + 2b(\dot{X}Y + X\dot{Y}) + 2X\dot{X}Y + X^2\dot{Y} \right] \end{aligned}$$

where the terms $(a + b^2)^2 Y$ terms is cancelled from the RHS and we get

$$\ddot{X} = \left[(a + b^2)^2 - 2b^2 \right] X + \lambda (a + b^2) \delta X + \lambda \left[\delta \dot{X} + \frac{2b^2}{(a + b^2)} X \dot{X} + 2b(\dot{X}Y + X\dot{Y}) + 2X\dot{X}Y + X^2\dot{Y} \right]$$

or,

$$\ddot{X} + \left[2b^2 - (a + b^2)^2 \right] X = \lambda \left[(a + b^2) \delta X + \delta \dot{X} + \frac{2b^2}{(a + b^2)} X \dot{X} + 2b(\dot{X}Y + X\dot{Y}) + 2X\dot{X}Y + X^2\dot{Y} \right]$$

Now, if we write ' $k = (a + b^2)$ ' with the frequency of oscillation $\omega = \sqrt{2b^2 - (a + b^2)^2} = \sqrt{2b^2 - k^2}$ the second order differential equation in X finally takes the desired form given by

$$\ddot{X} + \omega^2 X = \lambda \left[k \delta X + \delta \dot{X} + \frac{2b}{k} X \dot{X} + 2b(\dot{X}Y + X\dot{Y}) + 2X\dot{X}Y + X^2\dot{Y} \right]$$

which is our desired equation (4.12).

The second order differential equation in Y is obtained similarly by double differentiating the Eq. (4.11) as

$$\ddot{Y} = -\frac{2b^2}{(a + b^2)} \dot{X} - (a + b^2) \dot{Y} - \lambda \left[\frac{2b}{(a + b^2)} X \dot{X} + 2b(\dot{X}Y + X\dot{Y}) + 2X\dot{X}Y + X^2\dot{Y} \right]$$

or, substituting the expressions of \dot{X} and \dot{Y} we get,

$$\begin{aligned} \ddot{Y} = & -\frac{2b^2}{(a+b^2)} \left[(a+b^2)X + (a+b^2)Y + \lambda(\delta X + \Gamma) \right] \\ & - (a+b^2) \left[-\frac{2b^2}{(a+b^2)}X - (a+b^2)Y - \lambda(\Gamma) \right] \\ & - \lambda \left[\frac{2b}{(a+b^2)}X\dot{X} + 2b(\dot{X}Y + X\dot{Y}) + 2X\dot{X}Y + X^2\dot{Y} \right] \end{aligned}$$

where $\Gamma = \frac{b}{(a+b^2)}X^2 + 2bXY + X^2Y$.

Therefore we have,

$$\begin{aligned} \ddot{Y} = & -2b^2X - 2b^2Y - \lambda \frac{2b^2}{(a+b^2)}\delta X - \lambda \frac{2b^2}{(a+b^2)}\Gamma \\ & + 2b^2X + (a+b^2)^2Y + \lambda(a+b^2)\Gamma - \lambda \left[\frac{2b}{(a+b^2)}X\dot{X} \right. \\ & \left. + 2b(\dot{X}Y + X\dot{Y}) + 2X\dot{X}Y + X^2\dot{Y} \right] \end{aligned}$$

and finally ,

$$\begin{aligned} \ddot{Y} + \left[2b^2 - (a+b^2)^2 \right] Y = & \\ & \lambda \left[\left\{ (a+b^2) - \frac{2b^2}{(a+b^2)} \right\} \Gamma - \frac{2b^2}{(a+b^2)}\delta X \right] \\ & - \lambda \left[\frac{2b}{(a+b^2)}X\dot{X} + 2b(\dot{X}Y + X\dot{Y}) + 2X\dot{X}Y + X^2\dot{Y} \right] \end{aligned}$$

which can be put to the desired form with ' $k = (a+b^2)$ ' and $\omega = \sqrt{2b^2 - k^2}$ as

$$\begin{aligned} \ddot{Y} + \omega^2 Y = & \lambda \left[-\frac{\omega^2}{k}\Gamma - \frac{2b^2\delta}{k}X - \frac{2b}{k}X\dot{X} - 2b(X\dot{Y} + \dot{X}Y) \right. \\ & \left. - 2X\dot{X}Y - X^2\dot{Y} \right] \end{aligned}$$

which is Eq.(4.13)

4.5 Appendix B

RHS expansions of Eq. (4.21)

Equation (4.21) is given by

$$\begin{aligned} \ddot{X}_1 + \omega^2 X_1 = k\delta X_0 + \delta\dot{X}_0 + \frac{2b}{k}X_0\dot{X}_0 + 2b\dot{X}_0Y_0 + 2bX_0\dot{Y}_0 \\ + 2X_0\dot{X}_0Y_0 + X_0^2\dot{Y}_0 \end{aligned}$$

The Right hand side of the above equation is expanded in terms of the zeroth order solutions X_0 & Y_0 given by

$$X_0 = A \cos \alpha$$

and

$$Y_0 = -\frac{A\omega}{k} \sin \alpha - A \cos \alpha$$

. It is convenient to write down the expressions of \dot{X}_0 and \dot{Y}_0 here as

$$\dot{X}_0 = -A\omega \sin \alpha$$

and

$$\dot{Y}_0 = -\frac{A\omega^2}{k} \cos \alpha + A\omega \sin \alpha$$

Term wise calculation of Eq.(4.21) :

First term :

$$k\delta X_0 = k\delta A \cos \alpha$$

Second term :

$$\delta\dot{X}_0 = -\delta\omega A \sin \alpha$$

Third term:

$$\frac{2b}{k}X_0\dot{X}_0 = \frac{2b}{k}A \cos \alpha \{-A\omega \sin \alpha\} = -\frac{bA^2\omega}{k} \sin 2\alpha$$

Fourth term:

$$\begin{aligned}
 2b\dot{X}_0Y_0 &= 2b\{-A\omega \sin \alpha\}\left\{-\frac{A\omega}{k} \sin \alpha - A \cos \alpha\right\} \\
 &= \frac{2bA^2\omega^2}{k} \sin^2 \alpha + 2bA^2\omega \sin \alpha \cos \alpha \\
 &= \frac{bA^2\omega^2}{k} (1 - \cos 2\alpha) + bA^2\omega \sin 2\alpha \\
 &= \frac{bA^2\omega^2}{k} - \frac{bA^2\omega^2}{k} \cos 2\alpha + bA^2\omega \sin 2\alpha
 \end{aligned}$$

Fifth term:

$$\begin{aligned}
 2bX_0\dot{Y}_0 &= 2bA \cos \alpha \left[-\frac{A\omega^2}{k} \cos \alpha + A\omega \sin \alpha \right] \\
 &= -\frac{2bA^2\omega^2}{k} \cos^2 \alpha + 2bA^2\omega \sin \alpha \cos \alpha \\
 &= -\frac{bA^2\omega^2}{k} (1 + \cos 2\alpha) + bA^2\omega \sin 2\alpha \\
 &= -\frac{bA^2\omega^2}{k} - \frac{bA^2\omega^2}{k} \cos 2\alpha + bA^2\omega \sin 2\alpha
 \end{aligned}$$

Sixth term:

$$\begin{aligned}
 2X_0\dot{X}_0Y_0 &= 2A \cos \alpha (-A\omega \sin \alpha) \left(-\frac{A\omega}{k} \sin \alpha - A \cos \alpha \right) \\
 &= -A^2\omega \sin 2\alpha \left[-\frac{A\omega}{k} \sin \alpha - A \cos \alpha \right] \\
 &= \frac{A^3\omega^2}{k} \sin 2\alpha \sin \alpha + A^3\omega \sin 2\alpha \cos \alpha \\
 &= \frac{A^3\omega^2}{2k} \cos \alpha - \frac{A^3\omega^2}{2k} \cos 3\alpha + \frac{A^3\omega}{2} \sin 3\alpha + \frac{A^3\omega}{2} \sin \alpha
 \end{aligned}$$

Seventh term:

$$\begin{aligned}
 X_0^2 \dot{Y}_0 &= A^2 \cos^2 \alpha \left[-\frac{A\omega^2}{k} \cos \alpha + A\omega \sin \alpha \right] \\
 &= -\frac{A^3 \omega^2}{k} \cos^3 \alpha + A^3 \omega \cos^2 \alpha \sin \alpha \\
 &= -\frac{A^3 \omega^2}{k} \left[\frac{3}{4} \cos \alpha + \frac{1}{4} \cos 3\alpha \right] + \frac{A^3 \omega}{2} \sin 2\alpha \cos \alpha \\
 &= -\frac{3A^3 \omega^2}{4k} \cos \alpha - \frac{A^3 \omega^2}{4k} \cos 3\alpha + \frac{A^3 \omega}{4} \sin 3\alpha + \frac{A^3 \omega}{4} \sin \alpha
 \end{aligned}$$

In the light of the above expansions our Eq.(4.21) takes the following form if we collect the coefficients of various trigonometric terms :

$$\begin{aligned}
 \ddot{X}_1 + \omega^2 X_1 &= \left[-\delta\omega A + \frac{A^3 \omega}{2} + \frac{A^3 \omega}{4} \right] \sin \alpha \\
 &+ \left[k\delta A + \frac{A^3 \omega^2}{2k} - \frac{3A^3 \omega^2}{4k} \right] \cos \alpha \\
 &+ \left[-\frac{bA^2 \omega}{k} + 2bA^2 \omega \right] \sin 2\alpha \\
 &+ \left[-\frac{2bA^2 \omega^2}{k} \right] \cos 2\alpha \\
 &+ \left[-\frac{A^3 \omega^2}{2k} - \frac{A^3 \omega^2}{4k} \right] \cos 3\alpha \\
 &+ \left[\frac{A^3 \omega}{2} + \frac{A^3 \omega}{4} \right] \sin 3\alpha + \frac{bA^2 \omega^2}{k} - \frac{bA^2 \omega^2}{k}
 \end{aligned}$$

Hence Eq.(4.21) can be written in the following form:

$$\begin{aligned}
 \ddot{X}_1 + \omega^2 X_1 &= A_1 \sin \alpha + B_1 \cos \alpha + C_1 \sin 2\alpha \\
 &+ D_1 \cos 2\alpha + E_1 \sin 3\alpha + F_1 \cos 3\alpha
 \end{aligned}$$

where the constant coefficients A_1, B_1, C_1, D_1, E_1 and F_1 have the expressions given at page 61 of the present volume. Based on this the

solution of X_1 as obtained by application of renormalization group and after elimination of any divergences is given by :

$$X_1(t) = \frac{A_1}{4\omega^2} \sin \alpha + \frac{B_1}{4\omega^2} \cos \alpha - \frac{C_1}{3\omega^2} \sin 2\alpha \\ - \frac{D_1}{3\omega^2} \cos 2\alpha - \frac{E_1}{8\omega^2} \sin 3\alpha - \frac{F_1}{8\omega^2} \cos 3\alpha$$

and

$$\dot{X}_1 = \frac{A_1}{4\omega} \cos \alpha - \frac{B_1}{4\omega} \sin \alpha - \frac{2C_1}{3\omega} \cos 2\alpha \\ + \frac{2D_1}{3\omega} \sin 2\alpha - \frac{3E_1}{8\omega} \cos 3\alpha + \frac{3F_1}{8\omega} \sin 3\alpha$$

RHS expansions of Eq. (4.22)

Equation(4.22) is given as

$$\ddot{Y}_1 + \omega^2 Y_1 = -\frac{\omega^2 b}{k^2} X_0^2 - \frac{2b\omega^2}{k} X_0 Y_0 - \frac{\omega^2}{k} X_0^2 Y_0 - \frac{2b^2}{k} \delta X_0 \\ - \frac{2b}{k} X_0 \dot{X}_0 - 2b (X_0 \dot{Y}_0 + \dot{X}_0 Y_0) \\ - 2X_0 \dot{X}_0 Y_0 - X_0^2 \dot{Y}_0$$

Eq.(4.22) is now expanded in terms of the zeroth order solutions of \dot{X}_0 and \dot{Y}_0 given explicitly by

$$\dot{X}_0 = -A\omega \sin \alpha$$

and

$$\dot{Y}_0 = -\frac{A\omega^2}{k} \cos \alpha + A\omega \sin \alpha$$

Term wise calculation of Eq.(4.22) :

First term:

$$-\frac{\omega^2 b}{k^2} X_0^2 = -\frac{\omega^2 b}{k^2} A^2 \cos^2 \alpha = -\frac{\omega^2 b A^2}{2k^2} - \frac{\omega^2 b A^2}{2k^2} \cos 2\alpha$$

Second term:

$$\begin{aligned} -\frac{\omega^2}{k}2bX_0Y_0 &= -\frac{2\omega^2b}{k}A\cos\alpha\left[-\frac{A\omega}{k}\sin\alpha - A\cos\alpha\right] \\ &= \frac{\omega^3A^2b}{k^2}\sin 2\alpha + \frac{\omega^2bA^2}{k} + \frac{\omega^2bA^2}{k}\cos 2\alpha \end{aligned}$$

Third term:

$$\begin{aligned} -\frac{\omega^2}{k}X_0^2Y_0 &= -\frac{\omega^2}{k}A^2\cos^2\alpha\left[-\frac{A\omega}{k}\sin\alpha - A\cos\alpha\right] \\ &= \frac{\omega^3A^3}{2k^2}\sin 2\alpha\cos\alpha + \frac{\omega^2A^3}{k}\left[\frac{3}{4}\cos\alpha + \frac{1}{4}\cos 3\alpha\right] \\ &= \frac{\omega^3A^3}{4k^2}\sin 3\alpha + \frac{\omega^3A^3}{4k^2}\sin\alpha + \frac{3\omega^2A^3}{4k}\cos\alpha + \frac{\omega^2A^3}{4k}\cos 3\alpha \end{aligned}$$

Fourth term:

$$-\frac{2b^2}{k}\delta X_0 = -\frac{2b^2}{k}\delta A\cos\alpha$$

Fifth term:

$$-\frac{2b}{k}X_0\dot{X}_0 = -\frac{2b}{k}A\cos\alpha(-A\omega\sin\alpha) = \frac{bA^2\omega}{k}\sin 2\alpha$$

Sixth term:

$$\begin{aligned} -2bX_0\dot{Y}_0 &= -2bA\cos\alpha\left[-\frac{A\omega^2}{k}\cos\alpha + A\omega\sin\alpha\right] \\ &= \frac{2bA^2\omega^2}{k}\cos^2\alpha - bA^2\omega\sin 2\alpha \\ &= \frac{bA^2\omega^2}{k} + \frac{bA^2\omega^2}{k}\cos 2\alpha - bA^2\omega\sin 2\alpha \end{aligned}$$

Seventh term:

$$\begin{aligned} -2b\dot{X}_0Y_0 &= -2b(-A\omega\sin\alpha)\left(-\frac{A\omega}{k}\sin\alpha - A\cos\alpha\right) \\ &= -\frac{2bA^2\omega^2}{k}\sin^2\alpha - 2bA^2\omega\sin\alpha\cos\alpha \\ &= -\frac{bA^2\omega^2}{k} + \frac{bA^2\omega^2}{k}\cos 2\alpha - bA^2\omega\sin 2\alpha \end{aligned}$$

Eighth term:

$$\begin{aligned}
 2X_0\dot{X}_0Y_0 &= 2A \cos \alpha (-A\omega \sin \alpha) \left[-\frac{A\omega}{k} \sin \alpha - A \cos \alpha \right] \\
 &= \frac{2A^3\omega^2}{k} \sin^2 \alpha \cos \alpha + 2A^3\omega \sin \alpha \cos^2 \alpha \\
 &= \frac{A^3\omega^2}{k} \sin 2\alpha \sin \alpha + A^3\omega \sin 2\alpha \cos \alpha \\
 &= \frac{A^3\omega^2}{2k} \cos \alpha - \frac{A^3\omega^2}{2k} \cos 3\alpha + \frac{A^3\omega}{2} \sin 3\alpha + \frac{A^3\omega}{2} \sin \alpha
 \end{aligned}$$

Ninth term:

$$\begin{aligned}
 -X_0^2\dot{Y}_0 &= -(A^2 \cos^2 \alpha) \left[-\frac{A\omega^2}{k} \cos \alpha + A\omega \sin \alpha \right] \\
 &= \frac{A^3\omega^2}{k} \cos^3 \alpha - A^3\omega \cos^2 \alpha \sin \alpha \\
 &= \frac{3A^3\omega^2}{4k} \cos \alpha + \frac{A^3\omega^2}{4k} \cos 3\alpha - \frac{A^3\omega}{4} \sin 3\alpha - \frac{A^3\omega}{4} \sin \alpha
 \end{aligned}$$

As before, collecting the coefficients of the trigonometric terms Eq.(4.22) looks like:

$$\begin{aligned}
 \ddot{Y}_1 + \omega^2 Y_1 &= \left[\frac{\omega^3 A^3}{4k^2} + \frac{A^3\omega}{4} \right] \sin \alpha \\
 &+ \left[\frac{3\omega^2 A^3}{4k} - \frac{2b^2 \delta A}{k} + \frac{A^3\omega^2}{2k} + \frac{3A^3\omega^2}{4k} \right] \cos \alpha \\
 &+ \left[\frac{\omega^3 A^2 b}{k^2} + \frac{bA^2\omega}{k} - 2bA^2\omega \right] \sin 2\alpha \\
 &+ \left[-\frac{\omega^2 bA^2}{2k^2} + \frac{3\omega^2 bA^2}{k} \right] \cos 2\alpha \\
 &+ \left[\frac{\omega^3 A^3}{4k^2} + \frac{A^3\omega}{2} - \frac{A^3\omega}{4} \right] \sin 3\alpha \\
 &+ \left[\frac{\omega^2 A^3}{4k} - \frac{A^3\omega^2}{2k} + \frac{A^3\omega^2}{4k} \right] \cos 3\alpha \\
 &\quad - \frac{\omega^2 bA^2}{2k^2} + \frac{\omega^2 bA^2}{k} + \frac{bA^2\omega^2}{k} - \frac{bA^2\omega^2}{k}
 \end{aligned}$$

which is the same as writing

$$\ddot{Y}_1 + \omega^2 Y_1 = A_2 \sin \alpha + B_2 \cos \alpha + C_2 \sin 2\alpha + D_2 \cos 2\alpha + E_2 \sin 3\alpha + F_2$$

The explicit expressions of the constant coefficients A_2, B_2, C_2, D_2, E_2 and F_2 are given at Page 63. The solution of the equation for Y_1 is given as per prescription laid down in literature and application of renormalization group as :

$$Y_1 = \frac{A_2}{4\omega^2} \sin \alpha + \frac{B_2}{4\omega^2} \cos \alpha - \frac{C_2}{3\omega^2} \sin 2\alpha - \frac{D_2}{3\omega^2} \cos 2\alpha - \frac{E_2}{8\omega^2} \sin 3\alpha + \frac{F_2}{\omega^2}$$

The expression for \dot{Y}_1 which is found by differentiating the above solution for Y_1 is given by

$$\dot{Y}_1 = \frac{A_2}{4\omega} \cos \alpha - \frac{B_2}{4\omega} \sin \alpha - \frac{2C_2}{3\omega} \cos 2\alpha + \frac{2D_2}{3\omega} \sin 2\alpha - \frac{3E_2}{8\omega} \cos 3\alpha$$

4.6 Appendix C

Calculation of coefficient of $\sin \alpha$ in Eq.(4.28):

Eq.(4.28) is essentially the equation for second order calculations in the variable X_2 and is given by :

$$\begin{aligned} \ddot{X}_2 + \omega^2 X_2 = & k\delta X_1 + \delta \dot{X}_1 + \frac{2b}{k} (X_0 \dot{X}_1 + X_1 \dot{X}_0) + 2b (\dot{X}_0 Y_1 + Y_0 \dot{X}_1) \\ & + 2b (X_0 \dot{Y}_1 + X_1 \dot{Y}_0) + 2X_1 \dot{X}_0 Y_0 + 2X_0 \dot{X}_1 Y_0 \\ & + 2X_0 \dot{X}_0 Y_1 + 2X_1 X_0 \dot{Y}_0 + X_0^2 \dot{Y}_1 \end{aligned}$$

The RHS of the above equation is evaluated in detail using the expressions of X_0 , Y_0, \dot{X}_0 , \dot{Y}_0 , X_1 , Y_1 , \dot{X}_1 and \dot{Y}_1 from Appendix A and Appendix B. While evaluating the right-hand side of Eq.(4.28), we need to calculate only the terms giving secular $\sin \alpha$, and we may refrain from calculating all the terms, which will be quite a mammoth task and unnecessary from our perspective also. The coefficient of $\sin \alpha$ is the required expression with the help of which the amplitude flow equation at the 2nd order of perturbation is formulated.

Term wise calculation of Eq.(4.28) :

First term :

$$\begin{aligned} k\delta X_1 = k\delta \left[\frac{A_1}{4\omega^2} \sin \alpha + \frac{B_1}{4\omega^2} \cos \alpha + \dots \right] \\ = \frac{k\delta A_1}{4\omega^2} \sin \alpha + \frac{k\delta B_1}{4\omega^2} \cos \alpha + \dots \end{aligned}$$

Second term :

$$\delta \dot{X}_1 = \frac{\delta A_1}{4\omega} \cos \alpha - \frac{\delta B_1}{4\omega} \sin \alpha + \dots$$

Third term:

$$\begin{aligned}\frac{2b}{k}X_0\dot{X}_1 &= \frac{2b}{k}A \cos \alpha \left[-\frac{2C_1}{3\omega} \cos 2\alpha + \frac{2D_1}{3\omega} \sin 2\alpha + \dots \right] \\ &= -\frac{2bAC_1}{3\omega k} (\cos 3\alpha + \cos \alpha) + \frac{2bAD_1}{3\omega k} (\sin 3\alpha + \sin \alpha) + \dots \\ &= -\frac{2bAC_1}{3\omega k} \cos \alpha + \frac{2bAD_1}{3\omega k} \sin \alpha + \dots\end{aligned}$$

Fourth term :

$$\begin{aligned}\frac{2b}{k}\dot{X}_0X_1 &= \frac{2b}{k}(-A\omega \sin \alpha) \left[-\frac{C_1}{3\omega^2} \sin 2\alpha - \frac{D_1}{3\omega^2} \cos 2\alpha + \dots \right] \\ &= \frac{bA\omega C_1}{3\omega^2 k} (\cos \alpha - \cos 3\alpha) + \frac{bA\omega D_1}{3\omega^2 k} (\sin 3\alpha - \sin \alpha) + \dots \\ &= \frac{bAC_1}{3\omega k} \cos \alpha - \frac{bAD_1}{3\omega k} \sin \alpha + \dots\end{aligned}$$

Fifth term :

$$\begin{aligned}2b\dot{X}_0Y_1 &= 2b(-A\omega \sin \alpha) \left[-\frac{C_2}{3\omega^2} \sin 2\alpha - \frac{D_2}{3\omega^2} \cos 2\alpha + \frac{F_2}{\omega^2} + \dots \right] \\ &= \frac{bAC_2}{3\omega} (\cos \alpha - \cos 3\alpha) \\ &\quad + \frac{bAD_2}{3\omega} (\sin 3\alpha - \sin \alpha) - \frac{2bAF_2}{\omega} \sin \alpha + \dots \\ &= \frac{bAC_2}{3\omega} \cos \alpha + \left(-\frac{bAD_2}{3\omega} - \frac{2bAF_2}{\omega} \right) \sin \alpha + \dots\end{aligned}$$

Sixth term :

$$\begin{aligned}
 2b\dot{X}_1Y_0 &= 2b \left[-\frac{A\omega}{k} \sin \alpha - A \cos \alpha \right] \left[-\frac{2C_1}{3\omega} \cos 2\alpha + \frac{2D_1}{3\omega} \sin 2\alpha + \dots \right] \\
 &= -\frac{2bA\omega}{k} \sin \alpha \left[-\frac{2C_1}{3\omega} \cos 2\alpha + \frac{2D_1}{3\omega} \sin 2\alpha \right] \\
 &\quad - 2bA \cos \alpha \left[-\frac{2C_1}{3\omega} \cos 2\alpha + \frac{2D_1}{3\omega} \sin 2\alpha \right] + \dots \\
 &= \frac{2bAC_1}{3k} (\sin 3\alpha - \sin \alpha) - \frac{2bAD_1}{3k} (\cos \alpha - \cos 3\alpha) \\
 &\quad + \frac{2bAC_1}{3\omega} (\cos 3\alpha + \cos \alpha) - \frac{2bAD_1}{3\omega} (\sin 3\alpha + \sin \alpha) + \dots \\
 &= \left(\frac{2bAC_1}{3\omega} - \frac{2bAD_1}{3k} \right) \cos \alpha + \left(-\frac{2bAC_1}{3k} - \frac{2bAD_1}{3\omega} \right) \sin \alpha + \dots
 \end{aligned}$$

Seventh term:

$$\begin{aligned}
 2bX_0\dot{Y}_1 &= 2bA \cos \alpha \left[-\frac{2C_2}{3\omega} \cos 2\alpha + \frac{2D_2}{3\omega} \sin 2\alpha + \dots \right] \\
 &= -\frac{2bAC_2}{3\omega} (\cos 3\alpha + \cos \alpha) + \frac{2bAD_2}{3\omega} (\sin 3\alpha + \sin \alpha) + \dots \\
 &= \left(-\frac{2bAC_2}{3\omega} \right) \cos \alpha + \left(\frac{2bAD_2}{3\omega} \right) \sin \alpha + \dots
 \end{aligned}$$

Eighth term :

$$\begin{aligned}
 2bX_1\dot{Y}_0 &= 2b \left[-\frac{A\omega^2}{k} \cos \alpha + A\omega \sin \alpha \right] \left[-\frac{C_1}{3\omega^2} \sin 2\alpha - \frac{D_1}{3\omega^2} \cos 2\alpha + \dots \right] \\
 &= -\frac{2bA\omega^2}{k} \cos \alpha \left[-\frac{C_1}{3\omega^2} \sin 2\alpha - \frac{D_1}{3\omega^2} \cos 2\alpha \right] \\
 &\quad + 2bA\omega \sin \alpha \left[-\frac{C_1}{3\omega^2} \sin 2\alpha - \frac{D_1}{3\omega^2} \cos 2\alpha \right] + \dots \\
 &= \frac{bAC_1}{3k} (\sin 3\alpha + \sin \alpha) + \frac{bAD_1}{3k} (\cos 3\alpha + \cos \alpha) \\
 &\quad - \frac{bAC_1}{3\omega} (\cos \alpha - \cos 3\alpha) - \frac{bAD_1}{3\omega} (\sin 3\alpha - \sin \alpha) + \dots \\
 &= \left(\frac{bAC_1}{3k} + \frac{bAD_1}{3\omega} \right) \sin \alpha + \left(\frac{bAD_1}{3k} - \frac{bAC_1}{3\omega} \right) \cos \alpha + \dots
 \end{aligned}$$

Ninth term :

$$\begin{aligned}
2X_1\dot{X}_0Y_0 &= 2(-A\omega \sin \alpha) \left(-\frac{A\omega}{k} \sin \alpha - A \cos \alpha \right) X_1 \\
&= \left(\frac{2A^2\omega^2}{k} \sin^2 \alpha + A^2\omega \sin 2\alpha \right) X_1 \\
&= \frac{2A^2\omega^2}{k} \sin^2 \alpha \left[\frac{A_1}{4\omega^2} \sin \alpha + \frac{B_1}{4\omega^2} \cos \alpha - \frac{E_1}{8\omega^2} \sin 3\alpha - \frac{F_1}{8\omega^2} \cos 3\alpha + \dots \right] \\
&+ A^2\omega \sin 2\alpha \left[\frac{A_1}{4\omega^2} \sin \alpha + \frac{B_1}{4\omega^2} \cos \alpha - \frac{E_1}{8\omega^2} \sin 3\alpha - \frac{F_1}{8\omega^2} \cos 3\alpha + \dots \right] \\
&= \frac{2A^2A_1}{4k} \sin^3 \alpha + \frac{A^2B_1}{4k} (1 - \cos 2\alpha) \cos \alpha - \frac{A^2E_1}{8k} (1 - \cos 2\alpha) \sin 3\alpha \\
&- \frac{A^2F_1}{8k} (1 - \cos 2\alpha) \cos 3\alpha + \frac{A^2A_1}{4\omega} \sin 2\alpha \sin \alpha + \frac{A^2B_1}{4\omega} \sin 2\alpha \cos \alpha \\
&\quad - \frac{A^2E_1}{8\omega} \sin 3\alpha \sin 2\alpha - \frac{A^2F_1}{8\omega} \cos 3\alpha \sin 2\alpha + \dots \\
&= \frac{2A^2A_1}{4k} \left[\frac{3}{4} \sin \alpha - \frac{1}{4} \sin 3\alpha \right] - \frac{A^2B_1}{8k} \left[\cos 3\alpha + \cos \alpha \right] \\
&+ \frac{A^2B_1}{4k} \cos \alpha + \frac{A^2E_1}{16k} \left[\sin 5\alpha + \sin \alpha \right] + \frac{A^2F_1}{16k} \left[\cos 5\alpha + \cos \alpha \right] \\
&\quad + \frac{A^2A_1}{8\omega} \left[\cos \alpha - \cos 3\alpha \right] + \frac{A^2B_1}{8\omega} \left[\sin 3\alpha + \sin \alpha \right] \\
&\quad - \frac{A^2E_1}{16\omega} \left[\cos \alpha - \cos 5\alpha \right] - \frac{A^2F_1}{16\omega} \left[\sin 5\alpha - \sin \alpha \right] + \dots \\
&= \left[\frac{3A^2A_1}{8k} + \frac{A^2E_1}{16k} + \frac{A^2B_1}{8\omega} + \frac{A^2F_1}{16\omega} \right] \sin \alpha \\
&+ \left[-\frac{A^2B_1}{8k} + \frac{A^2B_1}{4k} + \frac{A^2F_1}{16k} + \frac{A^2A_1}{8\omega} - \frac{A^2E_1}{16\omega} \right] \cos \alpha + \dots
\end{aligned}$$

Tenth term:

$$\begin{aligned}
2X_0\dot{X}_1Y_0 &= 2A \cos \alpha \left[-\frac{A\omega}{k} \sin \alpha - A \cos \alpha \right] \dot{X}_1 \\
&= -\frac{A^2\omega}{k} \sin 2\alpha \left[\frac{A_1}{4\omega} \cos \alpha - \frac{B_1}{4\omega} \sin \alpha - \frac{3E_1}{8\omega} \cos 3\alpha + \frac{3F_1}{8\omega} \sin 3\alpha + \dots \right] \\
&\quad - A^2(1 + \cos 2\alpha) \left[\frac{A_1}{4\omega} \cos \alpha - \frac{B_1}{4\omega} \sin \alpha - \frac{3E_1}{8\omega} \cos 3\alpha + \frac{3F_1}{8\omega} \sin 3\alpha + \dots \right] \\
&= -\frac{A^2A_1}{8k} \left[\sin 3\alpha + \sin \alpha \right] + \frac{A^2B_1}{8k} \left[\cos \alpha - \cos 3\alpha \right] \\
&\quad + \frac{3A^2E_1}{16k} \left[\sin 5\alpha - \sin \alpha \right] - \frac{3A^2F_1}{16k} \left[\cos \alpha - \cos 5\alpha \right] \\
&\quad - \frac{A^2A_1}{4\omega} \cos \alpha + \frac{A^2B_1}{4\omega} \sin \alpha - \frac{A^2A_1}{8\omega} \left[\cos 3\alpha + \cos \alpha \right] \\
&\quad + \frac{A^2B_1}{8\omega} \left[\sin 3\alpha - \sin \alpha \right] + \frac{3A^2E_1}{16\omega} \left[\cos 5\alpha + \cos \alpha \right] \\
&\quad \quad - \frac{3A^2F_1}{16\omega} \left[\sin 5\alpha + \sin \alpha \right] + \dots \\
&= \left[-\frac{A^2A_1}{8k} - \frac{3A^2E_1}{16k} + \frac{A^2B_1}{4\omega} - \frac{A^2B_1}{8\omega} - \frac{3A^2F_1}{16\omega} \right] \sin \alpha \\
&\quad + \left[\frac{A^2B_1}{8k} - \frac{3A^2F_1}{16k} - \frac{A^2A_1}{4\omega} - \frac{A^2A_1}{8\omega} + \frac{3A^2E_1}{16\omega} \right] \cos \alpha + \dots
\end{aligned}$$

Eleventh term:

$$\begin{aligned}
2X_0\dot{X}_0Y_1 &= 2A \cos \alpha (-A\omega \sin \alpha) Y_1 \\
&= -A^2\omega \sin 2\alpha \left[\frac{A_2}{4\omega^2} \sin \alpha + \frac{B_2}{4\omega^2} \cos \alpha - \frac{E_2}{8\omega^2} \sin 3\alpha + \dots \right] \\
&= -\frac{A^2A_2}{8\omega} (\cos \alpha - \cos 3\alpha) - \frac{A^2B_2}{8\omega} (\sin 3\alpha + \sin \alpha) + \\
&\quad \quad \frac{A^2E_2}{16\omega} (\cos \alpha - \cos 5\alpha) + \dots \\
&= -\frac{A^2B_2}{8\omega} \sin \alpha + \left[-\frac{A^2A_2}{8\omega} + \frac{A^2E_2}{16\omega} \right] \cos \alpha + \dots
\end{aligned}$$

Twelfth term :

$$\begin{aligned}
2X_0X_1\dot{Y}_0 &= 2A \cos \alpha \left[-\frac{A\omega^2}{k} \cos \alpha + A\omega \sin \alpha \right] X_1 \\
&= -\frac{A^2\omega^2}{k} (1 + \cos 2\alpha) \left[\frac{A_1}{4\omega^2} \sin \alpha + \frac{B_1}{4\omega^2} \cos \alpha - \frac{E_1}{8\omega^2} \sin 3\alpha \right. \\
&\quad \left. - \frac{F_1}{8\omega^2} \cos 3\alpha + \dots \right] \\
&\quad + A^2\omega \sin 2\alpha \left[\frac{A_1}{4\omega^2} \sin \alpha + \frac{B_1}{4\omega^2} \cos \alpha - \frac{E_1}{8\omega^2} \sin 3\alpha \right. \\
&\quad \left. - \frac{F_1}{8\omega^2} \cos 3\alpha + \dots \right] \\
&= \frac{A^2A_1}{4k} \sin \alpha - \frac{A^2B_1}{4k} \cos \alpha - \frac{A^2A_1}{8k} [\sin 3\alpha - \sin \alpha] \\
&\quad - \frac{A^2B_1}{8k} [\cos 3\alpha + \cos \alpha] + \frac{A^2E_1}{16k} [\sin 5\alpha + \sin \alpha] \\
&\quad + \frac{A^2F_1}{16k} [\cos 5\alpha + \cos \alpha] + \frac{A^2A_1}{8\omega} [\cos \alpha - \cos 3\alpha] \\
&\quad + \frac{A^2B_1}{8\omega} [\sin 3\alpha + \sin \alpha] - \frac{A^2E_1}{16\omega} [\cos \alpha - \cos 5\alpha] \\
&\quad - \frac{A^2F_1}{16\omega} [\sin 5\alpha - \sin \alpha] + \dots \\
&= \left[-\frac{A^2A_1}{4k} + \frac{A^2A_1}{8k} + \frac{A^2E_1}{16k} + \frac{A^2B_1}{8\omega} + \frac{A^2F_1}{16\omega} \right] \sin \alpha \\
&\quad + \left[-\frac{A^2B_1}{4k} - \frac{A^2B_1}{8k} + \frac{A^2F_1}{16k} + \frac{A^2A_1}{8\omega} - \frac{A^2E_1}{16\omega} \right] \cos \alpha + \dots
\end{aligned}$$

Thirteenth term :

$$\begin{aligned}
 X_0^2 \dot{Y}_1 &= A^2 \dot{Y}_1 \cos^2 \alpha = \frac{A^2}{2} (1 + \cos 2\alpha) \dot{Y}_1 \\
 &= \frac{A^2}{2} \left[\frac{A_2}{4\omega} \cos \alpha - \frac{B_2}{4\omega} \sin \alpha \right] + \frac{A^2}{2} \cos 2\alpha \left[\frac{A_2}{4\omega} \cos \alpha - \frac{B_2}{4\omega} \sin \alpha \right. \\
 &\quad \left. - \frac{3E_2}{8\omega} \cos 3\alpha \right] + \dots \\
 &= \frac{A^2 A_2}{8\omega} \cos \alpha - \frac{A^2 B_2}{8\omega} \sin \alpha + \frac{A^2 A_2}{16\omega} [\cos 3\alpha + \cos \alpha] \\
 &\quad - \frac{A^2 B_2}{16\omega} [\sin 3\alpha - \sin \alpha] - \frac{3A^2 E_2}{32\omega} [\cos 5\alpha + \cos \alpha] + \dots \\
 &= \left[\frac{A^2 A_2}{8\omega} + \frac{A^2 A_2}{16\omega} - \frac{3A^2 E_2}{32\omega} \right] \cos \alpha \\
 &\quad + \left[-\frac{A^2 B_2}{8\omega} + \frac{A^2 B_2}{16\omega} \right] \sin \alpha
 \end{aligned}$$

Coefficient of $\sin \alpha$ (Q):

$$\begin{aligned}
 Q &= \frac{k\delta A_1}{4\omega^2} - \frac{\delta B_1}{4\omega} + \frac{2bAD_1}{3\omega k} - \frac{bAD_1}{3\omega k} - \frac{bAD_2}{3\omega} - \frac{2bAF_2}{\omega} - \frac{2bAC_1}{3k} \\
 &\quad - \frac{2bAD_1}{3\omega} + \frac{2bAD_2}{3\omega} + \frac{bAC_1}{3k} + \frac{bAD_1}{3\omega} + \frac{3A^2 A_1}{8k} + \frac{A^2 E_1}{16k} + \frac{A^2 B_1}{8\omega} \\
 &\quad + \frac{A^2 F_1}{16\omega} - \frac{A^2 A_1}{8k} - \frac{3A^2 E_1}{16k} + \frac{A^2 B_1}{4\omega} - \frac{A^2 B_1}{8\omega} - \frac{3A^2 F_1}{16\omega} - \frac{A^2 B_2}{8\omega} - \frac{A^2 A_1}{4k} \\
 &\quad + \frac{A^2 A_1}{8k} + \frac{A^2 E_1}{16k} + \frac{A^2 B_1}{8\omega} + \frac{A^2 F_1}{16\omega} - \frac{A^2 B_2}{8\omega} + \frac{A^2 B_2}{16\omega} \\
 &= \frac{kA_1 \delta}{4\omega^2} - \frac{B_1 \delta}{4\omega} + \frac{bAD_1}{3\omega k} + \frac{bAD_2}{3\omega} - \frac{bAD_1}{3\omega} - \frac{2bAF_2}{\omega} \\
 &\quad - \frac{bAC_1}{3k} + \frac{A^2 A_1}{8k} - \frac{A^2 E_1}{16k} + \frac{3A^2 B_1}{8\omega} - \frac{A^2 F_1}{16\omega} - \frac{3A^2 B_2}{16\omega}
 \end{aligned}$$

$$\begin{aligned}
&= \frac{k\delta}{4\omega^2} \left[\frac{3A^3\omega}{4} - \delta\omega A \right] - \frac{\delta}{4\omega} \left[k\delta A + \frac{A^3\omega^2}{4k} \right] + \frac{bA}{3\omega k} \left[-\frac{2bA^2\omega^2}{k} \right] \\
&\quad + \frac{bA}{3\omega} \left[\frac{3\omega^2 bA^2}{k} - \frac{\omega^2 bA^2}{2k^2} \right] - \frac{bA}{3\omega} \left[-\frac{2bA^2\omega^2}{k} \right] \\
&\quad - \frac{2bA}{\omega} \left[\frac{\omega^2 bA^2}{k} \left(1 - \frac{1}{2k} \right) \right] - \frac{bA}{3k} \left[2bA^2\omega - \frac{bA^2\omega}{k} \right] \\
&\quad + \frac{A^2}{8k} \left[\frac{3A^3\omega}{4} - \delta\omega A \right] - \frac{A^2}{16k} \left[\frac{3\omega A^3}{4} \right] + \frac{3A^2}{8\omega} \left[kA\delta + \frac{A^3\omega^2}{4k} \right] \\
&\quad - \frac{A^2}{16\omega} \left[-\frac{3A^3\omega^2}{4k} \right] - \frac{3A^2}{16\omega} \left[\frac{2A^3\omega^2}{k} - \frac{2b^2A\delta}{k} \right] \\
&= A^5 \left[\frac{3\omega}{32k} - \frac{3\omega}{64k} + \frac{3\omega}{32k} + \frac{3\omega}{64k} - \frac{3\omega}{8k} \right] \\
&+ A^3 \left[\frac{3k\delta}{16\omega} - \frac{\omega\delta}{16k} - \frac{2b^2\omega}{3k^2} + \frac{b^2\omega}{k} - \frac{b^2\omega}{6k^2} + \frac{2b^2\omega}{3k} - \frac{2b^2\omega}{k} \left(1 - \frac{1}{2k} \right) \right. \\
&\quad \left. - \frac{2b^2\omega}{3k} + \frac{b^2\omega}{3k^2} - \frac{\omega\delta}{8k} + \frac{3k\delta}{8\omega} + \frac{3b^2\delta}{8\omega k} \right] + A \left[-\frac{k\delta^2}{4\omega} - \frac{k\delta^2}{4\omega} \right]
\end{aligned}$$

which on simplification gives,

$$= A^5 \left[-\frac{6\omega}{32k} \right] + A^3 \left[\frac{3b^2\delta}{8\omega k} + \frac{9k\delta}{16\omega} - \frac{3\omega\delta}{16k} + \frac{b^2\omega}{2k^2} - \frac{b^2\omega}{k} \right] + A \left[-\frac{k\delta^2}{2\omega} \right]$$

Thus the final form of the coefficient of $\sin \alpha$ i.e., Q has been found to be a polynomial in 'A' as given above. From this expression the flow equation in the second order is easily obtained by writing -

$$\begin{aligned}
\left(\frac{dA}{dt} \right)_{2^{nd} order} &= -\frac{Q}{2\omega} \\
&= A^5 \left[\frac{3}{32k} \right] + A^3 \left[-\frac{3b^2\delta}{16\omega^2 k} - \frac{9k\delta}{32\omega^2} + \frac{3\delta}{32k} - \frac{b^2}{4k^2} + \frac{b^2}{2k} \right] \\
&\quad + A \left[\frac{k\delta^2}{4\omega^2} \right]
\end{aligned}$$

Finally, having obtained $\left(\frac{dA}{dt} \right)_{2^{nd} order}$ the final flow equation upto the second order is obtained by combining the first order flow equa-

tion and the second order flow equation and writing -

$$\left(\frac{dA}{dt}\right) = \left(\frac{dA}{dt}\right)_{1^{st} order} + \left(\frac{dA}{dt}\right)_{2^{nd} order}$$

or,

$$\left(\frac{dA}{dt}\right) = A^5 \left[\frac{3}{32k} \right] + A^3 \left[-\frac{3b^2\delta}{16\omega^2k} - \frac{9k\delta}{32\omega^2} + \frac{3\delta}{32k} - \frac{b^2}{4k^2} + \frac{b^2}{2k} - \frac{3}{8} \right] + A \left[\frac{k\delta^2}{4\omega^2} + \frac{\delta}{2} \right]$$

which is the final form of Eq.(4.36) with $\lambda = 1$.

Chapter 5

Prospects and Conclusion

In the present thesis, our primary focus has been to develop a method to effectively scan the limit cycle zone of the parameter space of a two-dimensional non-Linear type non-Linear Biochemical oscillator. The method developed in the last two chapters was based on and applied to the Sel'kov model of Glycolysis. The Sel'kov model was chosen as it is one of the oldest known biochemical reactions to show oscillatory behaviour and also due to the fact that the limit cycle region in the parameter space of this system has a large area, thus facilitating our analysis.

In the process of developing the method, we have shown an effective procedure for the application of perturbation theory in the case of two-dimensional non-linear oscillators. Perturbative renormalization group has been used to calculate the boundaries of the limit cycles for different values of parameters ' a ' and ' b ' of the system inside the limit cycle region of the parameter space ; then comparing the results with the numerically plotted result for the same pair of parameter values, it has been established that the results predicted by RG are in good agreement. During the calculation, the values of the system parameters ' a ' and ' b ' were changed as per our developed method, which needed the introduction of an external parameter ' δ ' in the system equations, thus facilitating the scanning of the parameter space of the system. Thus perturbative

renormalization group was used as a probe to establish the effectiveness of the method developed.

The third chapter of this volume presents a somewhat crude analytic method to scan the parameter space of the Sel'kov model of Glycolysis. In our efforts to keep the algebra simple and the procedure by which the external parameter ' δ ' was introduced in the system equations, we were constrained to keep the value of the external parameter ' δ ' small. As such, for bigger values of the parameter, our theory had failed to produce satisfactory results. Also, the method had failed to scan each and every point of the parameter space since variation in the value of ' δ ' only shifted the original system parameter values along a straight line, thus proving that the method needed some major improvements.

Improvements were brought about in our method by modifying the method in the fourth chapter. The major modification introduced was to use the original Jacobian of the system as a tool to introduce the external parameter ' δ ' in the system equations. This proved to be quite fruitful, as can be seen from the results in chapter 4. In the new procedure, there were no restrictions on the choice of the values for the external parameter ' δ ', and any point on the curves parametric in ' δ ' in Figure 4.1 can serve as a set of values of system parameters. In fact, ' δ ' provides a singular handle for changing both the parameter values of the system at one go.

Thus the method presented in this volume provides a systematic way of selecting parameter values needed for different experimental applications, where closed orbits from different parts of the parameter space are to be studied. This opens the way for detailed investigations into the shape and size of the limit cycles for different oscillating biochemical reactions for parameter values

suitably chosen from different regions of the limit cycle region of the parameter space. Another most important fact arising out of our analysis is the result that up to the first order in perturbation, the boundary of the limit cycle of a two-dimensional biochemical oscillator varies as $\sqrt{\delta}$.

In summary, the mathematical analysis presented in this volume can make way for experimentalists to choose parameters effectively from any region of the parameter space and thus open up ways to study the shape and size of the limit cycles for parameter values at different regions of the parameter space.

Bibliography

- [1] Morris W Hirsch, Stephen Smale, and Robert L Devaney. *Differential equations, dynamical systems, and an introduction to chaos*. Academic press, 2012.
- [2] Steven H Strogatz. *Nonlinear dynamics and chaos: with applications to physics, biology, chemistry, and engineering*. CRC press, 2018.
- [3] George David Birkhoff. *Dynamical systems*, volume 9. American Mathematical Soc., 1927.
- [4] Alfredo Medio and Marji Lines. *Nonlinear dynamics: A primer*. Cambridge University Press, 2001.
- [5] Daniel Kaplan and Leon Glass. *Understanding nonlinear dynamics*. Springer Science & Business Media, 1997.
- [6] Stephen Smale. Differentiable dynamical systems. *Bulletin of the American mathematical Society*, 73(6):747–817, 1967.
- [7] Albert Goldbeter et al. Biochemical oscillations and cellular rhythms. *Biochemical Oscillations and Cellular Rhythms*, 1997.
- [8] James Dickson Murray. *Mathematical Biology I. An Introduction*. Springer, 2002.
- [9] Irving R Epstein and John A Pojman. *An introduction to nonlinear chemical dynamics: oscillations, waves, patterns, and chaos*. Oxford university press, 1998.

- [10] Leah Edelstein-Keshet. *Mathematical models in biology*. SIAM, 2005.
- [11] Lee A Segel. *Modeling dynamic phenomena in molecular and cellular biology*. Cambridge University Press, 1984.
- [12] Wassim M Haddad and VijaySekhar Chellaboina. Nonlinear dynamical systems and control. In *Nonlinear Dynamical Systems and Control*. Princeton university press, 2011.
- [13] Lee A Segel et al. *Mathematical models in molecular cellular biology*. CUP Archive, 1980.
- [14] Albert Goldbeter. Computational approaches to cellular rhythms. *Nature*, 420(6912):238–245, 2002.
- [15] B Delamotte. Nonperturbative (but approximate) method for solving differential equations and finding limit cycles. *Physical Review Letters*, 70(22):3361, 1993.
- [16] Ebrahim Esmailzadeh, Davood Younesian, and Hassan Askari. Analytical methods in nonlinear oscillations. *Netherlands: Springer*, 2018.
- [17] Carl M Bender, Steven Orszag, and Steven A Orszag. *Advanced mathematical methods for scientists and engineers I: Asymptotic methods and perturbation theory*, volume 1. Springer Science & Business Media, 1999.
- [18] Dominic Jordan and Peter Smith. *Nonlinear ordinary differential equations: an introduction for scientists and engineers*. OUP Oxford, 2007.
- [19] Ji-Huan He. Some asymptotic methods for strongly nonlinear equations. *International journal of Modern physics B*, 20(10):1141–1199, 2006.

- [20] Lawrence Perko. Linear systems. In *Differential Equations and Dynamical Systems*, pages 1–63. Springer, 1991.
- [21] Stephen Wiggins, Stephen Wiggins, and Martin Golubitsky. *Introduction to applied nonlinear dynamical systems and chaos*, volume 2. Springer, 2003.
- [22] N Minorsky. Theoretical aspects of nonlinear oscillations. *IRE Trans. Circuit Theory*, 7(4):368–381, 1960.
- [23] J Schnakenberg. Simple chemical reaction systems with limit cycle behaviour. *Journal of theoretical biology*, 81(3):389–400, 1979.
- [24] Ali H Nayfeh and Dean T Mook. *Nonlinear oscillations*. John Wiley & Sons, 2008.
- [25] Jayanta K Bhattacharjee and Jyotirmoy Roy. Oscillators: Old and new perspectives. In *AIP Conference Proceedings*, volume 1582, pages 124–139. American Institute of Physics, 2014.
- [26] Polina Solomonovna Landa. *Nonlinear oscillations and waves in dynamical systems*, volume 360. Springer Science & Business Media, 2013.
- [27] Vladimir I Nekorkin. *Introduction to nonlinear oscillations*. John Wiley & Sons, 2015.
- [28] Amartya Sarkar, JK Bhattacharjee, Sagar Chakraborty, and DB Banerjee. Center or limit cycle: renormalization group as a probe. *The European Physical Journal D*, 64(2):479–489, 2011.
- [29] M Basso, R Genesio, and A Tesi. A frequency method for predicting limit cycle bifurcations. *Nonlinear Dynamics*, 13(4):339–360, 1997.

- [30] John Guckenheimer and Philip Holmes. *Nonlinear oscillations, dynamical systems, and bifurcations of vector fields*, volume 42. Springer Science & Business Media, 2013.
- [31] Jack K Hale and Hüseyin Koçak. *Dynamics and bifurcations*, volume 3. Springer Science & Business Media, 2012.
- [32] Debapriya Das, Dhruba Banerjee, and Jayanta K Bhattacharjee. Super-critical and sub-critical hopf bifurcations in two and three dimensions. *Nonlinear Dynamics*, 77(1):169–184, 2014.
- [33] Jayanta K Bhattacharjee, Sagar Chakraborty, and Amartya Sarkar. A methodology for classifying periodic orbits. In *Chaos Theory: Modeling, Simulation and Applications*, pages 120–126. World Scientific, 2011.
- [34] Bertrand Delamotte. A hint of renormalization. *American Journal of Physics*, 72(2):170–184, 2004.
- [35] Lin-Yuan Chen, Nigel Goldenfeld, and Yoshitsugu Oono. Renormalization group and singular perturbations: Multiple scales, boundary layers, and reductive perturbation theory. *Physical Review E*, 54(1):376, 1996.
- [36] Ronald E Mickens. *An introduction to nonlinear oscillations*. CUP Archive, 1981.
- [37] Yoshiki Kuramoto. *Chemical oscillations, waves, and turbulence*. Courier Corporation, 2003.
- [38] Chihiro Hayashi. Nonlinear oscillations in physical systems. In *Nonlinear Oscillations in Physical Systems*. Princeton University Press, 2014.
- [39] Oliver Nelles. Nonlinear dynamic system identification. In *Nonlinear System Identification*, pages 547–577. Springer, 2001.

- [40] Ali H Nayfeh and Balakumar Balachandran. *Applied non-linear dynamics: analytical, computational, and experimental methods*. John Wiley & Sons, 2008.
- [41] Ali H Nayfeh. *Introduction to perturbation techniques*. John Wiley & Sons, 2011.
- [42] Nigel Goldenfeld, Olivier Martin, Yoshitsugu Oono, and Fong Liu. Anomalous dimensions and the renormalization group in a nonlinear diffusion process. *Physical review letters*, 64(12):1361, 1990.
- [43] GC Paquette, Lin-Yuan Chen, Nigel Goldenfeld, and Y Oono. Structural stability and renormalization group for propagating fronts. *Physical review letters*, 72(1):76, 1994.
- [44] Mohammed Ziane. On a certain renormalization group method. *Journal of Mathematical Physics*, 41(5):3290–3299, 2000.
- [45] Amartya Sarkar and JK Bhattacharjee. Renormalization group as a probe for dynamical systems. In *Journal of Physics: Conference Series*, volume 319, page 012017. IOP Publishing, 2011.
- [46] Debapriya Das, Dhruva Banerjee, and Jayanta K Bhattacharjee. Finding limit cycles in self-excited oscillators with infinite-series damping functions. *The European Physical Journal D*, 69(3):1–13, 2015.
- [47] A Sarkar and JK Bhattacharjee. Renormalization group for nonlinear oscillators in the absence of linear restoring force. *EPL (Europhysics Letters)*, 91(6):60004, 2010.
- [48] EE Sel'kov. Self-oscillations in glycolysis. *Eur. J. Biochem*, 4:79–86, 1968.

- [49] Dhruva Banerjee and Jayanta K Bhattacharjee. Renormalization group and liénard systems of differential equations. *Journal of Physics A: Mathematical and Theoretical*, 43(6):062001, 2010.
- [50] Ayan Dutta, Debapriya Das, Dhruva Banerjee, and Jayanta K Bhattacharjee. Estimating the boundaries of a limit cycle in a 2d dynamical system using renormalization group. *Communications in Nonlinear Science and Numerical Simulation*, 57:47–57, 2018.
- [51] Ayan Dutta, Jyotipriya Roy, and Dhruva Banerjee. Predicting limit cycle boundaries deep inside parameter space of a 2d biochemical nonlinear oscillator using renormalization group. *International Journal of Bifurcation and Chaos*, 31(11):2150162, 2021.